Addition of malodorants to lighter gas – a study of the physical properties of mixtures of lighter gas and selected substances

Vasu Neela and Nicolas von Solms

Center for Phase Equilibria and Separation Processes (IVC-SEP)

Department of Chemical and Biochemical Engineering

Technical University of Denmark

Table of Contents

List of Tables ---------- **iv**

List of Figures ---------- **vi**

1 Introduction ---------- **1**

2 Background ---------- **4**

3 Chemical ingredients in inhalants ---------- **6**

4 Effects of butane volatile substance abuse ---------- **7**

4.1 Short term effect 7

4.2 Long term effect 7

5 Preventing volatile substance abuse ---------- **9**

6 The basic idea and its approach ---------- **10**

7 Theory and modeling ---------- **12**

7.1 CPA (Cubic-plus-Association) Equation of State 12

7.2 The COSMO-based thermodynamic model: 13

7.3 Malodorants 19

7.3.1 Triethylamine ---------- 21

7.3.2 Denatonium Benzoate (Bitrex) ---------- 21

7.3.3 Isobutyraldehyde ---------- 22

7.3.4 Tetrahydrothiophene ---------- 22

7.3.5 Dimethylsulfide ---------- 23

7.3.6 2, 2, 4-Trimethyl pentane ---------- 24

7.3.7 Picoline (2-methyl pyridine) ---------- 24

7.3.8 Eucalyptol (1.8 Cineole) ---------- 25

7.3.9 Nitrobenzene ---------- 25

7.3.10 1-Pentanol ---------- 26

7.3.11 Sulfuryl chloride ---------- 27

7.3.12 Cyanogen chloride ---------- 27

7.3.13 Bis-(2-chloroethyl) sulfide ---------- 28

7.3.14 Bis-(2-chloroethyl) ethylamine ---------- 28

7.3.15 Ethyldichloroarsine ---------- 29

7.3.16 Bromobenzylcyanide ---------- 30

7.3.17 Chloropicrin ---- 30
7.3.18 Diphenylcyanoarsine ---- 30
7.3.19 Ethyl mercaptan ---- 31
7.3.20 Bis(chloromethyl)ether ---- 32
7.3.21 2-Amino phenol ---- 32
7.3.22 Propyleneglycol ---- 33
7.3.23 s-Trioxane ---- 33
7.3.24 2-Chloroacetophenone ---- 34
7.3.25 Indole ---- 34
7.3.26 Pyridine ---- 35
7.3.27 *n*-Butylamine ---- 35
7.4 Estimation of pure compound parameters (CPA equation of state) 36
7.5 Sigma Profiles 38
7.6 Vapor-liquid Equilibria 57
8 Conclusion ---- 95
9 References ---- 96

List of Tables

Table 1: Death attributed to specific volatile substances in those under 18 from 1981-1990 .. 5
Table 2: Chemical ingredients in inhalants 6
Table 3 : Possible consequences from butane inhalant substances [9] 8
Table 4: Malodorants 19
Table 5: Properties of Triethylamine 21
Table 6: Properties of Denatonium benzoate (Bitrex) 22
Table 7: Properties of Isobutyraldehyde 22
Table 8: Properties of Tetrahydrothiophene 23
Table 9: Properties of Dimethylsulfide 23
Table 10: Properties of 2. 2. 4-Trimethyl pentane 24
Table 11: Properties of Picoline 25
Table 12: Properties of Eucalyptol 25
Table 13: Properties of Nitrobenzene 26
Table 14: Properties of 1-Pentanol 26
Table 15: Properties of sulfuryl chloride 27
Table 16: Properties of cyanogen chloride 28
Table 17: Properties of Bis-(2-chloroethyl) sulfide 28
Table 18: Properties of Bis-(2-chloroethyl) ethylamine 29
Table 19: Properties of Ethyl dichloroarsine 29
Table 20: Properties of Bromobenzylvyanide 30
Table 21: Properties of Trichloronitromethane 30
Table 22: Properties of Diphenylcyanoarsine 31
Table 23: Properties of Ethylmercaptan 31
Table 24: Properties of Bis (chloromethyl) ether 32
Table 25: Properties of 2-Aminophenol 32
Table 26: Properties of Propylene glycol 33
Table 27: Properties of s-Trioxane 33
Table 28: Properties of Chloroacetophenone 34
Table 29: Properties of Indole 34

Table 30: Properties of Pyridine 35
Table 31: Properties of butylamine 35
Table 32: CPA Parameters for the compounds involved in this study 36

List of Figures

Figure 1: Ideal solvation process in COSMO-based models [18] 13
Figure 2: Schematic illustration of contacting molecular cavities and contact interactions [14]. 15
Figure 3: Comparison of Triethylamine Vapor pressure between CPA, COSMOtherm and DIPPR 38
Figure 4: Comparison of Isobutyraldehyde Vapor pressure between CPA, COSMOtherm and DIPPR 39
Figure 5: Comparison of Tetrahydrothiophene Vapor pressure between CPA, COSMOtherm and DIPPR 39
Figure 6: Comparison of DimethylsulfideVapor pressure between CPA, COSMOtherm and DIPPR 40
Figure 7: Comparison of 2,2,4 Trimethylpentane Vapor pressure between CPA, COSMOtherm and DIPPR 41
Figure 8 Comparison of 2-MethylpyridineVapor pressure between CPA, COSMOtherm and DIPPR 41
Figure 9: Comparison of NitrobenzeneVapor pressure between CPA, COSMOtherm and DIPPR 42
Figure 10: Comparison of 1-Pentanol Vapor pressure between CPA, COSMOtherm and DIPPR 42
Figure 11: Comparison of Sulfurylchloride Vapor pressure between CPA, COSMOtherm and DIPPR 43
Figure 12: Comparison of CyanogenchlorideVapor pressure between CPA, COSMOtherm and DIPPR 43
Figure 13: Comparison of Ethylmercaptan Vapor pressure between CPA, COSMOtherm and DIPPR 44
Figure 14: Comparison of Bis(chloromethyl)ether Vapor pressure between CPA, COSMOtherm and DIPPR 44
Figure 15: Comparison of Propyleneglycol vapor pressure between CPA, COSMOtherm and DIPPR 45

Figure 16: Comparison of s-Trioxane vapor pressure between CPA, COSMOtherm and DIPPR 45
Figure 17: Comparison of Indole vapor pressure between CPA, COSMOtherm and DIPPR 46
Figure 18: Comparison of Pyridine vapor pressure between CPA, COSMOtherm and DIPPR 46
Figure 19: Comparison of Butylamine vapor pressure between CPA, COSMOtherm and DIPPR 47
Figure 20: Vapor-Liquid Equilibrium of Ethylmercaptan (1) / *n*-Butane (2) with CPA (Association scheme-2B) and COSMOtherm at 50^{o}C 49
Figure 21: Vapor-Liquid Equilibrium of Ethylmercaptan (1) / *n*-Butane (2) with CPA (Non association) and COSMOtherm at 50^{o}C 49
Figure 22: Vapor-Liquid Equilibrium of Ethylmercaptan (1) / *n*-Butane (2) with CPA (Association scheme-2B) and COSMOtherm at 100^{o}C 50
Figure 23: Vapor-Liquid Equilibrium of Ethylmercaptan (1) / *n*-Butane (2) with CPA (Non Association) and COSMOtherm at 100^{o}C 50
Figure 24: Sigma profiles for the lighter gas components (butane. isobutane and propane).. 51
Figure 25: Sigma profiles of 1,8 cineole, 1-pentanol and 2-methylpyridine 52
Figure 26: Sigma profiles of cyanogen chloride and dimethylsulfide 53
Figure 27: Sigma profiles for the sulfurylchloride and triethylamine 54
Figure 28: sigma profile for the ethyl mercaptan, Isobutanal and pyridine 55
Figure 29: sigma profile for the nitrobenzene and tetrahydrothiophene 55
Figure 30: sigma profile for the Bitrex anion and Bitrex cation 56
Figure 31: Vapor-Liquid equilibrium for Triethylamine (1) / *n*-Butane (2) at 25 ^{o}C. The solid curve shows the COSMOtherm predictions 58
Figure 32: The X-Y diagram for Triethylamine (1) / *n*-Butane (2) at 25 ^{o}C. The solid curve shows the COSMOtherm predictions 59
Figure 33: Vapor-Liquid equilibrium for Isobutyraldehyde (1) / *n*-Butane (2) at 25 ^{o}C. The solid curve shows the COSMOtherm predictions 60
Figure 34: The X-Y diagram for Isobutyraldehyde (1) / *n*-Butane (2) at 25 ^{o}C. The solid curve shows the COSMOtherm predictions 61

Figure 35: Vapor-Liquid equilibrium for Tetrahydrothiophene (1) / *n*-Butane (2) / at 25 ^{o}C. The solid curve shows the COSMOtherm predictions 62
Figure 36: The X-Y diagram for Tetrahydrothiophene (1) / *n*-Butane (2) at 25 ^{o}C. The solid curve shows the COSMOtherm predictions 62
Figure 37: Vapor-Liquid equilibrium for Dimethylsulfide (1) / *n*-Butane (2) at 25 ^{o}C. The solid curve shows the COSMOtherm predictions..... 63
Figure 38: The X-Y diagram for Dimethylsulfide (1) / *n*-Butane (2) at 25 ^{o}C. The solid curve shows the COSMOtherm predictions 64
Figure 39: Vapor-Liquid equilibrium for 2, 2, 4Trimethyl-2-pentane (1) / *n*-Butane (2) at 25 ^{o}C. The solid curve shows the COSMOtherm predictions 65
Figure 40: The X-Y diagram for 2, 2, 4 Trimethyl-2-pentane (1) / *n*-Butane (2) at 25 ^{o}C. The solid curve shows the COSMOtherm predictions..... 65
Figure 41: Vapor-Liquid equilibrium for 2-methylpyridine (1) / *n*-Butane (2) at 25 ^{o}C. The solid curve shows the COSMOtherm predictions..... 66
Figure 42: The X-Y diagram for 2-methylpyridine (1) / *n*-Butane (2) at 25 ^{o}C. The solid curve shows the COSMOtherm predictions 67
Figure 43: Vapor-Liquid equilibrium for 1, 8 Cineole (1) / *n*-Butane (2) at 25 ^{o}C. The solid curve shows the COSMOtherm predictions 68
Figure 44: The X-Y diagram for 1, 8 Cineole (1) / *n*-Butane (2) at 25 ^{o}C. The solid curve shows the COSMOtherm predictions 68
Figure 45: Vapor-Liquid equilibrium for Nitrobenzene (1) / *n*-Butane (2) at 25 ^{o}C. The solid curve shows the COSMOtherm predictions 69
Figure 46: The X-Y diagram for Nitrobenzene (1) / *n*-Butane (2) at 25 ^{o}C. The solid curve shows the COSMOtherm predictions 70
Figure 47: Vapor-Liquid equilibrium for 1-Pentanol (1) / *n*-Butane (2) at 25 ^{o}C. The solid curve shows the COSMOtherm predictions 71
Figure 48: The X-Y diagram for 1-Pentanol (1) / *n*-Butane (2) at 25 ^{o}C. The solid curve shows the COSMOtherm predictions 71
Figure 49: Vapor-Liquid equilibrium for Sulfuryl chloride (1) / *n*-Butane (2) at 25 ^{o}C. The solid curve shows the COSMOtherm predictions..... 72

Figure 50: The X-Y diagram for Sulfuryl chloride (1) / *n*-Butane (2) at 25 ^{o}C. The solid curve shows the COSMOtherm predictions 73
Figure 51: Vapor-Liquid equilibrium for Cyanogen chloride (1) / *n*-Butane (2) at 25 ^{o}C. The solid curve shows the COSMOtherm predictions..... 74
Figure 52: The X-Y diagram for Cyanogen chloride (1) / *n*-Butane (2) at 25 ^{o}C. The solid curve shows the COSMOtherm predictions 74
Figure 53: Vapor-Liquid equilibrium for Bis(2-chloroethyl)sulfide (1) / *n*-Butane (2) at 25 ^{o}C. The solid curve shows the COSMOtherm predictions 75
Figure 54: The X-Y diagram for Bis(2-chloroethyl)sulfide (1) / *n*-Butane (2) at 25 ^{o}C. The solid curve shows the COSMOtherm predictions..... 76
Figure 55: Vapor-Liquid equilibrium for Bis(2-chloroethyl)ethylamine (1) / *n*-Butane (2) at 25 ^{o}C. The solid curve shows the COSMOtherm predictions 77
Figure 56: Vapor-Liquid equilibrium for Bis(2-chloroethyl)ethylamine (1) / *n*-Butane (2) at 25 ^{o}C. The solid curve shows the COSMOtherm predictions 78
Figure 57: Vapor-Liquid equilibrium for Dichloroethylarsine (1) / *n*-Butane (2) at 25 ^{o}C. The solid curve shows the COSMOtherm predictions..... 79
Figure 58: The X-Y diagram for Dichloroethylarsine (1) / *n*-Butane (2) at 25 ^{o}C. The solid curve shows the COSMOtherm predictions 80
Figure 59: Vapor-Liquid equilibrium for Bromobenzylcyanide (1) / *n*-Butane (2) at 25 ^{o}C. The solid curve shows the COSMOtherm predictions 81
Figure 60: The X-Y diagram for Bromobenzylcyanide (1) / *n*-Butane (2) at 25 ^{o}C. The solid curve shows the COSMOtherm predictions 81
Figure 61: Vapor-Liquid equilibrium for Chloropicrin (1) / *n*-Butane (2) at 25 ^{o}C. The solid curve shows the COSMOtherm predictions 82
Figure 62: The X-Y diagram for Chloropicrin (1) / *n*-Butane (2) at 25 ^{o}C. The solid curve shows the COSMOtherm predictions 83
Figure 63: Vapor-Liquid equilibrium for Chloropicrin (1) / *n*-Butane (2) at 25 ^{o}C. The solid curve shows the COSMOtherm predictions 84
Figure 64: Vapor-Liquid equilibrium for Ethylmercaptan (1) / *n*-Butane (2) at 25 ^{o}C. The solid curve shows the COSMOtherm predictions..... 85

Figure 65: The X-Y diagram for Ethylmercaptan (1) / *n*-Butane (2) at 25 ^{o}C. The solid curve shows the COSMOtherm predictions 85
Figure 66: Vapor-Liquid equilibrium for Bis(chloromethyl)ether (1) / *n*-Butane (2) at 25 ^{o}C. The solid curve shows the COSMOtherm predictions 86
Figure 67: Vapor-Liquid equilibrium for 2-Amino phenol (1) / *n*-Butane (2) at 25 ^{o}C. The solid curve shows the COSMOtherm predictions..... 87
Figure 68: Vapor-Liquid equilibrium for Propylene glycol (1)/ *n*-Butane (2) at 25 ^{o}C. The solid curve shows the COSMOtherm predictions..... 88
Figure 69: Vapor-Liquid equilibrium for 1, 3, 5 Trioxane (1) / *n*-Butane (2) at 25 ^{o}C. The solid curve shows the COSMOtherm predictions..... 89
Figure 70: Vapor-Liquid equilibrium for Chloroacetophenone (1) / *n*-Butane (2) at 25 ^{o}C. The solid curve shows the COSMOtherm predictions 89
Figure 71: Vapor-Liquid equilibrium for Indole (1) / *n*-Butane (2) at 25 ^{o}C. The solid curve shows the COSMOtherm predictions 90
Figure 72: Vapor-Liquid equilibrium for Pyridine (1) / *n*-Butane (2) at 25 ^{o}C. The solid curve shows the COSMOtherm predictions 91
Figure 73: The X-Y diagram for Pyridine (1) / *n*-Butane (2) at 25 ^{o}C. The solid curve shows the COSMOtherm predictions 91
Figure 74: Vapor-Liquid equilibrium for Butylamine (1) / *n*-Butane (2) at 25 ^{o}C. The solid curve shows the COSMOtherm predictions 92
Figure 75: The X-Y diagram for Butylamine (1) / *n*-Butane (2) at 25 ^{o}C. The solid curve shows the COSMOtherm predictions 93
Figure 76: The X-Y diagram for possible additives (1) / *n*-Butane (2) at 25 ^{o}C. The solid curve shows the COSMOtherm predictions 94

1 Introduction

This project involves studying some relevant physical properties of mixtures created by adding agents to lighter gas which discourage its abuse. These additives are called "malodorants" here, although it is to be understood in a more general sense and includes any effect which discourages abuse (e.g. bittering agents, irritants, etc).

In this work, the majority of the compounds considered have been selected based on their unpleasant odor. The aim is to find a substance that has not only the correct physiological effect (discourages abuse) but also the correct physical behavior on addition to lighter gas (solubility, phase behavior). This means that the additive should not be too volatile (so that it disappears quickly if the lighter gas canister is held open for a short while – a process know as "weathering"). Conversely, it should not be too heavy (i.e. have a volatility much less than lighter gas) since it would then be required to be added in larger quantities in the liquid in order for it to be present in the vapor in sufficient quantities to have the required deterrent effect. This would also mean that in time the additive would be become more and more concentrated in the liquid and might finally affect the normal use of the gas canister. Finally, addition of the malodorants should not affect the normal use of lighter gas.

The influence of physical factors such as temperature, pressure and concentration of the selected substances with lighter gas is studied in this work. It should be emphasized that this report represents only one component in a larger study examining the possibility of adding malodorants to lighter gas and focuses on the physical chemistry or chemical engineering aspects of the problem. Issues of toxicity, for example, have not been taken into account although it may be mentioned that highly toxic substances such as mercaptans are already added to natural gas as malodorants in very small amounts, so the toxicity of the pure substance may not be the only factor that needs to be considered. Dosage and concentration are of course also relevant.

Lighter gas consists primarily of *n*-butane (referred to in the remainder of the report simply as butane) isobutane and propane. Butane is a volatile substance and is a gas at atmospheric temperature and pressure. It is stored as a liquid in lighters and lighter-gas refill cans by increasing its pressure. Butane's vapor pressure at room temperature (25 ^{o}C) is 2.28 atm which means that pure liquid butane in lighter gas containers is at a pressure of around

2.28 atm, depending on the temperature. The pressure of actual lighter gas is somewhat above this value due to the presence of the lighter isobutane and propane.

Cigarette lighter refill cans are the most commonly used butane product although butane is also used as a propellant in aerosols. There are a wide range of butane products including cigarette lighters and portable stoves. Butane is a colorless gas with a faintly disagreeable odor and it is poorly soluble in water. The lower explosive limit of butane is 1.9% and its toxicity is low. A typical lighter refill contains 54% *n*-butane, 20% isobutane, and 26% propane. Refill cans for stoves contain 71% *n*-butane, 28% isobutane, and 1% propane [2]. Butane is the main component of gas lighter refills and for the purposes of this investigation it is assumed that lighter gas is pure butane. This assumption is not expected to have an important influence on the results obtained here.

In this investigation we have used two thermodynamic models - Cubic-Plus-Association (CPA) and COSMOtherm to predict the phase behaviour of the mixtures studied. The CPA equation of state combines the very widely used Soave-Redlich-Kwong (SRK) equation of state combined with an extra expression which accounts specifically for hydrogen-bonding substances, such as amines or alcohols. This equation is applicable to multicomponent, multiphase equilibria for systems containing associating components. In this work, the CPA Equation of state is used to describe the vapor liquid equilibrium of additive (malodorants)-butane systems at different pressures and temperature is studied.

The COSMOtherm software also used in this work, and is a commercially available software program. Predictions from this model are generally very good at pressures which are not very elevated (for example the pressure of lighter gas at room temperature). COSMOtherm (Conductor like screening model) is a program that computes thermophysical data of fluid mixtures. COSMOtherm is developed based on COSMO-RS theory. COSMO-RS (Conductor like screening model for real solvents) is a theory of interacting molecular surfaces as computed by quantum (QM) continuum solvation models (CSMs). Quantum chemical methods originally developed for isolated molecules i.e. for molecules in a vacuum or a gas. The basis of the COSMO model is the ‘‘solvent accessible surface’’ of a solute molecule. COSMO places the molecule inside a cavity formed within a homogeneous medium, taken to be the solvent. COSMO is a valuable tool for the chemical engineering problems to find out the activity coefficients and other thermo physical data of compounds in

fluid phase. A small number of adjustable and universal parameters, the σ profiles, surfaces, volume of the molecules and the molecule-specific charge distribution are required to perform the COSMO-RS calculations [14].

COSMO-RS can be used for the prediction of vapor-liquid equilibria, liquid-liquid equilibria, solid-liquid equilibria, vapor pressures of pure compounds and mixtures, partition coefficients, heats of vaporization, activity coefficients, solubilities, excess Gibbs free energies, and excess enthalpies, etc. COSMO-RS has also been extended to ionic liquids. The equilibrium behavior of mixtures of various additives in butane is studied in terms primarily of their vapour-liquid equilibrium behaviour. This means that for a given composition of an additive in the butane liquid we are interested in the composition in the vapour phase and the overall pressure of the mixture. In some cases the additive is not soluble in butane and in these cases liquid-liquid equilibrium behaviour is observed (i.e. two separate liquid phases result, although there will be a small degree of mutual solubility of each component in the other liquid phase).

There is a very important difference between CPA and COSMOtherm which should be borne in mind: In order to use CPA (or indeed any equation of state model) *it is necessary to have experimental data available* for the pure components in the form of both liquid density and vapor pressure as a function of temperature. While this is usually not a problem for commonly occurring substances, this data is lacking for ten of the twenty-seven malodorants considered in this study. Even when pure-component data is available, there is no guarantee that predictions of the behavior of *binary* systems will be adequate. Experimental data for binary systems is even scarcer. Experimental data exists for only one binary system studied here – *n*-butane – ethyl mercaptan, which enables an assessment of the performance of the two models.

COSMOtherm on the other hand requires no experimental data (pure or binary) and is based solely on the chemical structure of the molecules combined with a quantum chemical calculation. This calculation only needs to be performed once to give a so-called charge surface and charge profile for the molecule, after which thermodynamic calculations can be done quickly and in a straightforward manner. Since no experimental data is required, COSMOtherm will not predict pure-component vapor pressures as accurately as CPA *for substances for which experimental data exists*, since the CPA parameters are fitted to the

experimental data. In general, however the uncertainty of prediction of pure-component vapor pressures was deemed to be acceptable, and in particular, COSMOtherm performed very well for the only binary system for which experimental data were available.

2 Background

Liquefied petroleum gas is used in cigarette lighter refills, small blow torches and camping gas stoves. The liquefied petroleum gas usually consists of butane, isobutane and propane in various proportions. Products other than cigarette lighter refills contain up to 40 % of unsaturated hydrocarbons. Butane is odorless and heavier than air, with a flash point of -40^{o}C and flammability limit of between 1.8 and 8.4% volume. *n*-butane, iso-butane and propane vaporize at ordinary temperature and atmospheric pressure, the boiling points of these are -0.5, -11.7 and -42.1 ^{o}C respectively.

Volatile substances are generally separated into four groups, namely volatile solvents, aerosols, gases and nitrites. Volatile solvents are liquids or semi solids which vaporize at room temperature. These products include paints, paint thinners and strippers, dry cleaning fluids, nail polish remover. Aerosols contain propellants and solvents. These include spray paints, hair sprays and vegetable oil sprays. The aerosols contain substances such as butane, toluene, propane and acetate. Volatile substances classified as “gases” include gas lighters, fire extinguishers, fuel gas, and anesthetic gases. These products contain butane, isopropane and nitrous oxide.

These products are often available in inexpensive packs and are thus attractive to misusers. Butane is most usually inhaled directly into the mouth from cigarette lighter refill cans. Cigarette lighter refills are misused by clenching the nozzle between teeth and pressing to release the gas. If the can is tilted then a jet of fluid cooled to at least -60 ^{o}C by expansion may be inhaled directly and there is also a risk of fire and explosion associated with the misuse of cigarette lighter refills. Butane gas affects the body about 5 minutes after inhalation and its effect lasts for 15-45 minutes. After this, the inhaler may feel nausea up to 9 to 12 hours. At the early stage of inhalation, the inhaler feels euphoria, a floating sensation, dizziness, slurred speech, sense of heightened power and hallucination. These symptoms may result in impulsive actions such as attacking other people [5].

In the United Kingdom 605 people under the ago of 18 have died from volatile substance abuse in the period 1981-1990. Table 1 shows the deaths attributed to specific products in those under 18 from 1981-1990 in United Kingdom [6] and the largest number of deaths was attributed due to butane gas cigarette lighter fuel.

Table 1: Death attributed to specific volatile substances in those under 18 from 1981-1990

Product	***No of deaths***	***Frequency (%)***
Butane gas lighter fuel	207	34.5
Calor gas (Propane)	7	1.2
Butane gas cylinder	10	1.7
PR spray	26	4.3
Fire extinguisher	33	5.5
Antiperspirants	88	14.7
Other sprays	15	4.5
Unknown spray canister	15	2.5
Evostick	35	5.8
Other glues	22	3.7
Dry cleaning agents	1	0.2
Other cleaning agents	30	5.0
Typewriter correcting fluid	67	11.2
Chloroform	3	0.5
Petrol	13	2.2
Unknown glues	15	0.8
Other products	11	1.8
Total	600	100

3 Chemical ingredients in inhalants

Solvents and volatile products contain many different chemicals. Table 2 shows the active ingredients present in a sampling of products. These chemicals include both gases and liquids [13].

Table 2: Chemical ingredients in inhalants

Product	***Major volatile components***
Adhesives	
Airplane glue	Toluene, ethyl acetate
Rubber cement	Hexane, toluene, methyl chloride, acetone, methylethylketone, methylbutylketone
Aerosols	
Spray paint	Butane, fluorocarbons, toluene, hydrocarbons
Hair spray	Butane, fluorocarbons, propane
Air fresheners	Butane, fluorocarbons
Fabric protection spray	Butane, trichloroethane
Computer cleaner	Dimethylether, hydrofluorocarbons
Cleaning products	
Degreaser	Tetrachloroethylene, trichloroethane, methanol
Spot remover	Xylene, petroleum distillates, trichloroethane
Solvents	
Nail polish remover	Acetone, ethyl acetate, toluene
Paint thinner	Toluene, methylene chloride, methanol, acetone
Correction fluid	Toluene, trichloroethylene, trichloroethane
Toluene	Methylbenzene
Lighter fluid	Butane, isopropane
Food products	
whippets	Nitrous oxide
Canned whipped cream	Nitrous oxide

4 Effects of butane volatile substance abuse

Volatile substances such as butane gas produce can be inhaled to induce a psychoactive, or mind altering effect [9]. Butane vapors displace oxygen and can result in loss of consciousness and directly damage lung tissue. The vapors are easily absorbed through the lungs and carried to the brain where they act to depress the central nervous systems [9].

4.1 Short term effect

The short term effects are most rapid and relatively brief in duration. Immediate effects may last only a minute or several minutes. These rapid effects are due to high lipid solubility which allows for rapid absorption from the lungs to blood stream. Hydrocarbons present in volatile substances are easily absorbed into fatty tissues in the brain where they act as depressants [10]. Intensive use of inhalants may result in irregular heart rhythms and sudden death. The sudden sniffing death is particularly related to inhalation of butane and propane fuels. Other inhalants, such as aerosols have been reported to induce sudden and fatal cardiac arrest, even in first time use. Recently, several deaths are associated with type correction fluid and lighter fluid [8]. Table 3 represents a range of possible consequences that may result from short term and long term chemical exposure [10].

4.2 Long term effect

A long term effect may present itself after prolonged exposure. These effects depend on the amount which is inhaled over a period of time. Long term use is linked with muscle weakness, reduced bone density, leukemia and other cancer [9]. Long term chemical exposure can cause damage to the liver, heart and lungs. A long term consequence of inhalant use depends on four factors: the user, the substance used, the context of use and culture of use. Long term solvent abuse may lead to permanent neurological damage.

Table 3 : Possible consequences from butane inhalant substances [9]

Short term effect	*Long term effect*
Euphoria/Feeling of well being	Chronic headache
Loss of inhibition	Sinusitis
Drowsiness/sedation	Tinnitus
Slurred speech/incoherence	Diminished cognitive function
Weakness	Nosebleeds
Nausea	Extreme tiredness
Vomiting	Red, watery eyes
Headaches	Shortness of breath
Loss of short term memory	Indigestion
Aggression	Dizziness
Hallucinations	Stomach ulcers
Uncoordinated movements	Chest pain or angina

5 Preventing volatile substance abuse

The following modifications have been proposed to prevent volatile substance abuse [10].

- Replacement of harmful or psycho- active components;
- Additions of deterrent chemicals such as odorants have been proposed to modify the butane gas in lighter refill cans. Research by the CSIRO in Australia concluded that adding mercaptans to butane gas at a level of 50 ppm would result in the product having unpleasant odor and emetic properties sufficient to deter misuse [1];
- Package modification;
- Modifying the butane cigarette lighter refill container, where the product is delivered from container to container (modification of nozzles of cans) ;
- Replacement of the abusable or toxic elements of the product with a non abusable alternative;
- Reformulation of products to remove or minimize abusable substances;
- Adding substances such as bittering agents (e.g. Bitrex) to make the product less appealing to inhalers;
- Ban on abusable chemicals (from legitimate products).

The purpose of this work is to consider a number of possible deterrent additives, and specifically whether it is possible to add these to lighter gas, from a physicochemical perspective.

6 The basic idea and its approach

The main objective of this work is to investigate compounds which are suitable for modifying the cigarette lighter fuel without affecting its performance. Compounds (malodorants) are selected based on physical and chemical properties such as compounds which are irritants, have an unpleasant odor or are bittering. The main volatile constituents of cigarette lighter and butane fuel gases are *n*-butane and isobutane. Butane is a straight chain aliphatic hydrocarbon gas at room temperature. The addition of mercaptans to butane gas has been shown not to affect the short term performance of butane-burning devices such as cigarette lighters but further research is required to assess the long term effect [1]. The focus of this work is on compounds *other* than those based on sulfur (such as hydrogen sulfide and mercaptans). However, a single comparison has been made for the system butane-ethyl mercaptan, since some binary experimental data is available for this system. This has enabled the theoretical approach used here to be verified.

The physical properties of malodorants and their mixtures have been calculated using the CPA equation of state and the COSMOtherm program. If experimental data for the pure compounds is available (they are available for 17 out of 27 compounds), pure component parameters can be found for the CPA equation of state by fitting the model to the experimental data. The behaviour of the binary system (butane-malodorant) can then be predicted. The COSMOtherm program can compute the physical properties of pure compounds and mixtures, without the need for experimental data. The results from the CPA model and the COSMOtherm program can then be compared with each other and with available experimental data (if available). Since there is only data for one binary system (butane – ethyl mercaptan) it is difficult to comment on which model is preferable. However, COSMOtherm performed very well for this system and our feeling is that the predictions of binary phase behaviour are reliable in nearly all cases studied here. CPA is probably as reliable, but can only be used if experimental data is available for the pure compounds.

COSMOtherm is a program that computes thermophysical data of fluids. This program is based on the COSMO-RS theory and the computational procedure is takes place in three steps. First, a molecule is “built” and a quantum chemistry calculation is performed in order to calculate a sigma potential and a sigma profile by COSMO-RS. This calculation is time-

consuming but is performed only once for each compound and the profiles are then stored in a database. In fact the sigma profiles for most of the malodorants considered here had already been calculated and were already available in the program's extensive database.

Vapor pressures and vapor liquid equilibrium calculations can then be performed for the pure compounds and for mixtures. These calculations are relatively quick. Section 7.5 discusses the sigma profiles and surfaces in detail.

7 Theory and modeling

7.1 CPA (Cubic-plus-Association) Equation of State

The CPA equation of state was developed by Kontogeorgis et al. [20,21]. This equation has been applied to systems containing mainly hydrocarbons with associating compounds. An associating compound is one which exhibits hydrogen bonding (such as water, alcohols and amines). This equation combines a so-called "physical" interaction with an association term which accounts for hydrogen bonding. The physical interactions are accounted for using the SRK (Soave-Redlich-Kwong) equation of state. This equation of state (SRK) is very widely used in the oil and gas industry and CPA was developed with this industry in mind – rather than develop a completely new equation of state, a term was simply added to the SRK equation to account for water, alcohols, etc. for which SRK was not performing adequately. In the absence of hydrogen bonding, CPA simply reduced to SRK. The result has been that CPA has been adopted by the oil industry (traditionally a rather conservative industry) because it can be readily integrated into existing software. A detailed description of the CPA equation of state can be found in Kontogeorgis et al [20, 21].

Without going into detail here, it is useful to know that the CPA equation of state requires five parameters to describe a single pure associating compound - three for the physical part, and two for the association part – an association energy (ε^{AB}) and an association volume $\left(\beta^{AB}\right)$. For a non-associating compound, such as butane, only three parameters are required. These parameters are determined by fitting to experimental data (saturated vapor pressures and liquid density) for the pure compound. An extensive collection of this data exists for many pure compounds (for example 17 of the 27 considered here). This compilation has been performed by the Design Institute for Physical Properties (DIPPR).

7.2 The COSMO-based thermodynamic model:

The COSMO model has been covered extensively in the literature [14, 18, 19], so only a comparatively short discussion is given here. The basis of COSMO-based model is the "solvent-accessible surface" of a solute molecule. These COSMO-based models generate a surface charge distribution. Figure 1 shows the ideal solvation process in the COSMO-based models [18].

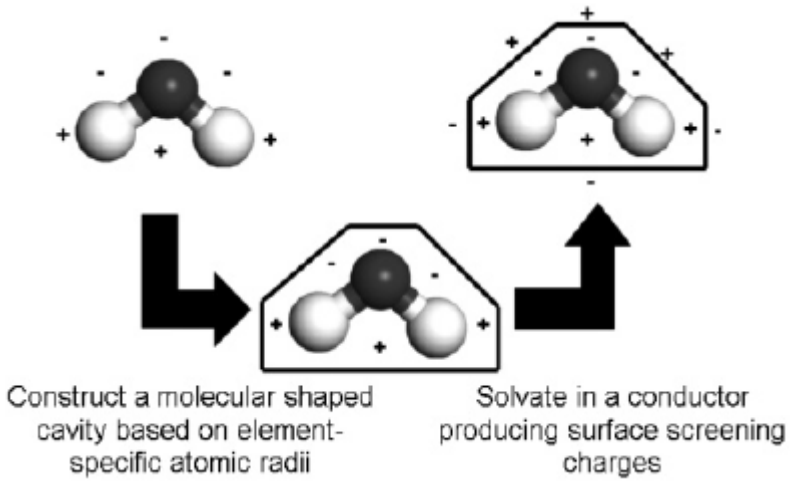

Figure 1: Ideal solvation process in COSMO-based models [18]

COSMO-based models construct a molecular-shaped cavity within a perfect conductor according to a specific set of rules and atom-specific dimensions. Then the molecule's dipole and higher moments draw charges from surrounding medium to the surface of the cavity to cancel the electric field both inside the conductor and tangential to the surface.

The induced surface charges on the solute surface in discretized space is given by the following equation(0)

$$\Phi_{tot} = \Phi_i + \Phi(q^*) = \Phi_i + Aq^* = 0 \qquad (7.1)$$

Φ_{tot} is the total potential on the cavity surface, Φ_i is the potential due to the charge distribution of solute molecule i, $\Phi(q^*)$ is the product of ideal screening charge q^* and coulomb interaction matrix A. This coulomb interaction matrix describes the potential interactions between surface charges and is a function of cavity geometry [18].

For the calculation of sigma profiles, a construction of the molecular–shaped cavity in the solvent continuum is required and surface segments need to be distributed over the cavity surface. The charge density distribution (σ profile, $p_i(\sigma)$) is calculated from the averaged surface charge densities. The charge distribution is represented as probability distribution of a molecular surface segment having a specific charge density. This probability distribution is called the sigma profile ($p_i(\sigma)$). The sigma profile for a molecule i is defined as

$$p_i(\sigma) = \frac{n_i(\sigma)}{n_i} = \frac{A_i(\sigma)}{A_i} \tag{7.2}$$

where $n_i(\sigma)$ is the number of segments with charge density σ in a single molecule i and $A_i(\sigma)$ is the total surface area from all these segments.

The probability of finding a segment with charge density σ in a mixture is the weighted sum of the σ profiles of all the components

$$p_s(\sigma) = \frac{\sum_i x_i n_i p_i(\sigma)}{\sum_i x_i n_i} = \frac{\sum_i x_i A_i p_i(\sigma)}{\sum_i x_i A_i} \tag{7.3}$$

The σ profile which is $p_i(\sigma)$ as a function of σ, quantifies the electronic properties of a fluid and is the most important characteristic of each species in the COSMO-RS model. The effective surface charge density can be calculated by using the following equation.

$$\sigma_m = \frac{\sum_n \sigma_n^* \frac{r_n^2 r_{av}^2}{r_n^2 + r_{av}^2} \exp\left(-\frac{d_{mn}^2}{r_n^2 + r_{av}^2}\right)}{\frac{r_n^2 r_{av}^2}{r_n^2 + r_{av}^2} \exp\left(-\frac{d_{mn}^2}{r_n^2 + r_{av}^2}\right)} \tag{7.4}$$

where σ_m is surface-charge density on segment m, r_n is the radius of the actual surface segment (assuming circular segments), r_{av} is the averaging radius (adjustable parameter), and d_{mn} is the distance between the two segments. The paired segments m and n have segment charge densities σ_m and σ_n respectively [16]. Sigma profiles and sigma surfaces are readily visualized – see section 7.5.

COSMO-RS theory

COSMO-RS is a theory of interacting molecular surfaces as computed by quantum chemical methods (QM). Quantum chemical methods originally developed for isolated molecules i.e. for molecules in vacuum or in gas phase. The COSMO-RS is basis of COSMO (conductor-like screening model), which belongs to the class of QM continuum solvation models (CSMs). These CSMs are an extension of the basic QM methods towards the description of liquid phases. CSMs are describes the molecule in solution through a quantum chemical calculation of solute molecule with surrounding solvent as a continuum [14].

COSMO theory of real solvents integrates concepts from quantum chemistry, dielectric continuum models, electrostatic surface interactions and statistical thermodynamics. Basically QM-COSMO calculations provide a discrete surface around a molecule embedded in a virtual conductor. Figure 2 shows that each segment i is characterized by its area a_i on the surface and the screening charge density σ_i on this segment. A liquid is now considered to be an ensemble of closely packed ideally screened molecules as shown in Figure 2. The system has to be compressed in order to get close packing and the molecules are slightly deformed from their original positions.

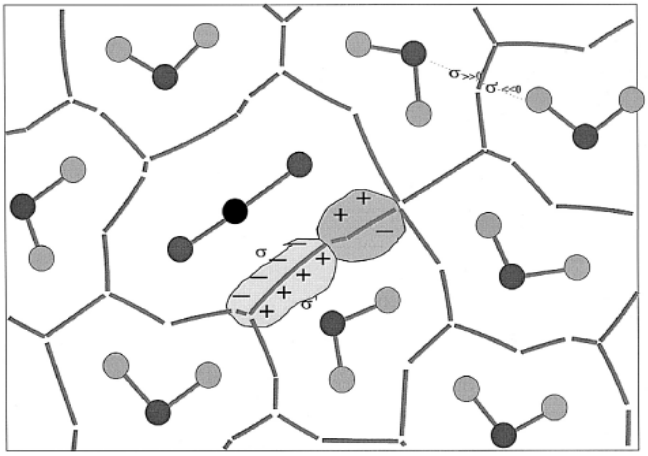

Figure 2: Schematic illustration of contacting molecular cavities and contact interactions [14].

Each piece of molecular surface is in close contact with another one. Assuming that each molecule is enclosed by virtual conductor and then the electrostatic interaction arises from the contact of two different screening charge densities (SCDs). The energy difference between the real situation of such contact and ideally screened situation is defined as a local interaction energy, which results from the contact of molecules. The difference between the

screening charge densities σ and σ' of a contact pair is a measure of the misfit of the SCD on both segments in the real system, compare to the situation inside the ideal conductor.

$$E_{misfit}(\sigma,\sigma') = a_{eff}\frac{\alpha'}{2}(\sigma+\sigma')^2 \tag{7.5}$$

where a_{eff} is the effective contact area between two surface segments and α' is an energy factor.

Hydrogen bonding can also described between two adjacent SCDs. Hydrogen bonding donors having a strongly negative SCD and acceptors have strongly positive SCDs. If two polar pieces of surface with opposite polarity are in contact with each other then hydrogen bonding occurs. This interaction energy is expressed as

$$E_{HB} = a_{eff}c_{HB}\min(0;\min(0;\sigma_{donor}+\sigma_{HB})\max(0;\sigma_{donor}-\sigma_{HB})) \tag{7.6}$$

where c_{HB} and σ_{HB} are adjustable parameters. COSMO-RS can also counts the van der Waals interaction between segments by the following expression

$$E_{vdW} = a_{eff}(\tau_{vdW}+\tau'_{vdW}) \tag{7.7}$$

where τ_{vdW} and τ'_{vdW} are element specific adjustable parameters. The van der Waals energy depends only on the element type of the atoms that are involved in surface contact. Statistical thermodynamics provides the link between microscopic surface interaction energies and macroscopic thermodynamic properties of a liquid. Since in COSMO-RS all molecular interactions consist of local pair-wise interactions of surface segments, the statistical averaging can be done in the ensemble of interacting surface pieces. The composition of the surface segment ensemble with respect to the interaction can be described by sigma profiles. The sigma profile of the whole system/mixture is just the sum of the σ-profiles of the components X_i weighted with their mole fraction in the mixture x_i

$$p_s(\sigma) = \sum_{i\in S} x_i p^{x_i}(\sigma) \tag{7.8}$$

The chemical potential of a surface segment with SCD σ in an ensemble described by normalized distribution function $p_s(\sigma)$ is given by

$$\mu_s(\sigma) = -\frac{RT}{a_{eff}}\ln\left[\int p_s(\sigma')\exp\left(\frac{a_{eff}}{RT}\left(\mu_s(\sigma')-E_{misfit}(\sigma,\sigma')-E_{HB}(\sigma,\sigma')\right)\right)d\sigma'\right] \tag{7.9}$$

$\mu_s(\sigma)$ is a measure of the affinity of the system S to a surface of polarity σ. It is a characteristic function of each system and is called "σ potential". The COSMO-RS representation of molecular interactions is namely the σ profiles and σ potentials of compounds and mixtures.

COSMO-RS is also able to provide a reasonable estimate of a pure compounds chemical potential in the gas phase

$$\mu_{Gas}^{X_i} = E_{Gas}^{X_i} - E_{COSMO}^{X_i} - E_{vdW}^{X_i} + \omega_{Ring} n_{Ring}^{X_i} + \eta_{Gas} RT \tag{7.10}$$

where $E_{Gas}^{X_i}$ and $E_{COSMO}^{X_i}$ are the quantum chemical total energies of the molecule in the gas phase and in the COSMO conductor respectively. $E_{vdW}^{X_i}$ is the van der Waals energy of X_i. The remaining contributions consist of a correction term for ring shaped molecule with $n_{Ring}^{X_i}$ being the number of ring atoms in the molecule. ω_{Ring} is an adjustable parameter and the parameter η_{Gas} provides the link between the reference states of the system's free energy in the gas phase and in the liquid [14].

Once the chemical potential of pure compound has been computed in solution and in the ideal gas phase, the vapor pressure of the pure compound can be calculated as:

$$P_{vap}^{X_i}(T) = \exp\left(\frac{\mu_{X_i}^{X_i} - \mu_{Gas}^{X_i}}{kT}\right) \tag{7.11}$$

Where $P_{vap}^{X_i}$ is the vapor pressure of pure compound X_i, k is the Boltzmann constant, T is the temperature and $\mu_{X_i}^{X_i}$ is the pseudo-chemical potential of pure compound X_i in a liquid X_i.

After the vapor pressure of the pure compound has been calculated, COSMO-RS can predict vapor liquid equilibrium in mixtures using the standard thermodynamic relation:.

$$\gamma_S^{Xi} = \exp\left(\frac{\mu_S^{X_i} - \mu_{X_i}^{X_i}}{RT}\right) \tag{7.12}$$

$$p^{total} = \sum_i p_{vap}^{X_i} x_i \gamma_S^{X_i} \tag{7.13}$$

$$y_i = \frac{p_{vap}^{X_i} x_i \gamma_S^{X_i}}{p^{tot}} \tag{7.14}$$

In equation (7.12) γ_S^{Xi} is the activity coefficient of pure compound X_i in solution which is considered the continuum medium according to COSMO model, p^{total} is the total vapor pressure of the mixture that is used to predict the vapor liquid equilibrium diagram, X_i is the mole fraction of compounds in the liquid phase and Y_i is the mole fraction of compounds in the gas phase. The vapor liquid equilibrium calculations in COSMO-RS are thus done based on vapor pressure and the activity coefficients of the compounds in solution.

7.3 Malodorants

These compounds were initially chosen based on their deterrent effect (mainly odor) and then checked for suitability with respect to their physical properties (phase behavior and solubility). The compounds selected for study are shown in Table 4.

Table 4: Malodorants

S.No	Malodorants	CAS-number	Chemical formula	Deterrent effect	DIPPR database
1.	Triethylamine	121-44-8	C6H15N	Strong fishy	Yes
2.	Denatonium benzoate	3734-33-6	C28H34N2O3	Bitter taste	No
3.	Isobutyraldehyde	78-84-2	C4H8O	Extremely unpleasant	Yes
4.	Tetrahydrothiophene	110-01-0	C4H8S	Strong unpleasant odor	Yes
5.	Dimethylsulfide	75-18-3	C2H6S	Unpleasant odor	Yes
6.	2,2,4 Trimethylpentane	540-84-1	C8H18	Gasoline/Petrol	Yes
7.	Picoline(2-Methylpyridine)	109-06-8	C6H7N	Unpleasant (strong) odor	Yes
8.	Eucalyptol (1,8 Cineole)	470-82-6	C10H180	Strong aromatic and spicy	No
9.	Nitrobenzene	98-95-3	C6H5NO2	bitter (Almond-like odor)	Yes
10.	1-Pentanol	71-41-0	C5H12O	Characteristic odor, stench	Yes
11.	Sulfurylchloride	7791-25-5	SO2Cl2	Bitter, Pungent odor, irritating	Yes
12.	Cyanogenchloride	506-77-4	CClN	Bitter, Pungent odor, irritating	Yes
13.	Bis-(2-chloroethyl)sulfide	505-60-2	C4H8Cl2S	Garlic or Horse radish	No
14.	Bis-(2-chloroethyl)ethylamine	538-07-8	C6H13Cl2N	Faint, Fishy, or musty	No
15.	Ethyldichloroarsine	598-14-1	C2H5AsCl2	Fruity but biting and irritating	No
16.	Bromobenzylcyanide	16532-79-9	C8H6BrN	Soured or rotting fruit	No
17.	Chloropicrin	76-06-2	CCl3NO2	Stinging, pungent odor	No
18.	Diphenylcyanoarsine	23525-22-6	C13H10AsN	Garlic and bitter almonds	No
19.	Ethylmercaptan	75-08-1	C2H6S	Garlic odor	Yes
20.	Bis(chloromethyl)ether	542-88-1	C2CH4Cl2O	Strong unpleasant odor	Yes
21.	2-Aminophenol	95-55-6	C8H7NO	Phenol-like (strong irritating)	No
22.	Propyleneglycol	57-55-6	C3H8O2	Mild odor	Yes
23.	s-Trioxane	110-88-3	C3H6O3	Irritating odor	Yes
24.	2-Chloroacetophenone	532-27-4	C8H7ClO	Eye, throat, skin irritant	No
25.	Indole	120-72-9	C8H7N	Unpleasant (strong)	Yes
26.	Pyridine	110-86-1	C5H5N	Characteristic fish like smell	Yes

27.	Butylamine	109-73-9	C4H11N	Characteristic fish like smell	Yes

A brief discussion of each component follows in sections 7.3.1 – 7.3.27.

7.3.1 Triethylamine

Triethylamine occurs as a colorless flammable liquid and it is soluble in water and other organic solvents. It has been selected based on its strong fishy ammonia-like odor. The properties of triethylamine are shown in Table 5.

Molecular Structure:

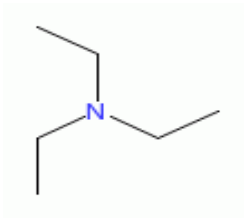

Table 5: Properties of Triethylamine

Triethylamine	Odor	Strong fishy
	Molecular Weight	101.19 kg/kmol
	Critical Temperature	535.15 K
	Critical Pressure	30.4 bar
	Critical Volume	0.39 m³/kmol
	Melting Point	158.45 K
	Normal Boiling Point	361.92 K
	Liquid Molar Volume	0.139672 m³/kmol

7.3.2 Denatonium Benzoate (Bitrex)

Denatonium Benzoate has an extremely bitter taste. It is easily soluble in water, alcohol and other solvents. Bitrex is not a very toxic substance and has been added to a wide range of chemicals to deter ingestion. Addition of Bitrex to alcohol makes it unfit for consumption. It is also added to all kinds of harmful liquids including solvents, paints, varnishes, toiletries and other household products. The physical and chemical properties are shown in Table 6.

Molecular Structure:

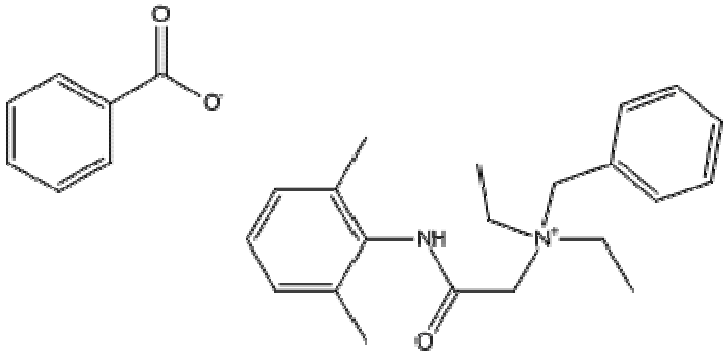

Table 6: Properties of Denatonium benzoate (Bitrex)

Denatonium benzoate	Odor	Bitter taste
	Molecular Weight	446.581 kg/kmol
	Freezing/Melting Point	163-170 ^{o}C

It is considered that this comparatively large molecule would not be a suitable deterrent additive to butane because of its low vapor pressure. However it is included here for completeness since it is one of the few examples of deterrents which is actually added to commercial products.

7.3.3 Isobutyraldehyde

Isobutyraldehyde (isobutanal) is a liquid at ambient temperatures and is soluble in water. It is considered a highly flammable liquid which can easily be ignited by heat, spark or flame. Isobutanal is selected based on its unpleasant smell. The physical and chemical properties are shown in Table 7.

Molecular Structure:

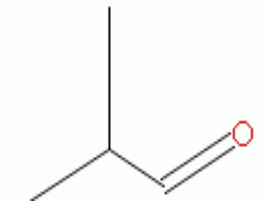

Table 7: Properties of Isobutyraldehyde

Isobutyraldehyde	Odor	Extremely unpleasant smell
	Molecular Weight	72.10572 kg/kmol
	Critical Temperature	507 K
	Critical Pressure	41.0 bar
	Critical Volume	0.263 m³/kmol
	Freezing/Melting Point	208.15 K
	Normal Boiling Point	337.25 K
	Liquid Molar Volume	0.0920264 m³/kmol

7.3.4 Tetrahydrothiophene

Tetrahydrothiophene (thiolane) is a heterocyclic organic compound. It consists of a five-membered ring containing four carbon atoms and one sulfur atom. It has a strong unpleasant

odor and is used as an odorant in natural gas. Thiolane is easily soluble in water but is insoluble in other solvents such as ether and ethanol.

Molecular Structure:

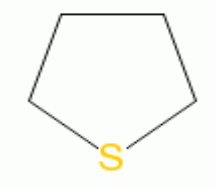

Table 8: Properties of Tetrahydrothiophene

Tetrahydrothiophene	Odor	Strong unpleasant odor
	Molecular Weight	88.17132 kg/kmol
	Critical Temperature	631.95 K
	Critical Pressure	51.6 bar
	Critical Volume	0.249 m³/kmol
	Melting Point	176.99 K
	Normal Boiling Point	394.267 K
	Liquid Molar Volume	0.0887032 m³/kmol

7.3.5 Dimethylsulfide

Dimethyl sulfide is a low molecular weight organosulfur compound with a garlic-like odor. It is stable and incompatible with strong oxidizing agents. This compound is slightly soluble in water. It is used as a flavor in other products. The physical and chemical properties are shown in Table 9.

Molecular Structure:

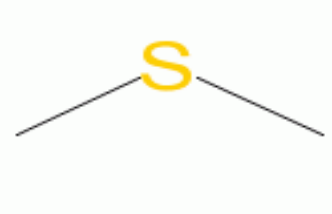

Table 9: Properties of Dimethylsulfide

Dimethylsulfide	Odor	Garlic like odor
	Molecular Weight	62.13404 kg/kmol
	Critical Temperature	503.04 K
	Critical Pressure	55.3 bar
	Critical Volume	0.201 m³/kmol

	Melting Point	174.88 K
	Normal Boiling Point	310.48 K
	Liquid Molar Volume	0.0737373 m³/kmol

7.3.6 2, 2, 4-Trimethyl pentane

Isooctane is clear, colorless liquid which smells like gasoline. It is used as a solvent and to determine the octane number of fuels.

Molecular Structure:

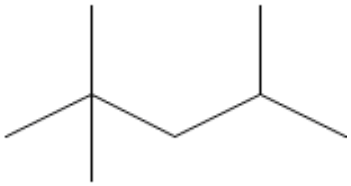

Table 10: Properties of 2. 2. 4-Trimethyl pentane

2,2,4 Trimethylpentane	Odor	Gasoline smell
	Molecular Weight	114.22852 kg/kmol
	Critical Temperature	543.8 K
	Critical Pressure	25.7 bar
	Critical Volume	0.468 m³/kmol
	Freezing/Melting Point	165.777 K
	Normal Boiling Point	372.388 K
	Liquid Molar Volume	0.165478 m³/kmol

7.3.7 Picoline (2-methyl pyridine)

Picoline is a colorless liquid at room temperature and pressure. It is obtained from coal tar and has a putrid fish-like odor. Picoline is useful as a solvent and as a raw material for various chemical products used in polymers, textiles, fuels and pharmaceuticals. The properties are shown in Table 10.

Molecular Structure:

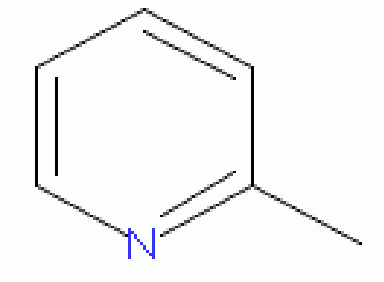

Table 11: Properties of Picoline

2-Methylpyridine (Picoline)	Odor	Unpleasant (Strong)
	Molecular Weight	93.12648 kg/kmol
	Critical Temperature	621 K
	Critical Pressure	46.0 bar
	Critical Volume	0.335 m³/kmol
	Melting Point	206.44 K
	Normal Boiling Point	402.55 K
	Liquid Molar Volume	0.0990828 m³/kmol

7.3.8 Eucalyptol (1.8 Cineole)

Eucalyptol is obtained from oil of eucalyptus and it is natural organic compound. It is a colorless liquid and having strong aromatic odor. It is used in flavoring, fragrances and cosmetics. It is also ingredient in many brands of mouthwash and cough suppressant. The properties are shown in Table 12.

Molecular Structure:

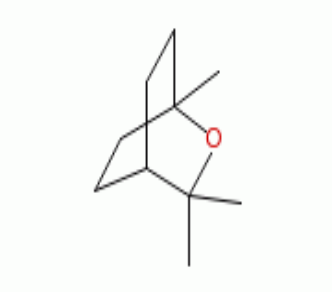

Table 12: Properties of Eucalyptol

Eucalyptol (1, 8 Cineole)	Odor	Strong aromatic odor and spicy
	Molecular Weight	154.249
	Freezing/Melting Point	1.5 ^{o}C
	Normal Boiling Point	176-177 ^{o}C

7.3.9 Nitrobenzene

Nitrobenzene is an aromatic nitro compound with an odor resembling that of bitter almonds. It is colorless to pale yellow, oily liquid or as greenish yellow crystals. Mostly nitrobenzene is used in the manufacturing of aniline. Nitrobenzene is used in pesticides, rubber chemicals,

pharmaceuticals and dyes. It is also used as solvent in petroleum refining and synthesis of other organic compounds. The properties are shown in Table 13.

Molecular Structure:

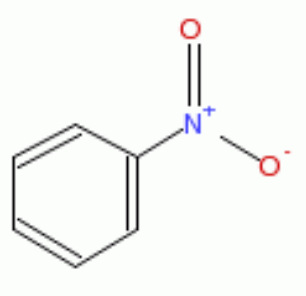

Table 13: Properties of Nitrobenzene

Nitrobenzene	Odor	Strong bitter (Almond-like odor)
	Molecular Weight	123.11 kg/kmol
	Critical Temperature	719.00 K
	Critical Pressure	44.0 bar
	Critical Volume	0.35 m³/kmol
	Melting Point	278.91 K
	Normal Boiling Point	483.95 K
	Liquid Molar Volume	0.10 m³/kmol

7.3.10 1-Pentanol

1-Pentanol is clear, colorless liquid with characteristic choking odor. It is obtained by the fermentation of starches and from the distillation of petroleum. The physical and chemical properties are shown in Table 14.

Molecular Structure:

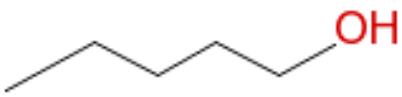

Table 14: Properties of 1-Pentanol

1-Pentanol	Odor	Characteristic odor. stench
	Molecular Weight	88.1482 kg/kmol
	Critical Temperature	588.1 K
	Critical Pressure	38.97 bar
	Critical Volume	0.326 m³/kmol
	Melting Point	195.56 K
	Normal Boiling Point	410.9 K

	Liquid Molar Volume	0.10854 m³/kmol

7.3.11 Sulfuryl chloride

Sulfuryl chloride is colorless liquid and having a pungent odor. It is used as chlorinating and dehydrating agent and boils at 69 ^{o}C. It is decomposed by hot water and alkaline substances. It is soluble in most organic solvents like benzene, chloroform, carbon tetrachloride and acetic acid. The chemical and physical properties are shown in Table 15.

Molecular Structure:

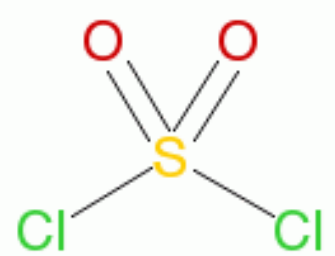

Table 15: Properties of sulfuryl chloride

Sulfurylchloride	Odor	Bitter, Pungent odor, irritating
	Molecular Weight	134.9698 kg/kmol
	Critical Temperature	545 K
	Critical Pressure	46.1 bar
	Critical Volume	0.234 m³/kmol
	Melting Point	219 K
	Normal Boiling Point	342.55 K

7.3.12 Cyanogen chloride

Cyanogen chloride is a colorless, highly volatile liquid with a pungent, biting odor. This compound is selected because of its tearing and irritating properties. Normally cyanogen chloride is non-persistent and is used as a quick-acting casualty agent.

Molecular Structure:

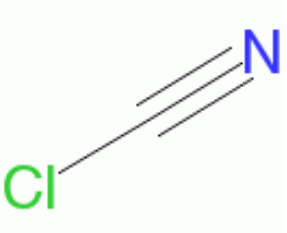

Table 16: Properties of cyanogen chloride

Cyanogenchloride	Odor	Pungent, biting and irritating
	Molecular Weight	61.4704 kg/kmol
	Critical Temperature	449 K
	Critical Pressure	59.9 bar
	Critical Volume	0.163 m³/kmol
	Melting Point	266.65 K
	Normal Boiling Point	286 K
	Liquid Molar Volume	0.0524536 m³/kmol

7.3.13 Bis-(2-chloroethyl) sulfide

Bis-(2-chloroethyl) sulfide is a colorless to amber-colored liquid with garlic like odor and it is more stable in storage. This compound is lighter than water and small droplets will float on water surfaces and present a hazard. It was selected because of its garlic like odor. The effects from this compound are vomiting, fever and skin reddening. The physical and chemical properties are shown in Table 17.

Molecular Structure:

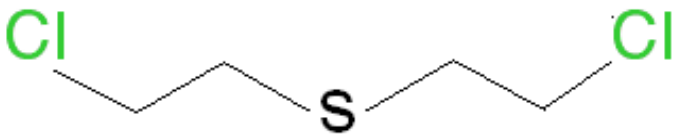

Table 17: Properties of Bis-(2-chloroethyl) sulfide

Bis-(2-chloroethyl) sulfide	Odor	Garlic or horse radish
	Molecular Weight	159.08
	Freezing/Melting Point	14.45 ^{o}C
	Normal Boiling Point	227.8 ^{o}C

7.3.14 Bis-(2-chloroethyl) ethylamine

Bis-(2-chloroethyl) ethylamine is more volatile, colorless liquid with a fishy or musty odor. It was selected because of its fishy odor and it is easily soluble in organic solvents. Severe vapor exposure will result in redness of the skin, causing irritation and itching.

Molecular Structure:

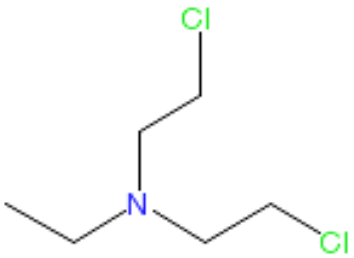

Table 18: Properties of Bis-(2-chloroethyl) ethylamine

Bis-(2-chloroethyl) ethylamine	Odor	Faint, fishy, or musty
	Molecular Weight	170.08
	Freezing/Melting Point	-34 ^{o}C
	Normal Boiling Point	194 ^{o}C

It is considered that this comparatively large molecule with a high boiling point would not be a suitable deterrent additive to butane.

7.3.15 Ethyldichloroarsine

Table 19 shows the physical and chemical properties of ethyldichloroarsine and it is a liquid with a fruity but biting and irritating odor. It is selected due to its biting and irritating odor. It is easily soluble in alcohol and acetone. Arsine-containing agents irritate the eyes and the liquid may produce severe eye injury.

Molecular Structure:

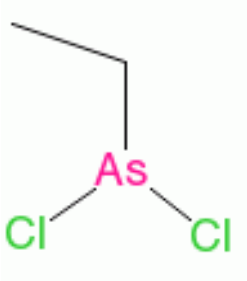

Table 19: Properties of Ethyl dichloroarsine

Ethyldichloroarsine	Odor	Fruity but biting and irritating
	Molecular Weight	174.88 kg/kmol
	Melting Point	Less than -65 ^{o}C
	Normal Boiling Point	156 ^{o}C

7.3.16 Bromobenzylcyanide

Bromobenzylcyanide was the first tearing agent used and it produces irritation and tearing of the eyes with pain in the forehead. It is mainly considered based on the fact that it is an irritant. The physical and chemical properties are shown in Table 20.

Molecular Structure:

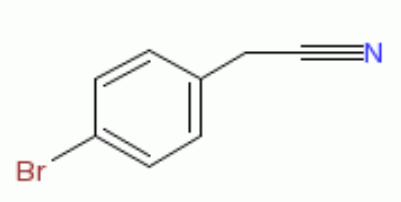

Table 20: Properties of Bromobenzylvyanide

Ethyldichloroarsine	Odor	Soured or rotting fruit. Irritant, tearing agent
	Molecular Weight	196 kg/kmol
	Melting Point	25.5 ^{o}C
	Normal Boiling Point	242 ^{o}C

7.3.17 Chloropicrin

Chloropicrin is a pungent. Colorless, oily liquid and it was shown in Table 21. It is very volatile and a powerful irritant. The vapors cause irritation, coughing and vomiting. It is considered based on odor and its solubility in organic solvents.

Molecular Structure:

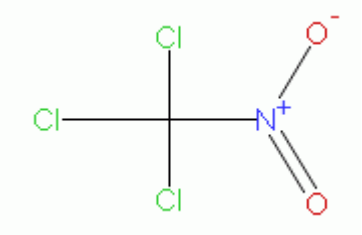

Table 21: Properties of Trichloronitromethane

Chloropicrin	Odor	Stinging. Pungent odor
	Molecular Weight	164.375 kg/kmol
	Freezing/Melting Point	-69 ^{o}C
	Normal Boiling Point	112 ^{o}C

7.3.18 Diphenylcyanoarsine

The properties of diphenylcyanoarsine are shown in Table 22. This compound produces strong irritation, vomiting and it is selected based on its odor of garlic and bitter almonds.

Molecular Structure:

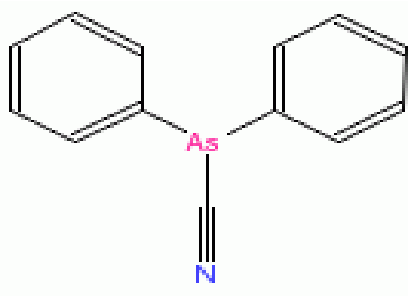

Table 22: Properties of Diphenylcyanoarsine

Diphenylcyanoarsine	Odor	Garlic and bitter almonds
	Molecular Weight	255.147 kg/kmol
	Freezing/Melting Point	-31.5 ^{o}C
	Normal Boiling Point	350 ^{o}C

7.3.19 Ethyl mercaptan

Ethyl mercaptan is a colorless liquid and it has a strong garlic odor. Mercaptans are added to fuel at the refinery and local distribution centers. Addition of mercaptans to petrol increases sulfur levels. It is included here partly because some experimental data for the binary system ethyl mercaptan – butane exists.

Molecular Structure:

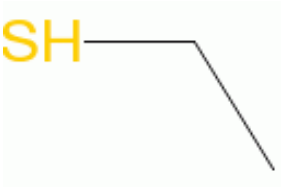

Table 23: Properties of Ethylmercaptan

Ethylmercaptan	Odor	Garlic odor
	Molecular Weight	62.13404 kg/kmol
	Critical Temperature	499.15 K
	Critical Pressure	54.9 bar
	Critical Volume	0.207 m³/kmol
	Melting Point	125.26 K
	Normal Boiling Point	308.153 K
	Liquid Molar Volume	0.0746133 m³/kmol

7.3.20 Bis(chloromethyl)ether

Bis(chloromethyl)ether is a chemical with a strong unpleasant odor. It is clear liquid at room temperature, but readily evaporates into air. Table 24 shows the physical and chemical properties of Bis(chloromethyl)ether.

Molecular Structure:

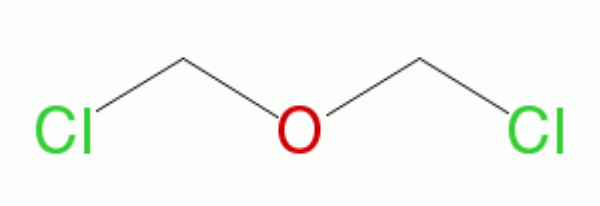

Table 24: Properties of Bis (chloromethyl) ether

Bis(chloromethyl)ether	Odor	Strong unpleasant odor
	Molecular Weight	114.95856 kg/kmol
	Critical Temperature	579 K
	Critical Pressure	45.8 bar
	Critical Volume	0.258 m³/kmol
	Melting Point	231.65 K
	Normal Boiling Point	378 K
	Liquid Molar Volume	0.0876502 m³/kmol

7.3.21 2-Amino phenol

2-Amino phenol is used as an intermediate for azo and sulfur dyes. It is off-white in color and has a strong irritating odor. This compound is selected based on odor and solubility properties. The physical and chemical properties are shown in Table 25.

Molecular Structure:

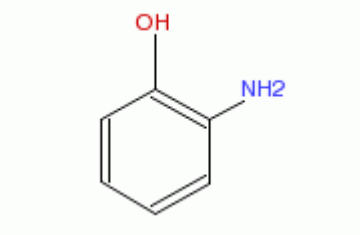

Table 25: Properties of 2-Aminophenol

2-Aminophenol	Odor	Phenol-like (strong irritating)
	Molecular Weight	109.13 kg/kmol
	Melting Point	172 ^{o}C
	Normal Boiling Point	164 ^{o}C

7.3.22 Propyleneglycol

Propyleneglycol is a colorless, viscous and hydroscopic liquid and it is used in anti freezing solutions, hydraulic fluids, and as a solvent. The physical and chemical properties are shown in Table 26.

Molecular Structure:

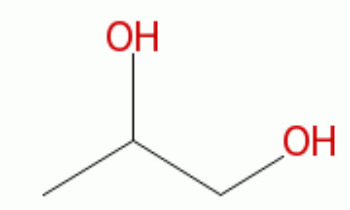

Table 26: Properties of Propylene glycol

Propyleneglycol	Odor	Mildodor
	Molecular Weight	76.09442 kg/kmol
	Critical Temperature	626 K
	Critical Pressure	61 bar
	Critical Volume	0.239 m³/kmol
	Melting Point	213.15 K
	Normal Boiling Point	460.75 K
	Liquid Molar Volume	0.0736939 m³/kmol

7.3.23 s-Trioxane

s-Trioxane is a stable cyclic trimer of formaldehyde with a chloroform odor. It is a colorless, crystalline solid. It is easily soluble in water at room temperature and the physical and chemical properties are shown in Table 27.

Molecular Structure:

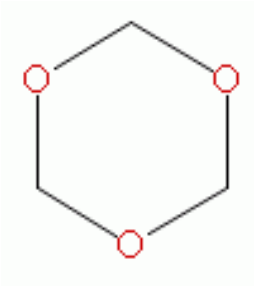

Table 27: Properties of s-Trioxane

s-Trioxane	Odor	Irritating odor
	Molecular Weight	90.07794 kg/kmol
	Critical Temperature	604 K
	Critical Pressure	58.2 bar
	Critical Volume	0.224 m³/kmol

	Melting Point	334.65 K
	Normal Boiling Point	387.65 K
	Liquid Molar Volume	0.0766816 m³/kmol

7.3.24 2-Chloroacetophenone

Chloroacetophenone has is easily soluble in organic solvents. In higher concentrations it causes a tingling sensation, irritation, burning and pain of the nose and throat. Is used in tear gas and chemical mace. The physical and chemical properties are shown in Table 28.

Molecular Structure:

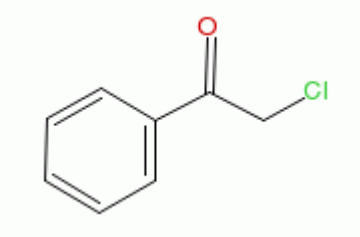

Table 28: Properties of Chloroacetophenone

Chloroacetophenone	Odor	Fragrant: similar to apple blossoms. Irritant to nose and throat
	Molecular Weight	154.59 kg/kmol
	Melting Point	54 °C
	Normal Boiling Point	248 °C

7.3.25 Indole

Indole is colorless and has an unpleasant odor. It occurs naturally in human feces and has an intense fecal odor. The physical and chemical properties are shown in Table 28.

Molecular Structure:

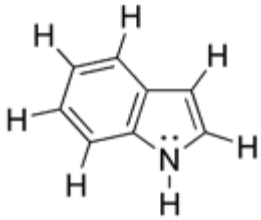

Table 29: Properties of Indole

Indole	Odor	Unpleasant (strong)
	Molecular Weight	117,14788 kg/kmol
	Critical Temperature	790 K
	Critical Pressure	43 bar
	Critical Volume	0,431 m³/kmol
	Melting Point	326,15 K

	Normal Boiling Point	526,15 K

7.3.26 Pyridine

Pyridine is a liquid with a fish-like odor. It is used as intermediate in making dyes, food flavorings, pharmaceuticals, rubber chemicals and adhesives. The physical and chemical properties are shown in Table 30.

Molecular Structure:

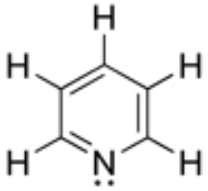

Table 30: Properties of Pyridine

Pyridine	Odor	Characteristic fish like smell
	Molecular Weight	79.0999 kg/kmol
	Critical Temperature	619.95 K
	Critical Pressure	56.3 bar
	Melting Point	231.53 K
	Normal Boiling Point	388.41 K

7.3.27 *n*-Butylamine

Butylamine is a liquid having a fishy, ammonia-like odor common to amines. It is used as an ingredient in the manufacture of pesticides, pharmaceuticals, and emulsifiers. The physical and chemical properties are shown in Table 31.

Molecular Structure:

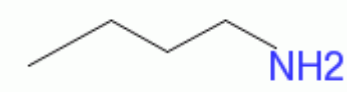

Table 31: Properties of butylamine

Butylamine	Odor	Characteristic fish like smell
	Molecular Weight	73.13684 kg/kmol
	Critical Temperature	531.9 K
	Critical Pressure	42 bar
	Melting Point	224.05 K
	Normal Boiling Point	350.55 K

7.4 Estimation of pure compound parameters (CPA equation of state)

The CPA equation of state has up to five adjustable pure compound parameters. The five parameters for pure associating compounds are, three for the physical part, a_0, C_1 and b; and two for the association part - association energy (ε^{AB}) and association volume $\left(\beta^{AB}\right)$.

These parameters are determined by regression of saturated vapor pressures and liquid density data over a wide temperature range, usually ranging from (close to) the triple point to (close to) critical point. The vapor pressure and liquid density of pure compounds are taken from the DIPPR database (which is a collection of experimental data). However, only 17 out of 27 malodorants are available in the DIPPR database. CPA parameters for these 17 compounds are shown in table 32. Of these, 9 are considered to be associating. Most associating compounds are considered to have two association sites (known as the 2B scheme) but some, such as water are considered to have 4 associating sites. Of the substances considered in this study, only propylene glycol has 4 associating sites

Table 32: CPA Parameters for the compounds involved in this study

Compound	CPA Parameters					RMSPE		
	a_0 [bar cm^{6}mol^{-2}]	b [cm^{3}mol^{-1}]	c_1	ε^{AB} [bar cm^{3}mol^{-1}]	β^{AB} *1000	ERR. P	ERR. D	Association Scheme
Triethylamine	19502531	115.95	0.78212	131495.6	77.2426	0.0018	0.0059	2B
Butylamine	16832281	84.09	0.75803	117612.3	33.8039	0.0014	0.0049	2B
Pyridine	18845285	71.58	0.77061	133372.1	0.69330	0.0012	0.0059	2B
Isobutyraldehyde	16890366	76.97	0.91279	109697.9	0.509004	0.0028	0.0069	2B
Ethylmercaptan	9330709	59.11	0.58262	112655.5	97.924	0.0013	0.004	2B
2,2,4 Trimethylpentane	32142567	139.06	0.87691	-	-	0.0052	0.0111	-
Dimethylsulfide	12718442	58.99	0.70002	-	-	0.0088	0.0131	-
Sulfurylchloride	15972215	68.41	0.75793	-	-	0.02	0.06	-
Cyanogenchloride	8438040	41.41	0.76412	-	-	0.0236	0.009	-
1-Pentanol	23179121	97.29	0.92138	215043.2	2.64607	0.0008	0.0081	2B
Tetrahydrothiophene	18801411	77.9	0.58312	122342	46.51	0.0005	0.0042	2B
Bis(chloromethyl)ether	19260947	76.77	0.88853	-	-	0.0076	0.0078	-
Propyleneglycol	13798206	67.67	0.74271	197598.1	11.953	0.0261	0.0186	4C
2-Methylpyridine	23246503	87.74	0.86376	-	-	0.0059	0.0059	-
Nitrobenzene	32605440	98.38	0.8447	-	-	0.0167	0.021	-
Indole	35614137	101.82	0.9411	-	-	0.0108	0.0094	-
s-Trioxane	16960394	65.42	0.87733	110119.1	2.048	0.0031	0.0059	2B

n-Butane	13447507	74.64	0.72748	-	-	0.0027	0.0111	-
Propane	9154695	58.69	0.66653	-	-	0.003	0.0131	-
Isobutane	12935743	75.1	0.71322	-	-	0.0083	0.0173	-

Comparison of the CPA and COSMOtherm performance with Experimental data:

The malodorants' pure-component parameters for the CPA model are found by fitting to vapor pressure and liquid density data. The parameters are shown in the table 32. The property that is of interest to us is vapor pressure, so we compare the performance of the models on this property. Figures 3-19 show the vapor pressure as a function of temperature for the 17 compounds where we have experimental data. In all cases, the vapor pressure from CPA is in excellent agreement with experiment. This is to be expected, since the parameters were obtained in order to *ensure* good agreement for this property. However, in the absence of experimental data, CPA cannot be used. From the comparisons with COSMOtherm, we can see that in most cases, the prediction (based only on the chemical structure of the compound) is acceptable. This gives us some confidence that the pure-component vapor pressures for the ten compounds for which no experimental data exists, should be satisfactorily predicted by COSMOtherm.

Figure 3 shows the vapor pressure of triethylamine at different temperatures for CPA (with 2B association scheme for triethylamine) and COSMOtherm. These results are compared with the DIPPR correlations (based on experiment). As expected, the CPA equation of state is able to represent correctly the pure triethylamine vapor pressure for triethylamine. COSMOtherm tends to overpredict the vapor pressure at higher temperatures. However at the temperature of relevance (around a room temperature of 293 K) the prediction is satisfactory. The vapor pressures of the remaining 16 malodorants for which we have experimental data are shown in Figure 4 to Figure 19. Predictions from COSMOtherm are generally very good, especially at around room temperature. Compounds for which COSMOtherm performs less well are 2,2,4-trimethyl pentane (figure 7), sulfuryl chloride (figure 11), bis(chloromethyl)ether (figure 14), s-trioxane (figure 16) and indole (figure 17). The vapor pressure of bis(chloromethyl)ether (figure 14) is particularly poorly represented. The reason for this is not clear. However, in general COSMOtherm does a good job of representing the vapor pressure of the pure substances, which leads us to believe that we can

accept the vapor pressure predicted for the other ten compounds where we have no experimental data.

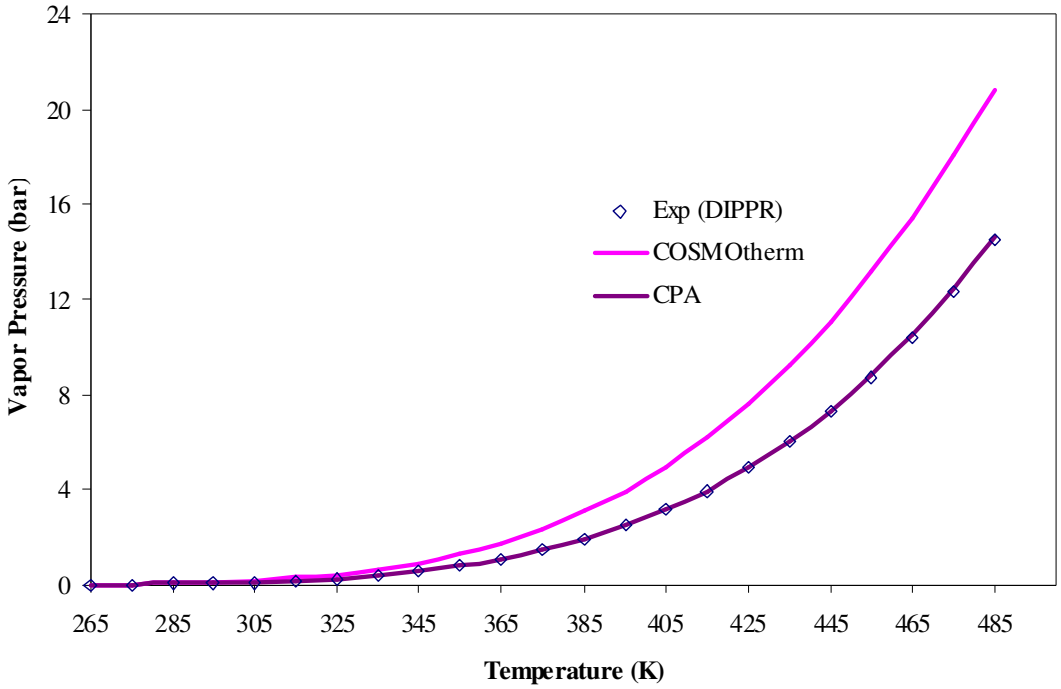

Figure 3: Comparison of Triethylamine Vapor pressure between CPA, COSMOtherm and DIPPR

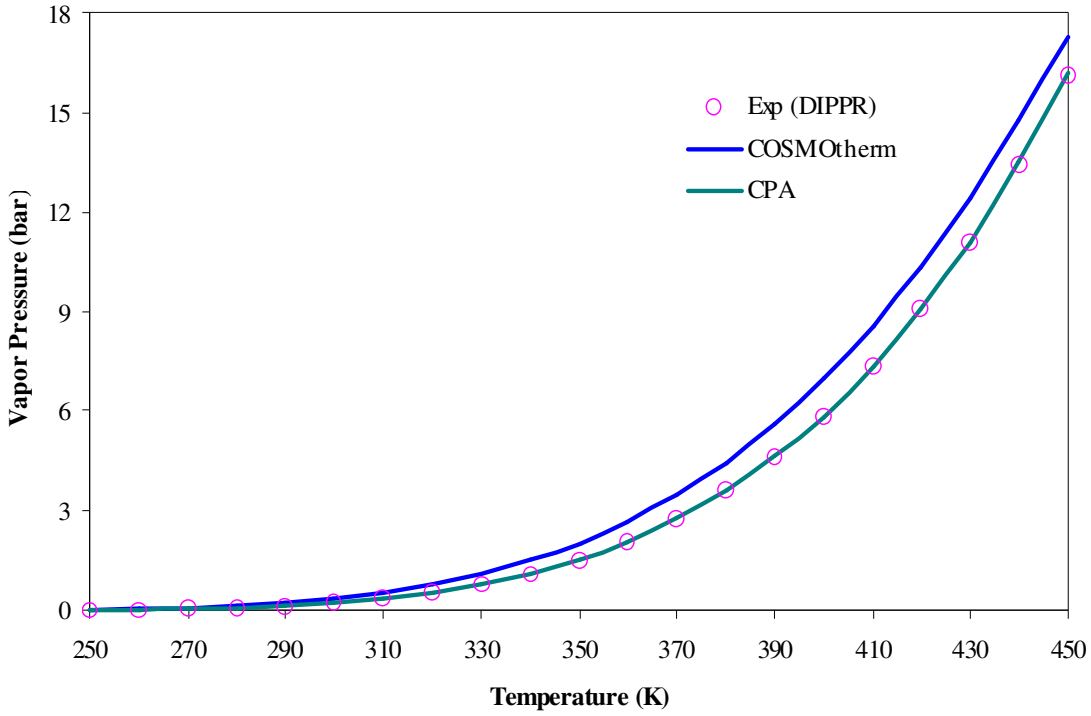

Figure 4: Comparison of Isobutyraldehyde Vapor pressure between CPA, COSMOtherm and DIPPR

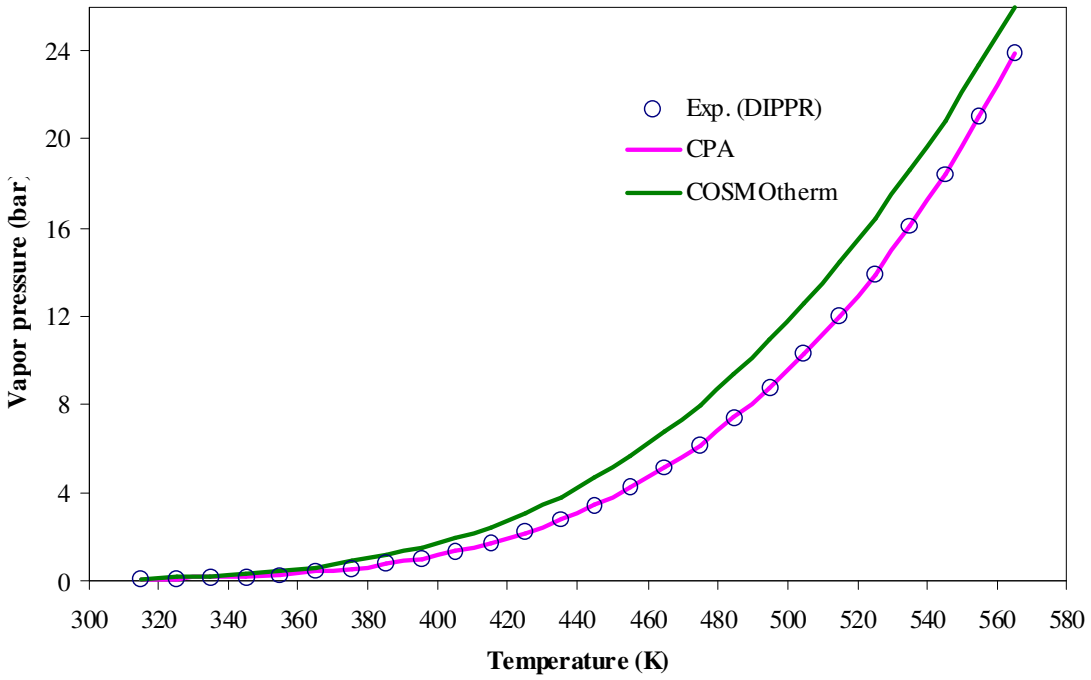

Figure 5: Comparison of Tetrahydrothiophene Vapor pressure between CPA, COSMOtherm and DIPPR

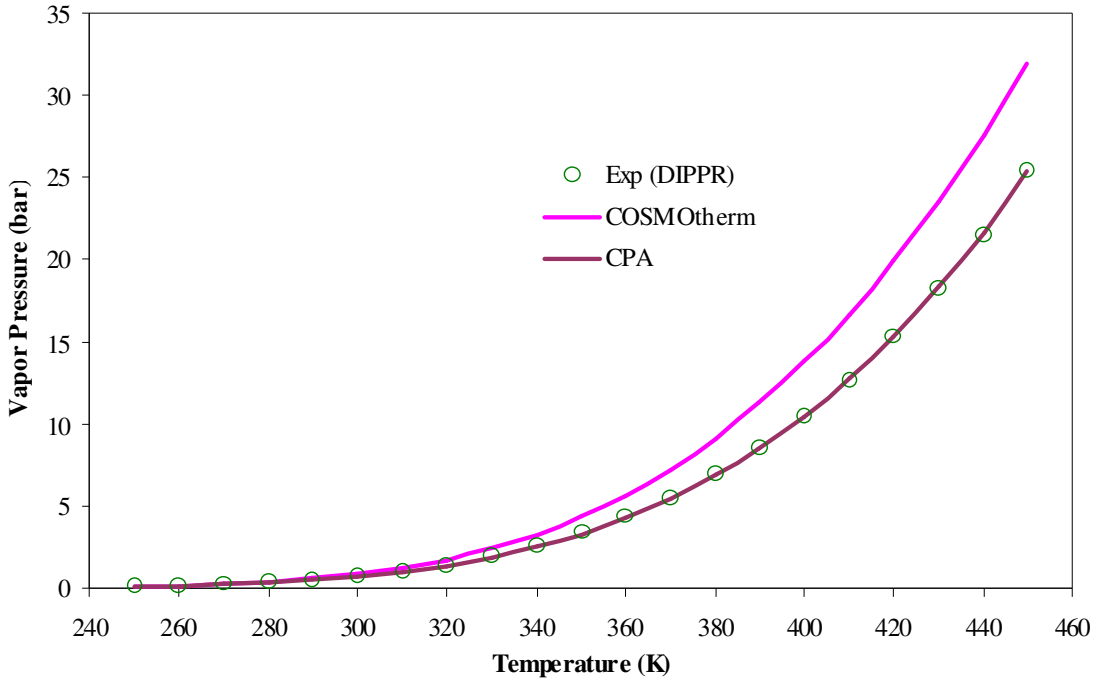

Figure 6: Comparison of DimethylsulfideVapor pressure between CPA, COSMOtherm and DIPPR

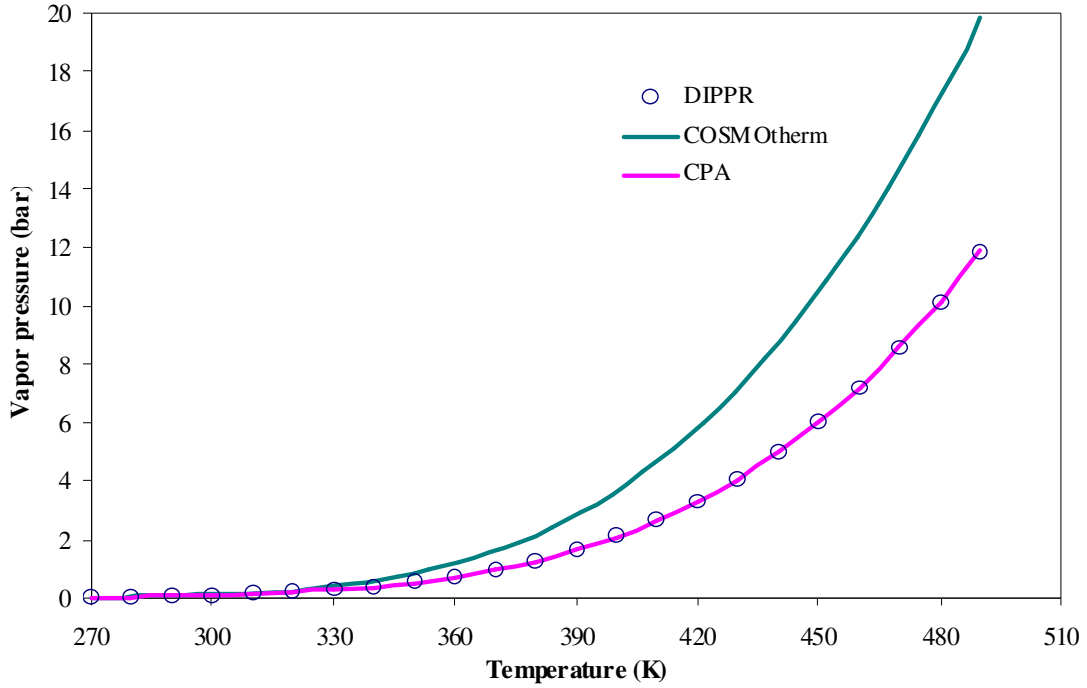

Figure 7: Comparison of 2,2,4 Trimethylpentane Vapor pressure between CPA, COSMOtherm and DIPPR

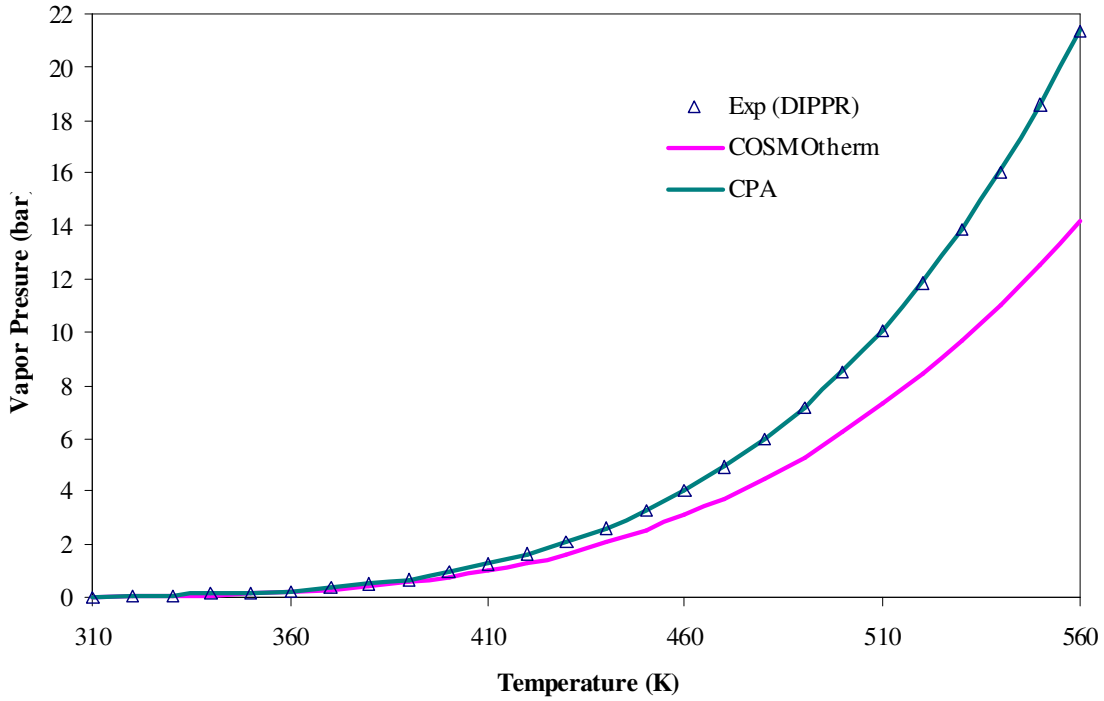

Figure 8 Comparison of 2-MethylpyridineVapor pressure between CPA, COSMOtherm and DIPPR

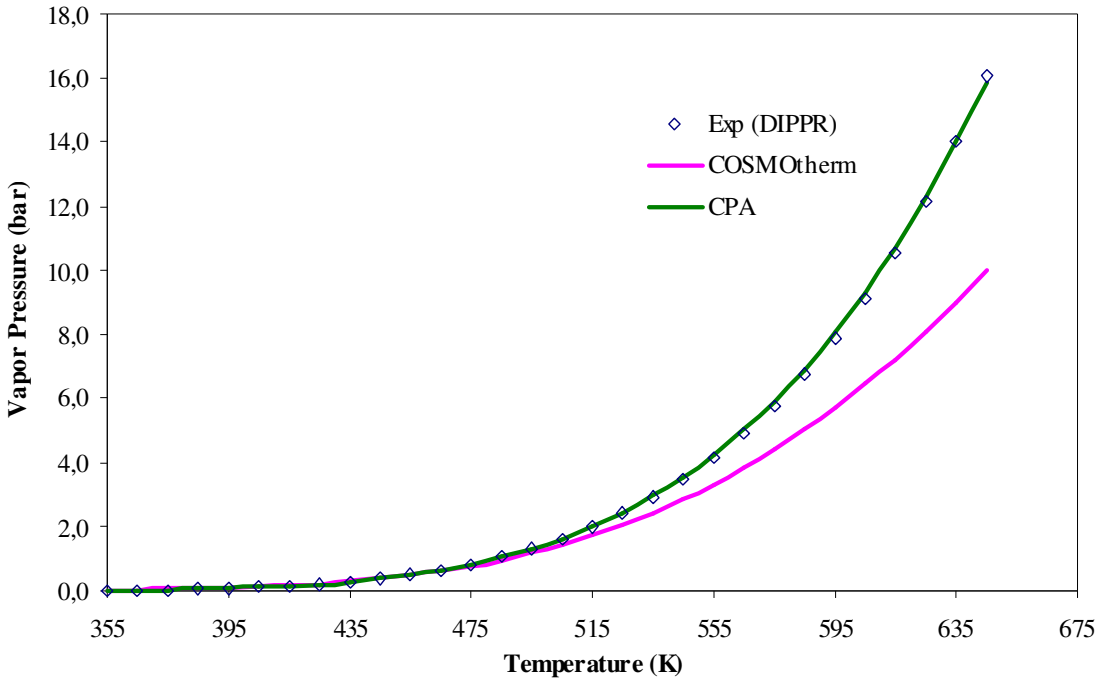

Figure 9: Comparison of NitrobenzeneVapor pressure between CPA, COSMOtherm and DIPPR

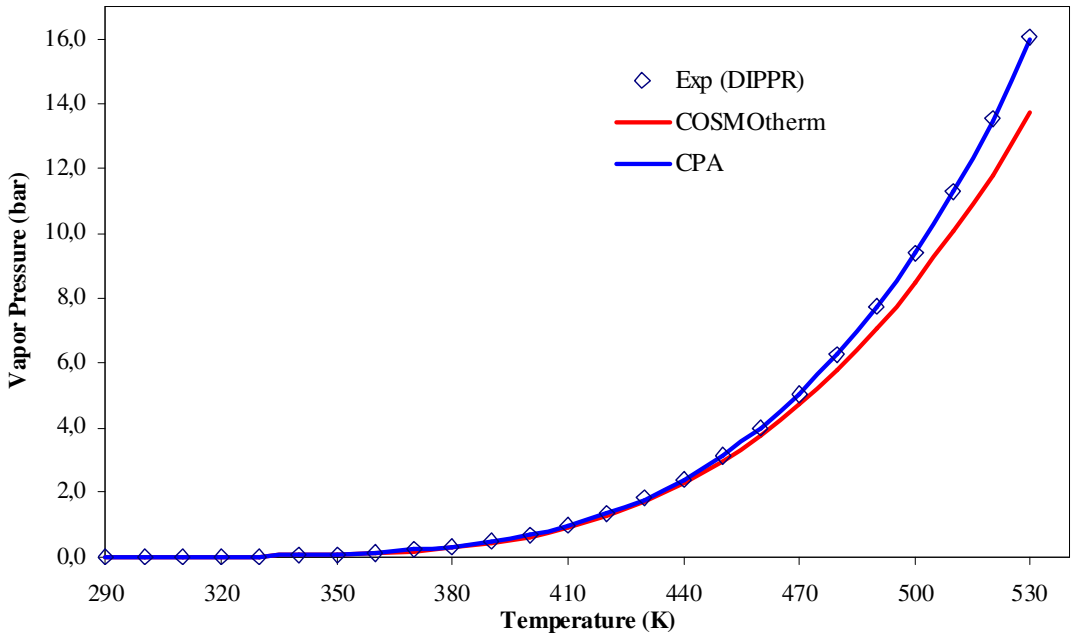

Figure 10: Comparison of 1-Pentanol Vapor pressure between CPA, COSMOtherm and DIPPR

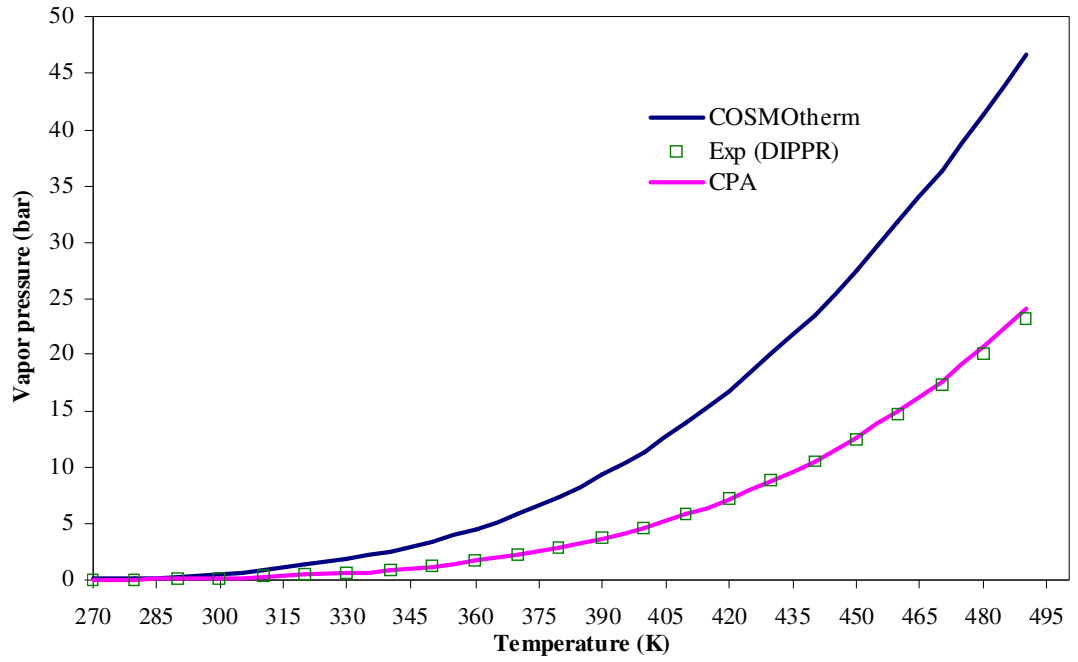

Figure 11: Comparison of Sulfurylchloride Vapor pressure between CPA, COSMOtherm and DIPPR

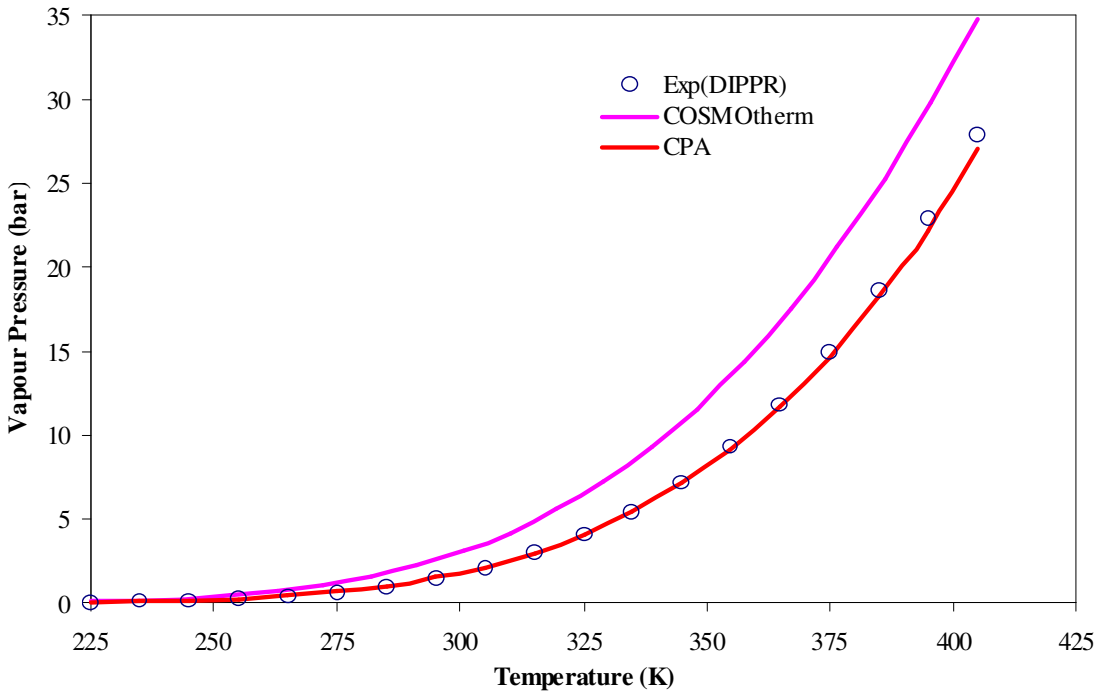

Figure 12: Comparison of CyanogenchlorideVapor pressure between CPA, COSMOtherm and DIPPR

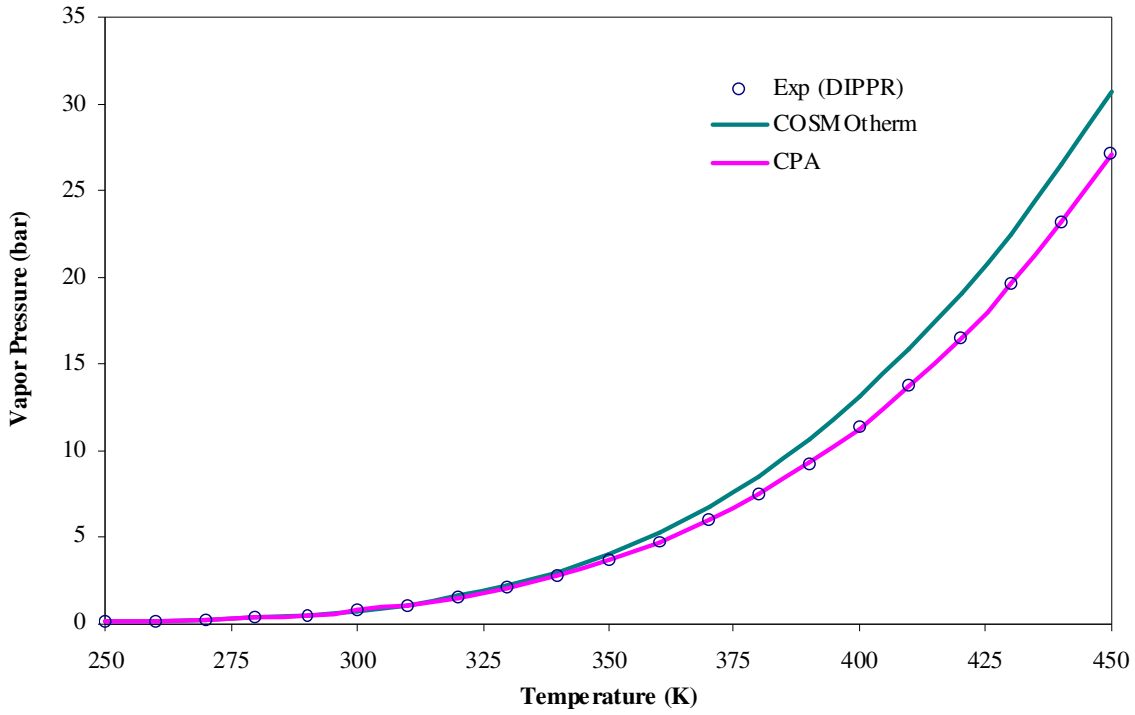

Figure 13: Comparison of Ethylmercaptan Vapor pressure between CPA, COSMOtherm and DIPPR

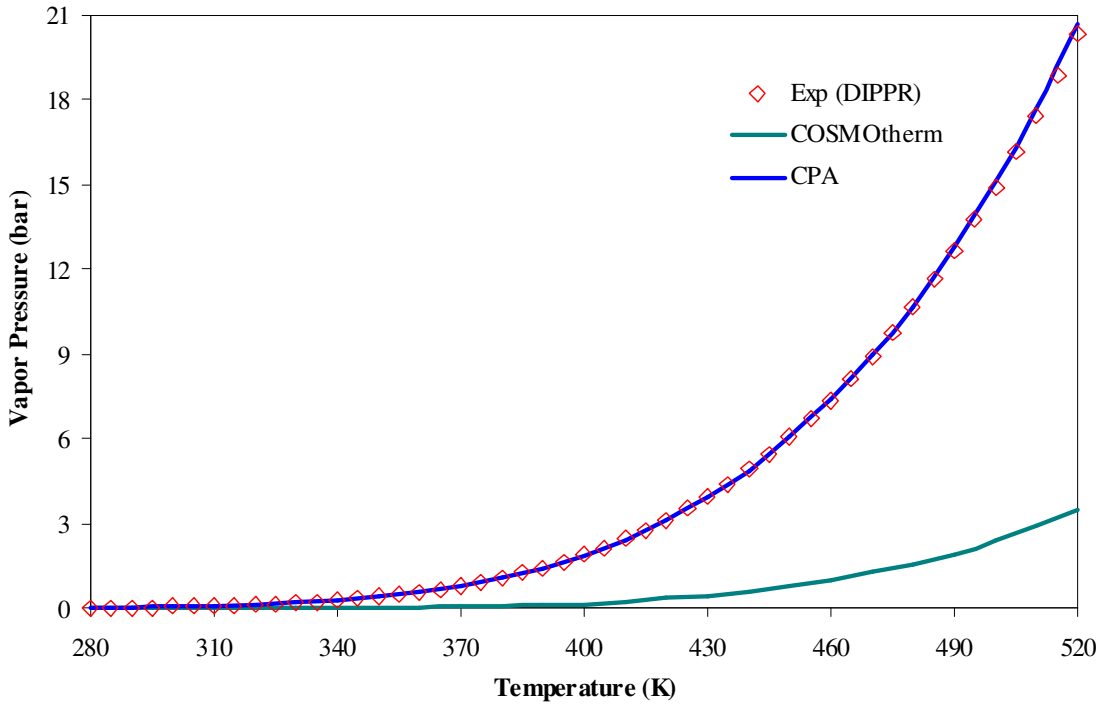

Figure 14: Comparison of Bis(chloromethyl)ether Vapor pressure between CPA, COSMOtherm and DIPPR

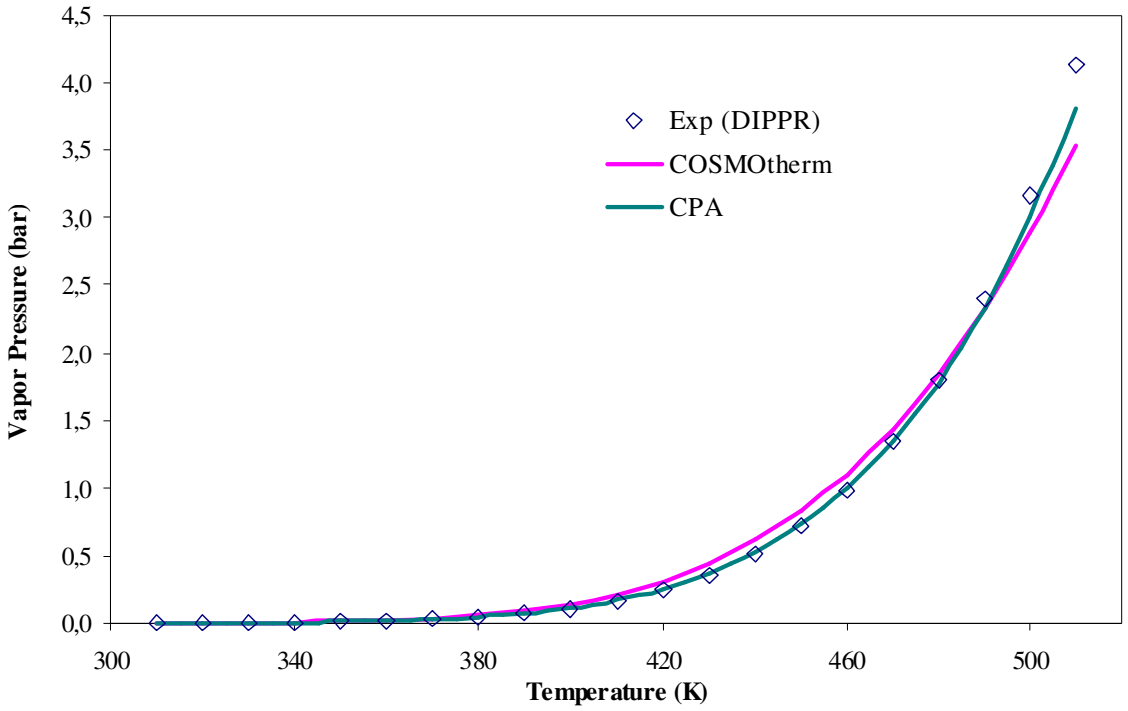

Figure 15: Comparison of Propyleneglycol vapor pressure between CPA, COSMOtherm and DIPPR

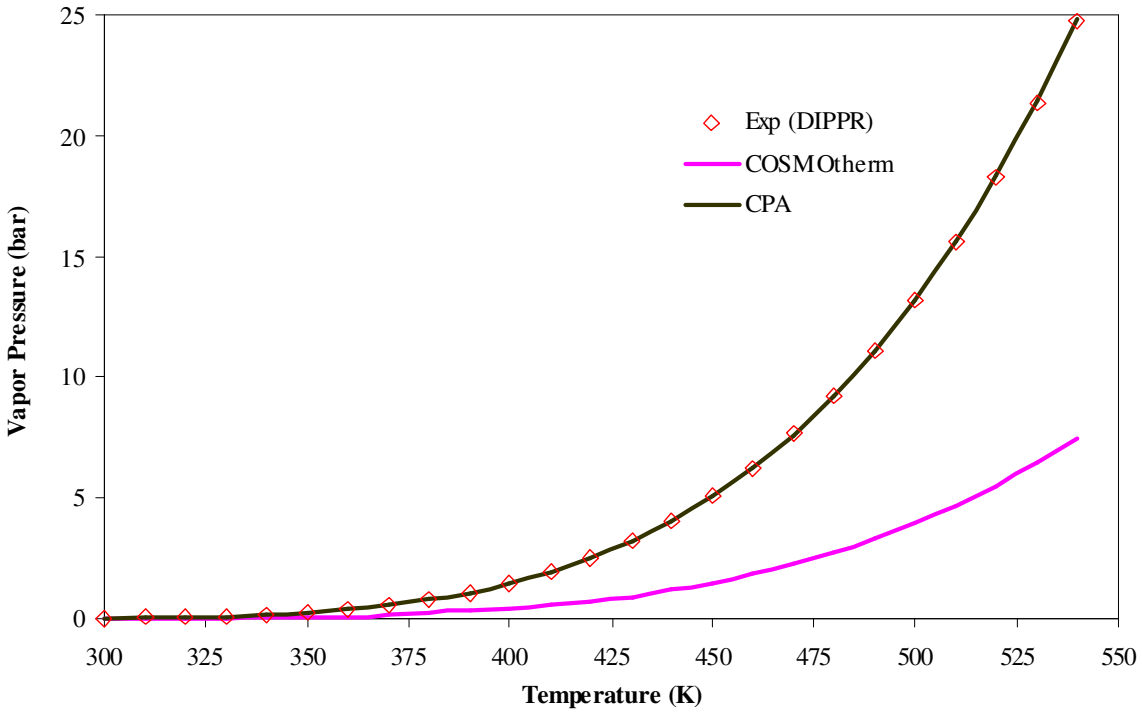

Figure 16: Comparison of s-Trioxane vapor pressure between CPA, COSMOtherm and DIPPR

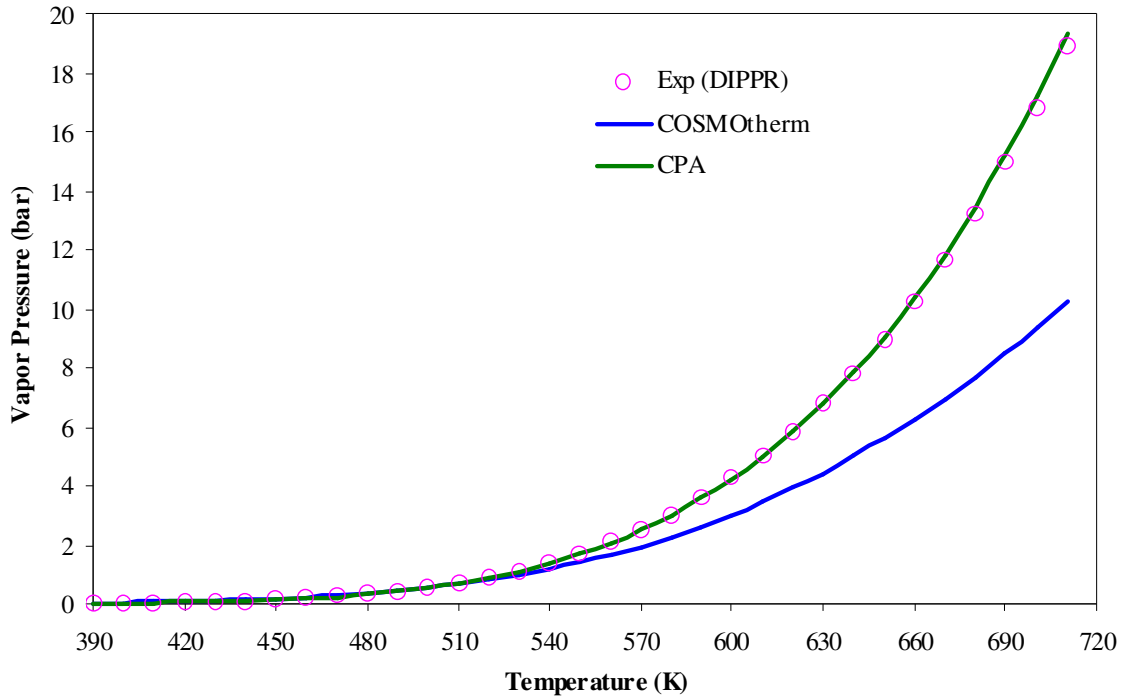

Figure 17: Comparison of Indole vapor pressure between CPA, COSMOtherm and DIPPR

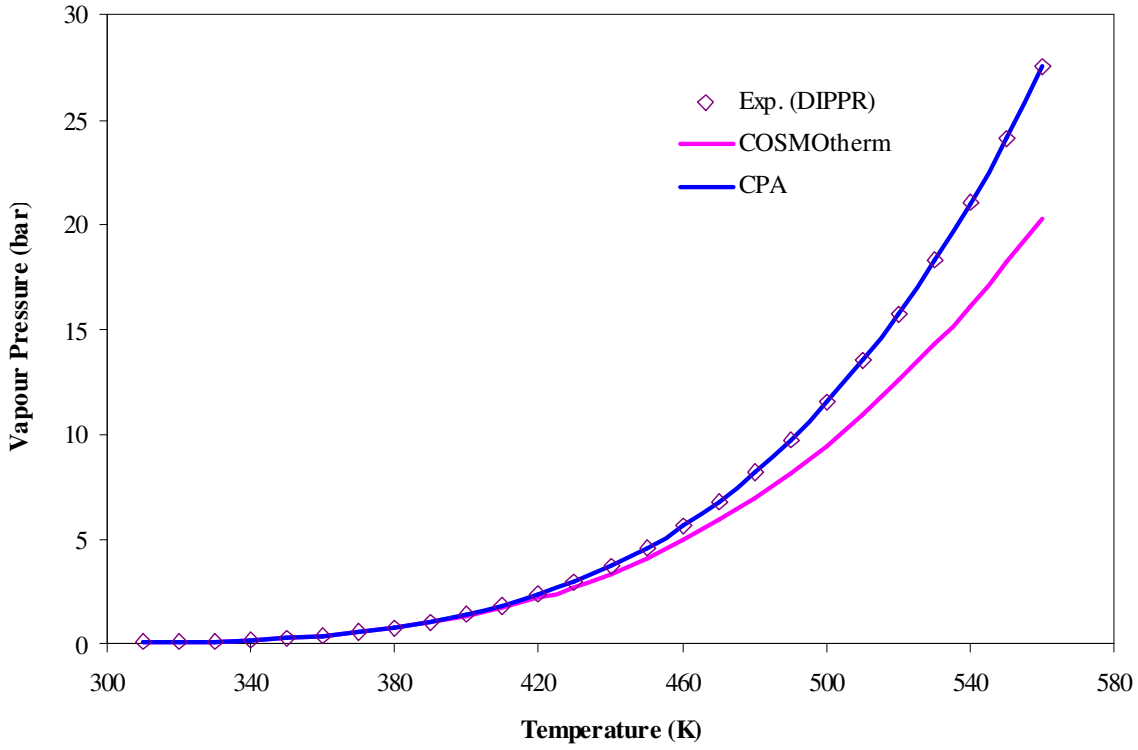

Figure 18: Comparison of Pyridine vapor pressure between CPA, COSMOtherm and DIPPR

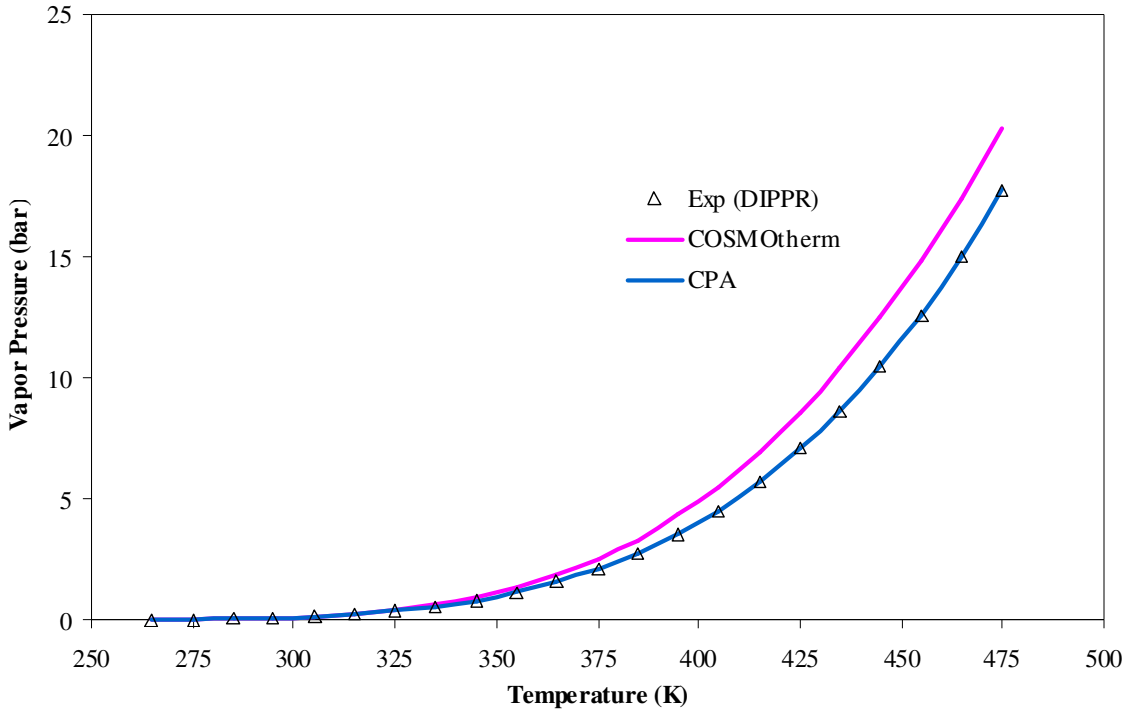

Figure 19: Comparison of Butylamine vapor pressure between CPA, COSMOtherm and DIPPR

Ideally the models should be verified using the kind of binary data that is of interest to us. The only binary pair for which we have data is butane-ethyl mercaptan, at temperatures of 50 °C and 100 °C, i.e. at temperatures higher than those of interest. Nevertheless a comparison can give us an idea of whether the models give us the correct behavior. Figures 20-23 show pressure composition diagrams for this binary mixture. Figures 20 and 21 show the behavior at a temperature of 50 °C. A discussion of this type of diagram is in order here: when x1=y1=0, we have pure butane and the vapor pressure is 5 bar (the vapor pressure of pure butane at 50 °C). For x1=y1=1, we have pure ethyl mercaptan and the vapor pressure is about 1.75 bar. Both models (as expected) give the correct endpoints. At intermediate pressure (e.g. 3 bar) the mixture splits into a vapor and liquid in equilibrium with compositions of around y1=0.45 and x1=0.8 respectively, i.e. ethyl mercaptan, being the heavier component, tends to concentrate in the liquid phase. The top line gives the liquid composition, while the lower line is the vapor composition. Figure 20 shows that COSMO does a good job of predicting the phase behavior of this binary mixture. The lines for CPA are if ethyl mercaptan is considered to be hydrogen bonding. The prediction is not that good, but the experimental data can be correlated using a so-called binary interaction parameter (*kij*), an adjustable

parameter which can help the agreement between the theory and the data. CPA predicts a maximum in the pressure at a concentration of about x1=0.1, which is not what the data shows. This cannot completely be corrected for with a binary parameter. Figure 21 shows the results if ethyl mercaptan is considered to be non-associating. The agreement is better here, although the COSMOtherm predictions are still better. In this case CPA can be made to agree very closely with the data by using a binary interaction parameter. The problem with this binary parameter, however, is that one must have the experimental data in advance. Figures 22 and 23 make the same point, at a temperature of 100 °C. Based on the results for pure component and binary data (where data is available), it was proposed to continue modeling with COSMOtherm alone, since results with CPA require at least pure-component data, and the predictions of the behavior of binary mixtures seems to be better with COSMOtherm.

The following points are considered to use COSMOtherm program in this work instead of CPA equation of state to calculate the physical properties.

- The performance of COSMOtherm is better for the single binary mixture where we have data compared to the CPA equation of state
- Lack of pure component data in DIPPR database. The pure compound data (vapor pressure and liquid density) is necessary to estimate the pure compound (and mixture) properties with CPA.
- Some of the compounds used in this work are not available in the DIPPR database.
- The COSMOtherm program can be used to compute the thermodynamic properties of pure compounds and mixtures for which no data is available.

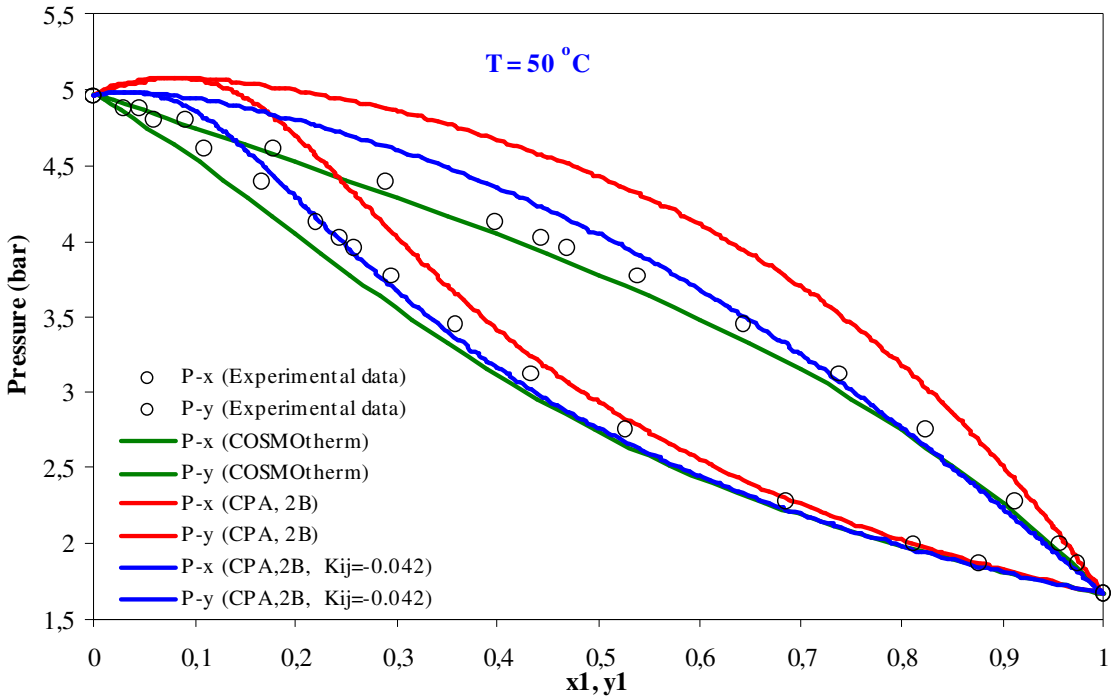

Figure 20: Vapor-Liquid Equilibrium of Ethylmercaptan (1) / *n*-Butane (2) with CPA (Association scheme-2B) and COSMOtherm at 50°C

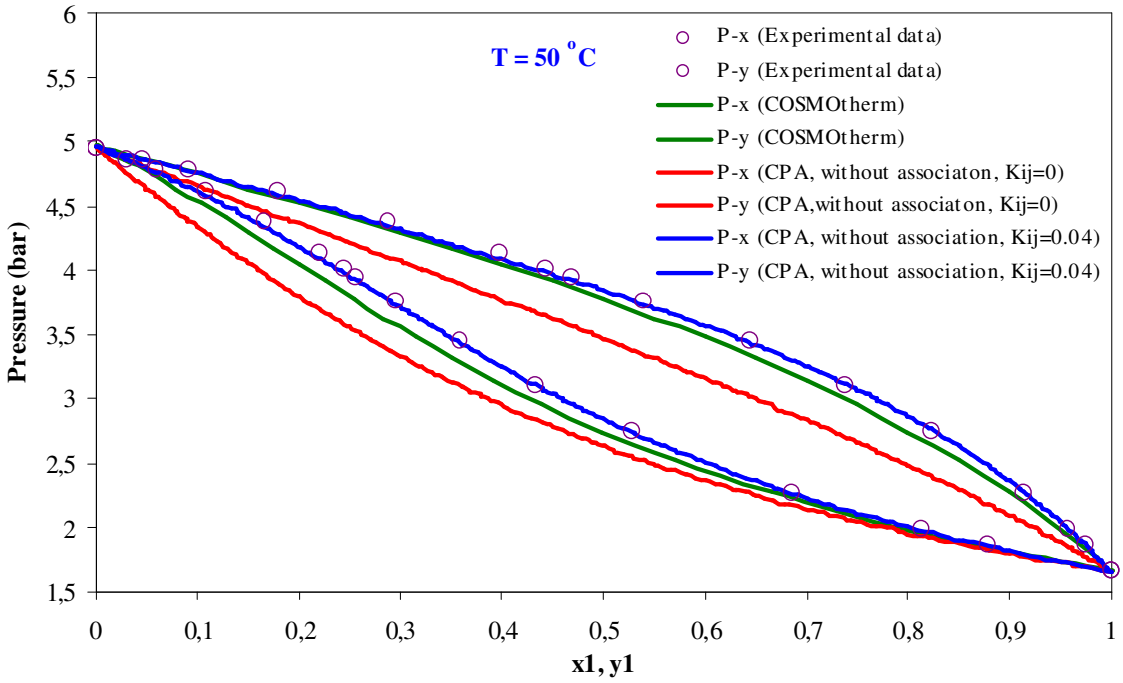

Figure 21: Vapor-Liquid Equilibrium of Ethylmercaptan (1) / *n*-Butane (2) with CPA (Non association) and COSMOtherm at 50°C

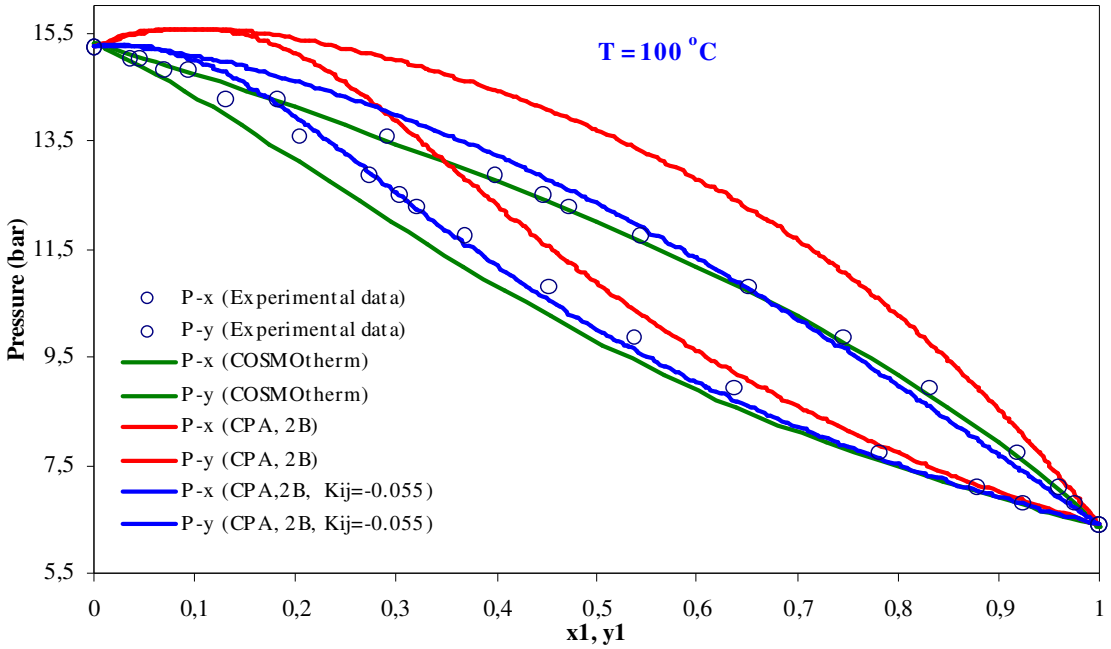

Figure 22: Vapor-Liquid Equilibrium of Ethylmercaptan (1) / *n*-Butane (2) with CPA (Association scheme-2B) and COSMOtherm at 100°C

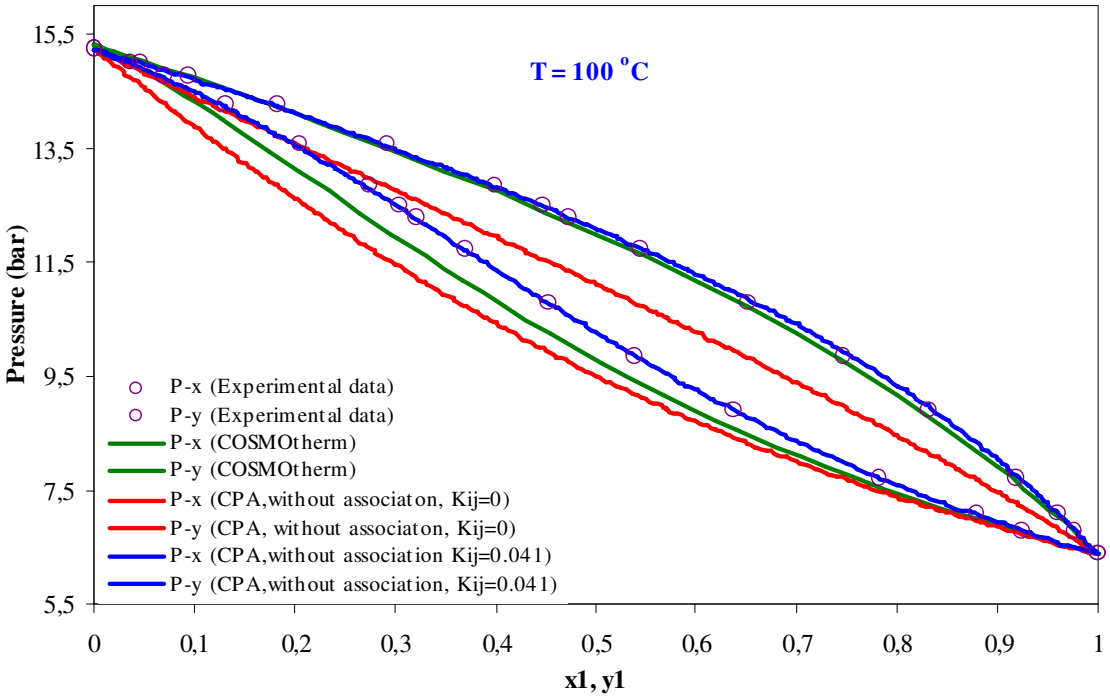

Figure 23: Vapor-Liquid Equilibrium of Ethylmercaptan (1) / *n*-Butane (2) with CPA (Non Association) and COSMOtherm at 100°C

7.5 Sigma Profiles

The first step in a COSMOtherm calculation is to calculate the sigma profiles and surfaces for the selected compounds. The majority of these were already in the existing database and did not require computation. This program needs COSMO files to generate sigma profiles for the compounds which are selected as malodorants. The charge distribution is represented as probability distribution of a molecular surface segment having a specific charge density. This probability distribution is called sigma profile ($p_i(\sigma)$). The surface charge density of lighter gas components (butane, isobutane and propane) and the resulting σ-profile of each component are shown in Figure 24 .

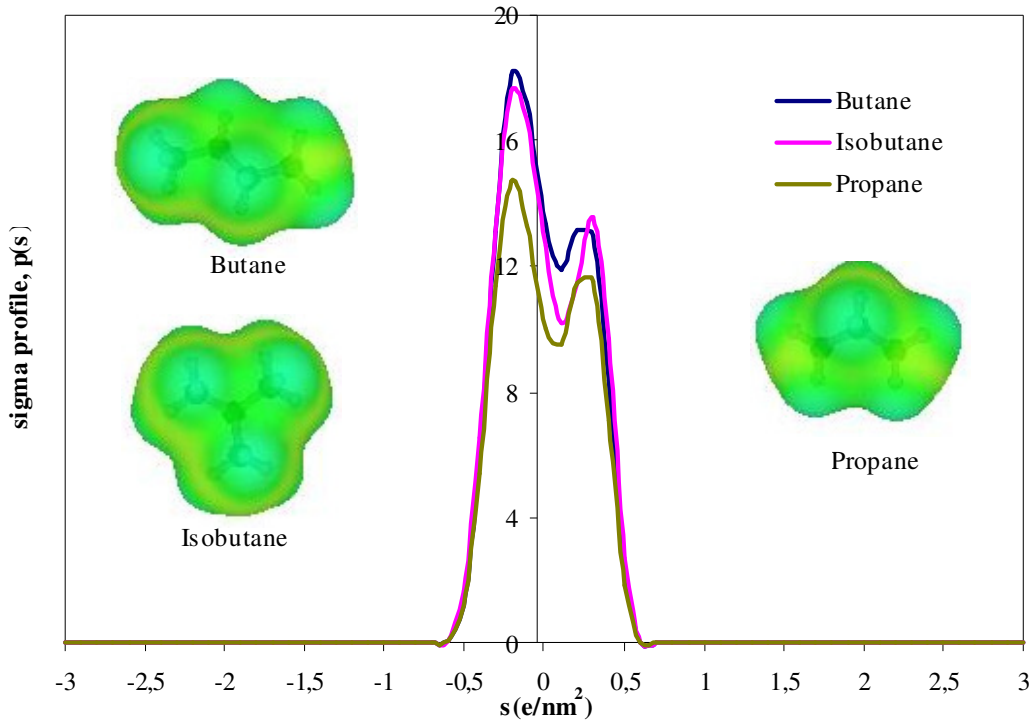

Figure 24: Sigma profiles for the lighter gas components (butane, isobutane and propane).

These three compounds are alkanes and do not have significant electrostatic moments. Consequently the σ-profiles are rather narrow. Two peaks are detected from the above diagram, resulting from the hydrogen on the negative side and from the carbon on the positive side. The corresponding σ-profiles of the butane, isobutane and propane range from -0.6 to +0.6e/nm^2. The area under the curve represents the total surface area of the

compound. The σ-profiles of other alkanes look very similar and mainly differ in height according to the differences in the total surface area.

The polarization charge densities and σ-profiles of some other compounds are shown in Figure 25. The σ-profiles of 1,8 cineole and 1-pentanol range from -0.6 to +0.6e/nm^2. On the surface of 1-pentanol (bottom left in Figure 25), the deep blue area identifies the polar hydrogen atom and deep red region represents the lone pair oxygen. The red region on the surface of the 1,8 cineole (top left Figure 25) identifies the polar oxygen.

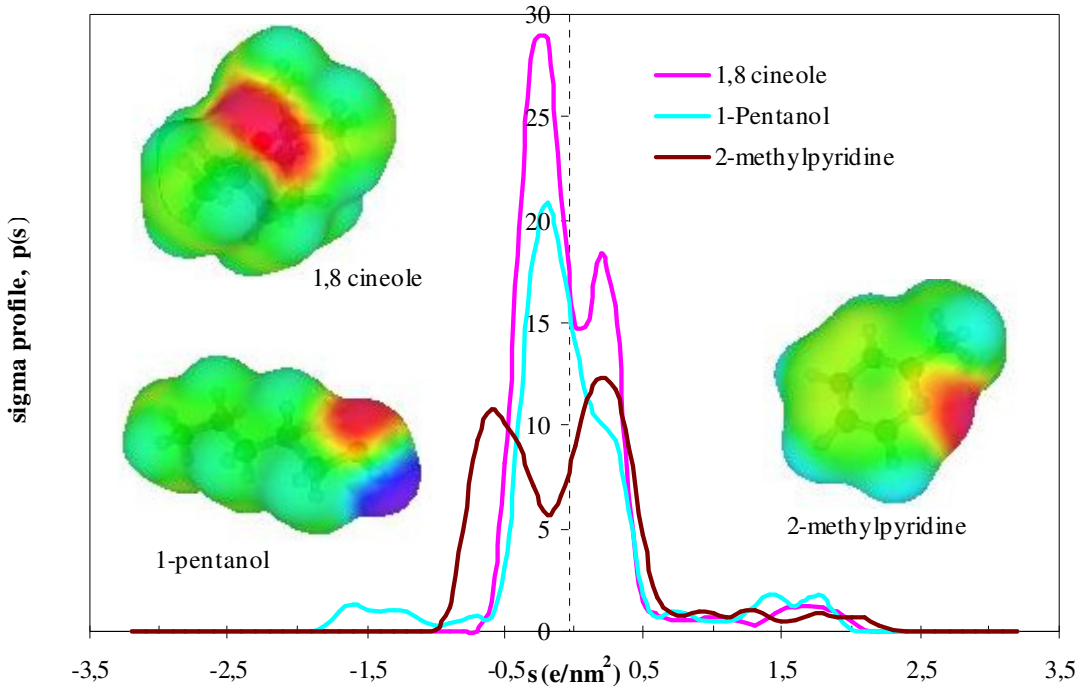

Figure 25: Sigma profiles of 1,8 cineole, 1-pentanol and 2-methylpyridine

The σ-profile of 2-methyl pyridine shows a highly polarized charge density – typical of hydrogen-bonding compounds. The sigma surface and σ-profile of cyanogenchloride, dimethylsulfide and butylamine are shown in Figure 26. The sigma surface of cyanogenchloride mainly appears green but the chlorine atom shows some blue region and yellow with red showing the nitrogen. The sigma profile and sigma surface of sulfurylchloride and triethylamine are shown in Figure 27. The surface of triethylamine shows a very strong lone-pair on the nitrogen. The polarization charge density ranges from -0.8 to +0.8 e/nm^2. The butylamine sigma profile is similar to butane, except that it is broader and the polarization of the amine group is visible as a red and blue region on the surface.

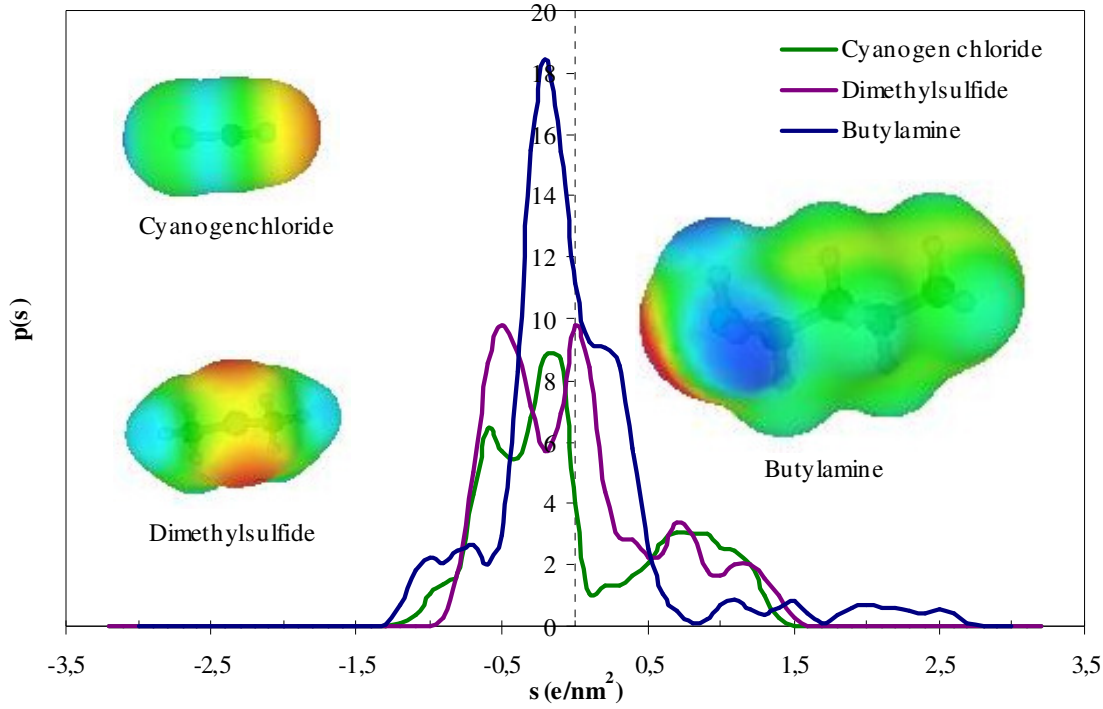

Figure 26: Sigma profiles of cyanogen chloride and dimethylsulfide

The sigma surface of sulfurylchloride (left side in Figure 27) mainly appears green with the chlorine atoms show blue region and oxygen atom shows yellow region.

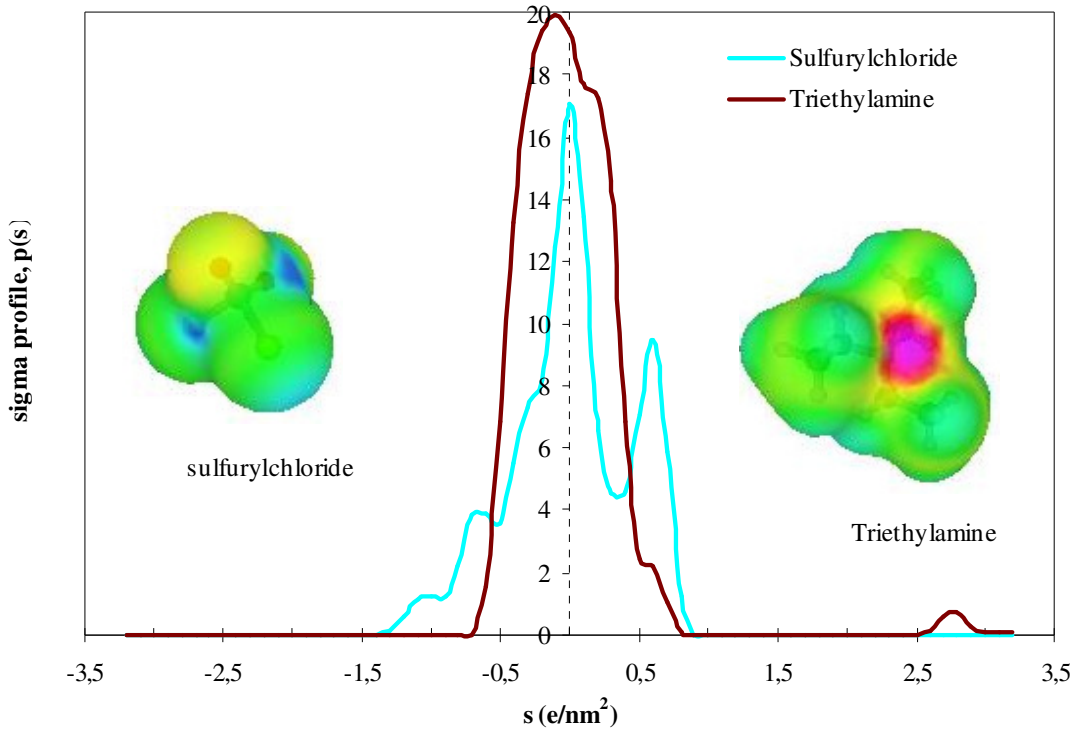

Figure 27: Sigma profiles for the sulfurylchloride and triethylamine

The sigma profile and sigma surface of ethyl mercaptan, isobutanal and pyridine are shown in Figure 28. The deep red region on the surface of isobutanal represents the lone pair oxygen and the light blue color identifies the polar hydrogen. The sigma profile of nitrogen–containing compounds like pyridine, nitrobenzene (Figure 29) show a strong lone pair on the nitrogen. The polarization charge density ranges from +1.1 to 2.5 e/nm^2.

The sulfur lone pairs are much weaker in ethyl mercaptan. The red region on the surface identifies the sulfur and the blue region represents the hydrogen. Ethyl mercaptan thus has a weak hydrogen bond.

The sigma profile and sigma surface of nitrobenzene and tetrahydrothiophene are shown in Figure 29. The blue area in the surface of nitrobenzene identifies the nitrogen and two yellow regions represent the lone pair oxygen. The red region on tetrahydrothiophene surface shows the sulfur atom.

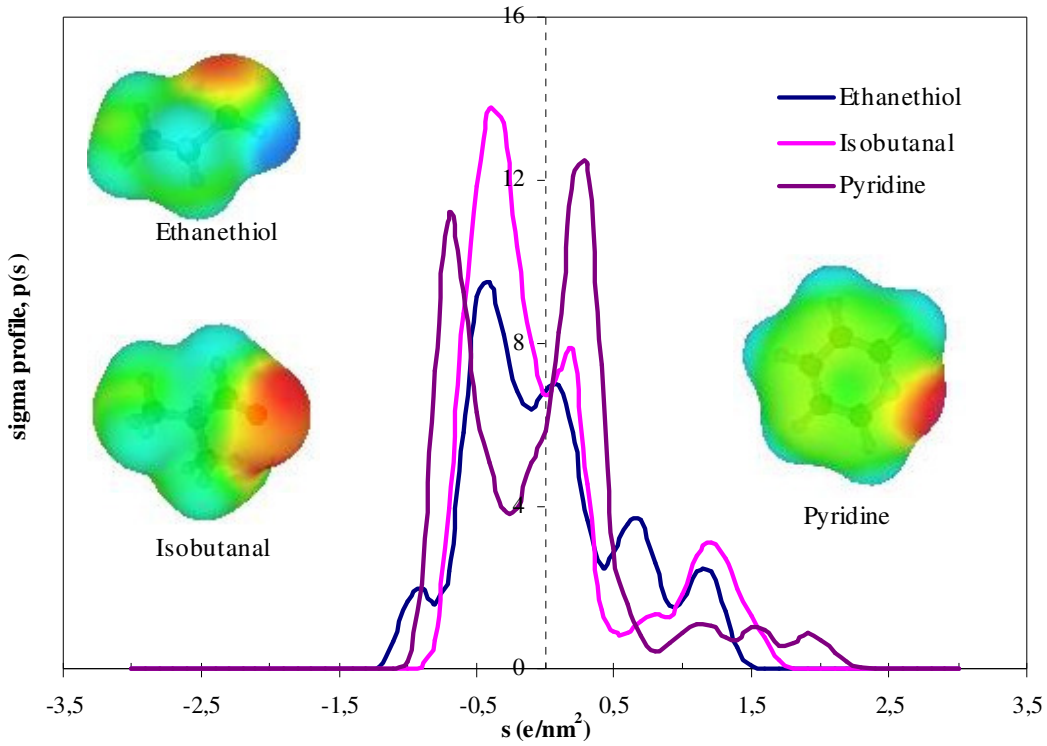

Figure 28: sigma profile for the ethyl mercaptan, Isobutanal and pyridine

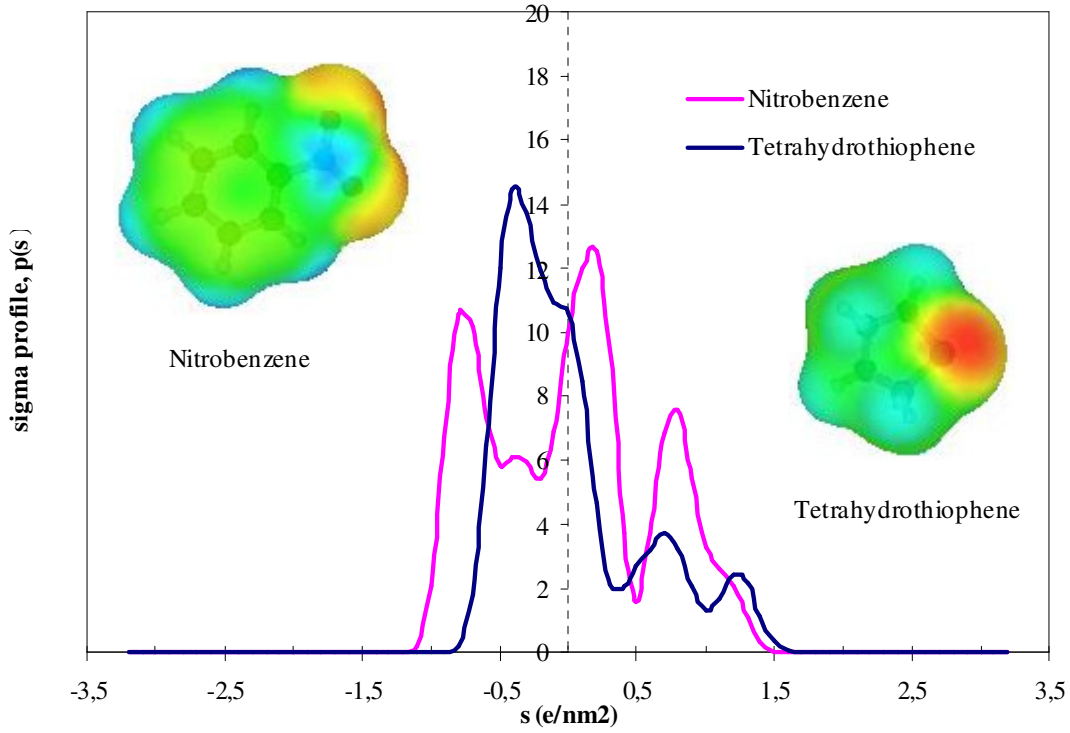

Figure 29: sigma profile for the nitrobenzene and tetrahydrothiophene

The sigma profile and sigma surface of bitrex anion and cation are shown in Figure 30. Both are high molecular weight compounds and their sigma profiles and sigma surfaces were not in the database but were generated using a quantum chemistry program. In particular the high negative charge represented by the anion is visible as a large red region.

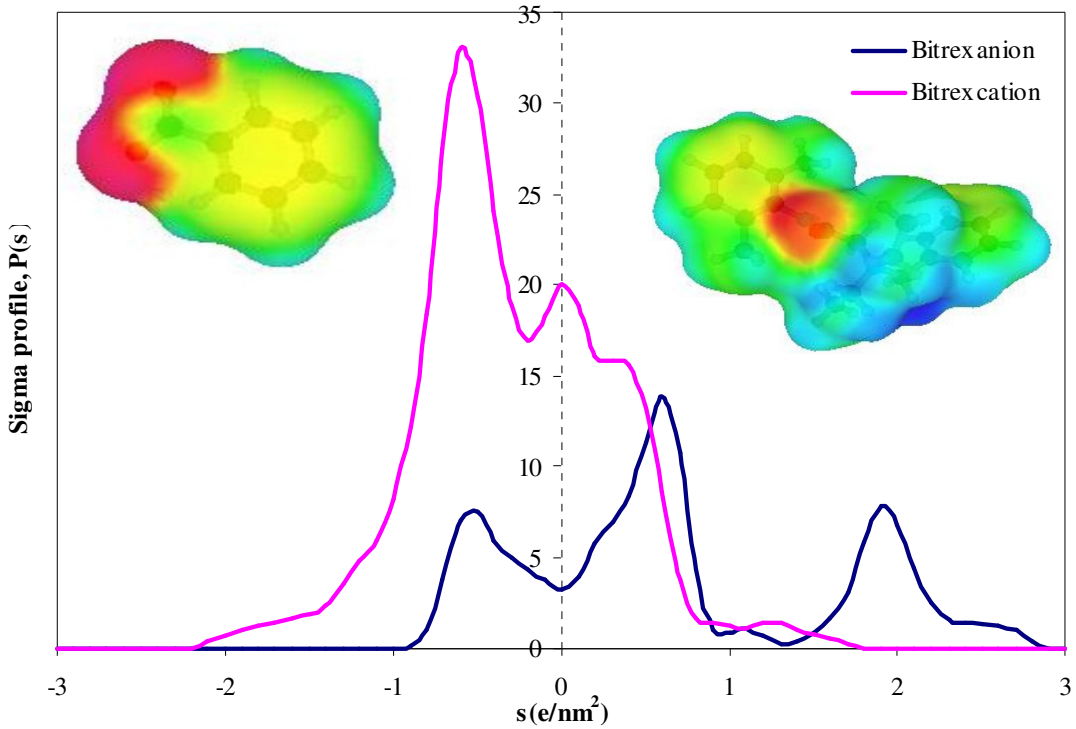

Figure 30: sigma profile for the Bitrex anion and Bitrex cation

7.6 Vapor-liquid Equilibria

Phase equilibrium calculations are done using COSMOtherm as described above. Phase diagrams are calculated for a fixed temperature (isothermal, room temperature, assumed to be 25 °C). What the program calculates is the pure component vapor pressure and activity coefficient as a function of the liquid compositions. The total pressure is then calculated using the equation:

$$p^{(tot)} = \sum_i p_i^0 x_i \gamma_i \tag{7.13}$$

The p_i^0 are pure compounds vapor pressures for compounds i (which are known), x_i are the mole fractions of the compounds in the liquid phase and γ_i are the activity coefficients of the compounds as predicted by COSMOtherm. Vapor mole fractions are then obtained by the ratio of partial and total vapor pressures.

$$y_i = p_i^0 x_i \gamma_i \Big/ p^{(tot)} \tag{7.14}$$

The liquid-liquid equilibrium properties can be calculated by using an analogous relation

$$X_i^{\mathrm{I}} \gamma_i^{\mathrm{I}} = X_i^{\mathrm{II}} \gamma_i^{\mathrm{II}} \tag{7.15}$$

where subscripts I and II denote the two liquid phases. This calculation is required in the case where two liquid phases form. Our phase diagrams are calculated at a fixed temperature. There are two common ways to plot the phase equilibrium for binary systems. One way is to plot mole fraction vs. temperature at constant pressure and another is to plot mole fraction vs. pressure at constant temperature. These plots are referred to as *P-xy* and *T-xy* plots. Since normal use of lighter gas occurs at a constant temperature, we have chosen to represent the phase behavior as *P-xy* diagrams.

Triethylamine – n-Butane binary system

The compounds triethylamine (1) and *n*-butane (2) are selected from database in COSMOtherm and the vapor-liquid phase diagram is then calculated at a fixed temperature (25 °C) in COSMOtherm. Figure shows the vapor liquid equilibrium data for triethylamine (1) / *n*-butane (2) at 25 °C. In this Figure, if the pressure were increased to P_1 everything would be liquid and the pressure to drop below P_5 the mixture is gas at any composition. If the pressure is reduced from P_1, the first vapor molecule forms at a pressure of P_2. This is the boiling point pressure of triethylamine at 25 °C. For the equilibrium pressure line P_4 the liquid mole fraction of triethylamine is given by the blue line while the lower curve (pink line) is the vapor mole fraction of triethylamine.

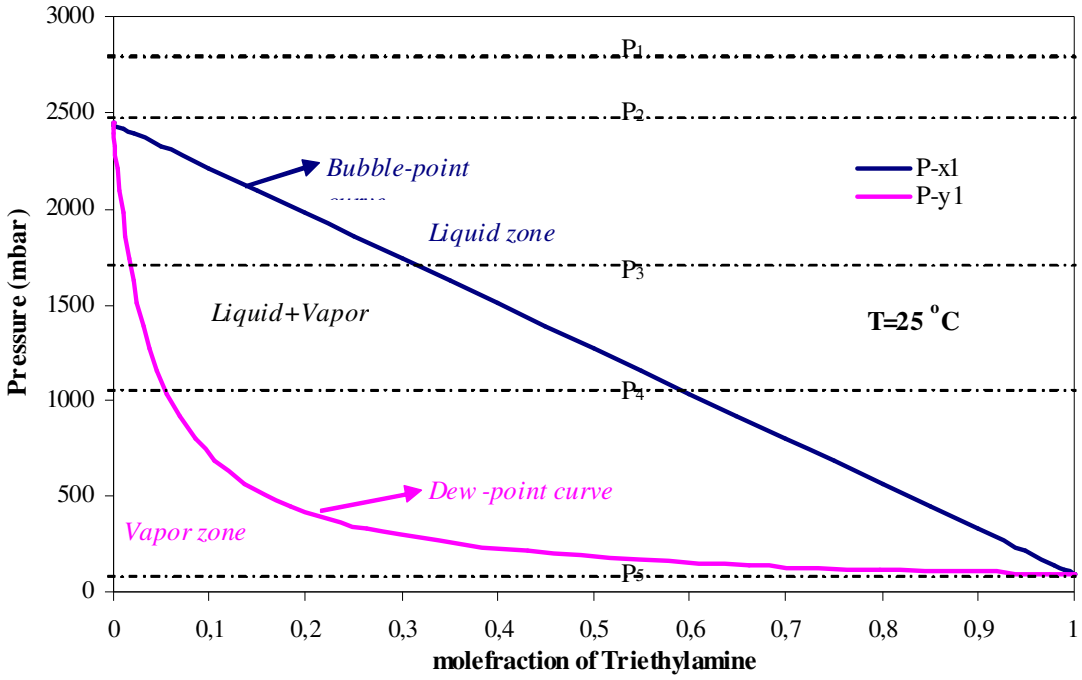

Figure 31: Vapor-Liquid equilibrium for Triethylamine (1) / *n*-Butane (2) at 25 °C. The solid curve shows the COSMOtherm predictions

For example if the liquid contained about 32% triethylamine, the pressure would be about 1700 mbar (the blue line at P_3). At this pressure the vapour composition would be about 3% (where P_3 intersects the pink line). Figure shows the mole fraction of triethylamine in the vapor phase as a function of its concentration in the liquid phase. This diagram is created

from Figure and contains no more information – it is just convenient to see directly how the vapor composition depends on the liquid composition. Thus we can more easily see that for a liquid composition of, say, 5%, the vapor composition is 0.2%. In this study, we are looking for substances which can be added in small amounts, so the region of the phase diagram that is of most interest is near the origin (close to pure butane). We are also looking for compounds which have a similar volatility to butane (so the vapor and liquid phase compositions are comparable).

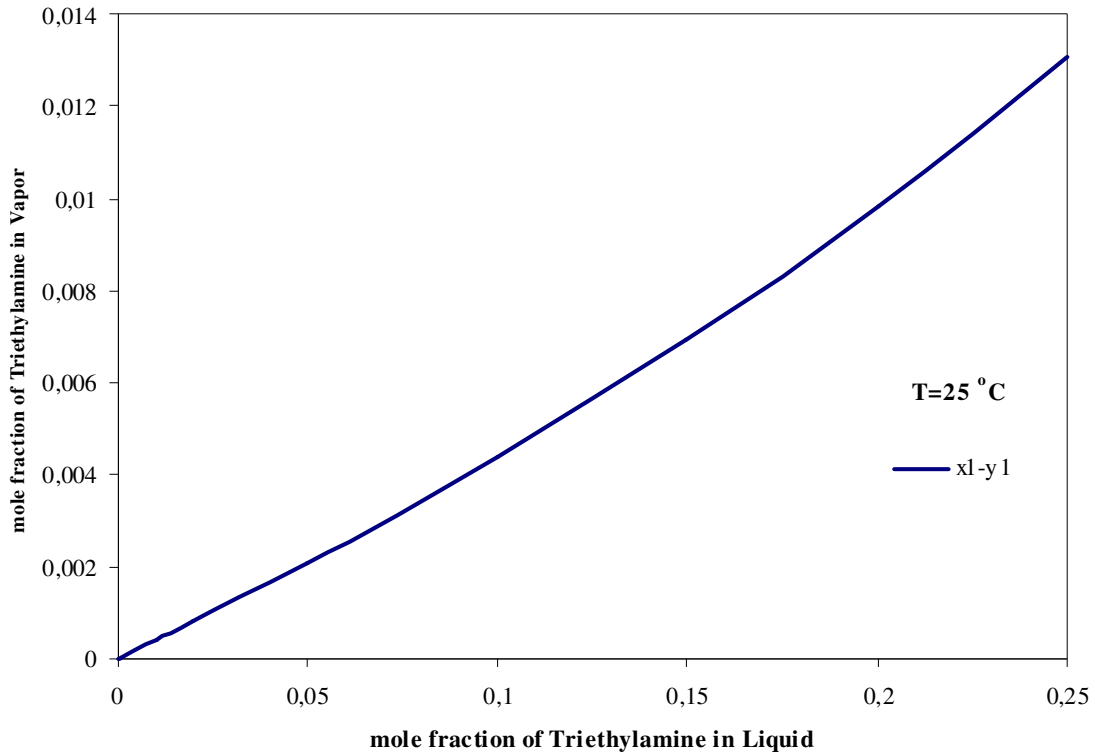

Figure 32: The X-Y diagram for Triethylamine (1) / *n*-Butane (2) at 25 °C. The solid curve shows the COSMOtherm predictions

The malodorant concentration needs to be low because the addition of these compounds should not affect the normal use of the lighter gas. The *y-x* phase diagrams are thus shown at low concentrations.

Isobutyraldehyde – n-Butane binary system

The Figure shows the vapor liquid equilibrium data for isobutyraldehyde (1)/*n*-butane (2) at fixed temperature 25 °C. Figure shows the mole fraction of triethylamine in both phases and a point on the equilibrium curve separated into the mole fraction of the vapor that is isobutyraldehyde on the y-axis and the mole fraction of liquid that is isobutyraldehyde on the x-axis. The remaining mole fraction in both cases is *n*-Butane.

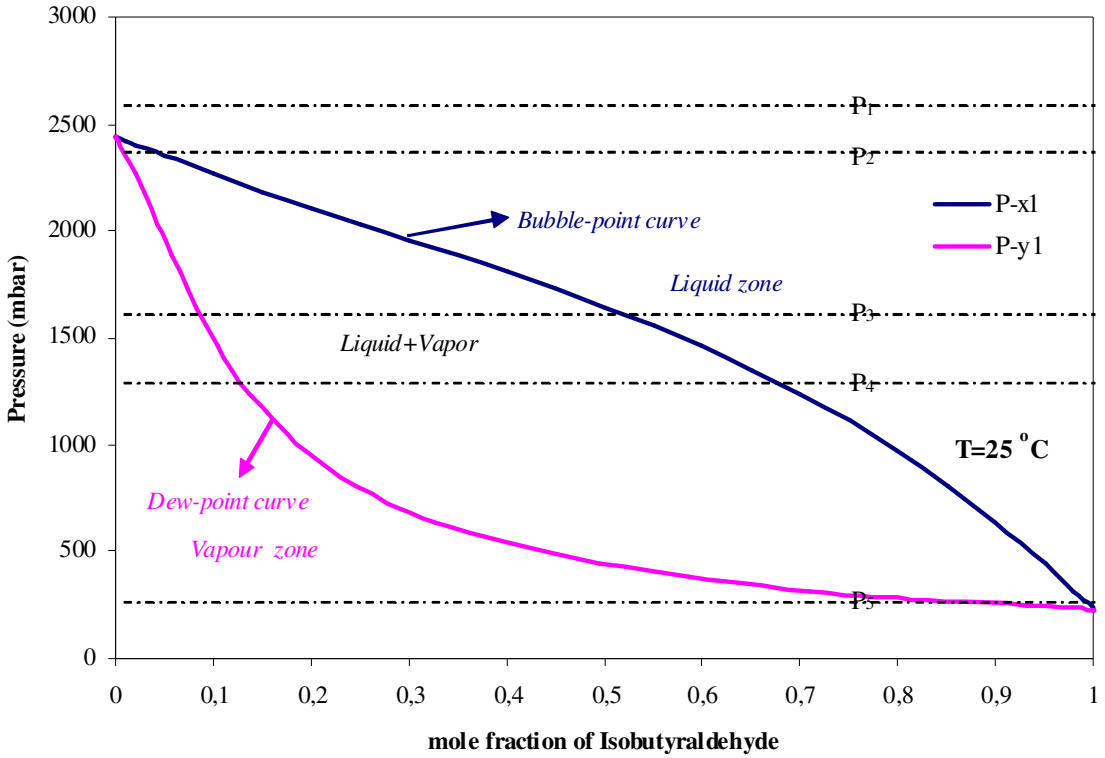

Figure 33: Vapor-Liquid equilibrium for Isobutyraldehyde (1) / *n*-Butane (2) at 25 °C. The solid curve shows the COSMOtherm predictions

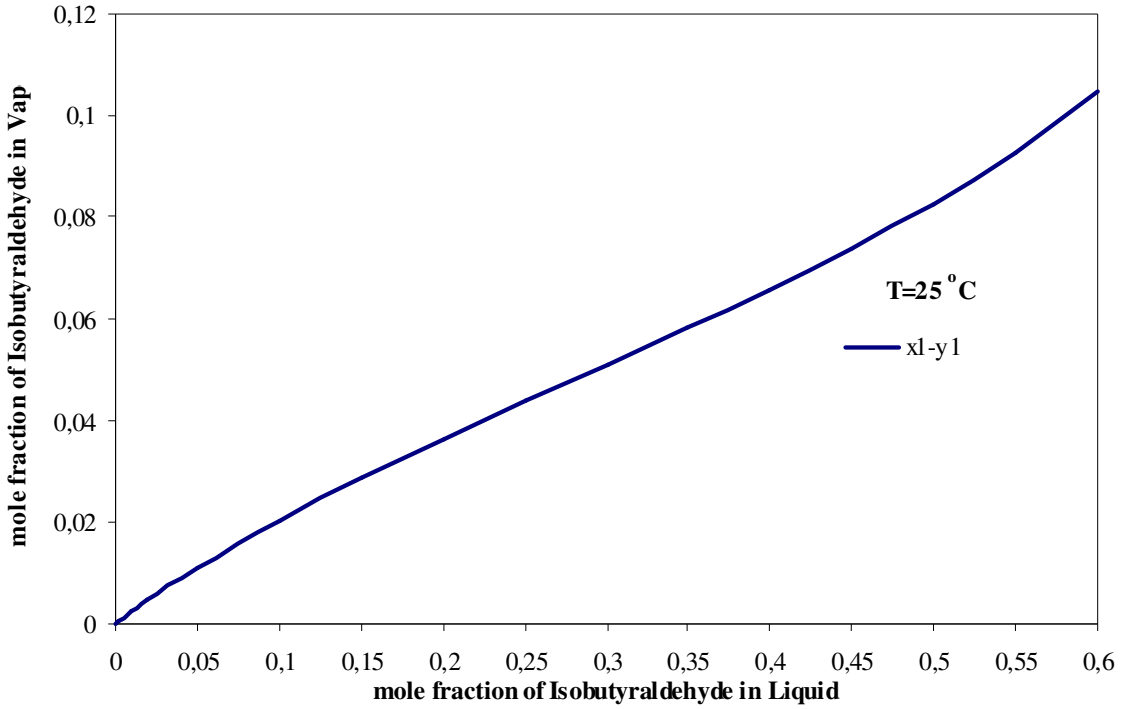

Figure 34: The X-Y diagram for Isobutyraldehyde (1) / *n*-Butane (2) at 25 °C. The solid curve shows the COSMOtherm predictions

Tetrahydrothiophene – n-Butane binary system

The Figure shows the vapor liquid equilibrium data for tetrahydrothiophene (1)/*n*-butane (2) at fixed temperature 25 °C. Figure shows the mole fraction of tetrahydrothiophene in vapor and liquid phases. A point on the equilibrium curve separated into the mole percentage of the vapor that is substance tetra hydrothiophene on the y-axis and the mole percentage of liquid that is tetrahydrothiophene on the x-axis. The remaining mole percentage in both cases is *n*-butane.

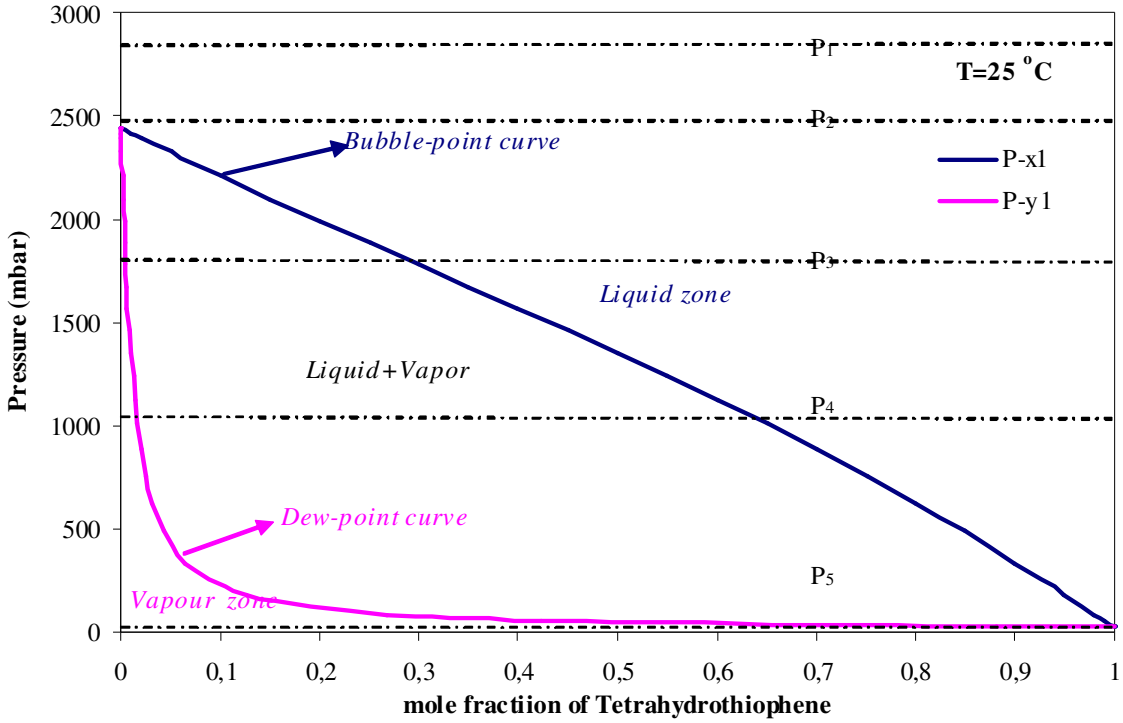

Figure 35: Vapor-Liquid equilibrium for Tetrahydrothiophene (1) / *n*-Butane (2) / at 25 °C. The solid curve shows the COSMOtherm predictions

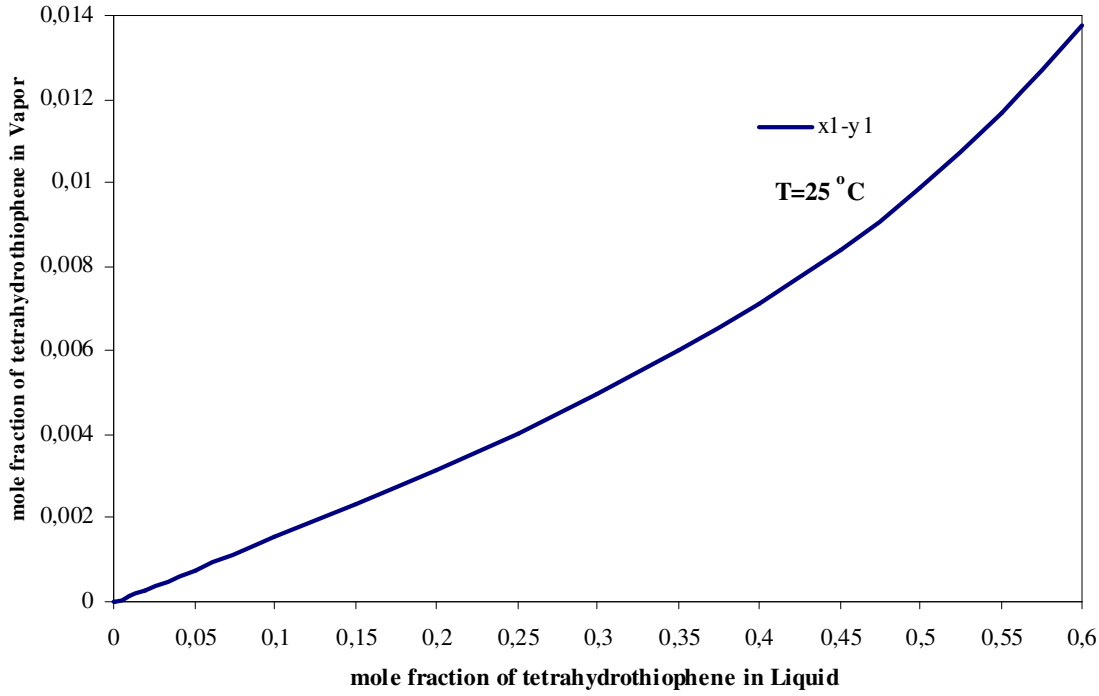

Figure 36: The X-Y diagram for Tetrahydrothiophene (1) / *n*-Butane (2) at 25 °C. The solid curve shows the COSMOtherm predictions

Dimethylsulfide – n-Butane binary system

The Figure shows the vapor liquid equilibrium data for dimethylsulfide (1)/*n*-butane (2) at fixed temperature 25 °C and the vapor-liquid phase diagram is calculated by using COSMOtherm. Figure shows the amount of dimethylsulfide in vapor and liquid phases. A point on this curve shows the variations of dimethylsulfide in liquid that is in equilibrium with dimethylsulfide in vapor at different pressures. The remaining mole percentage in both cases is *n*-Butane.

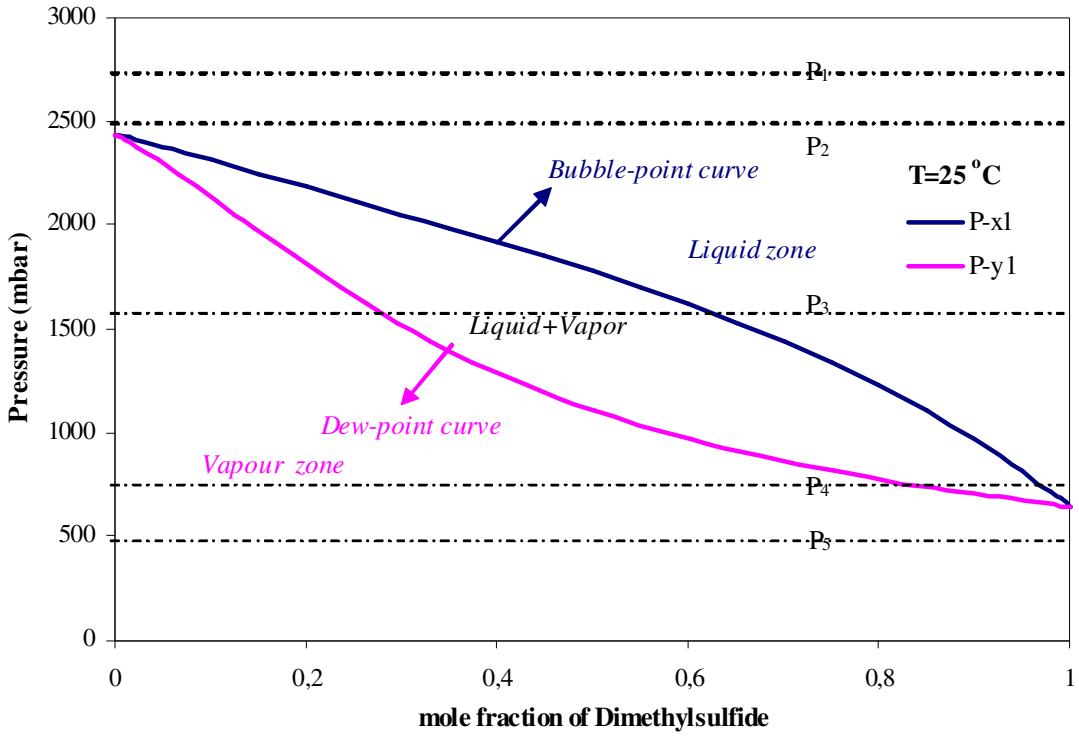

Figure 37: Vapor-Liquid equilibrium for Dimethylsulfide (1) / *n*-Butane (2) at 25 °C. The solid curve shows the COSMOtherm predictions

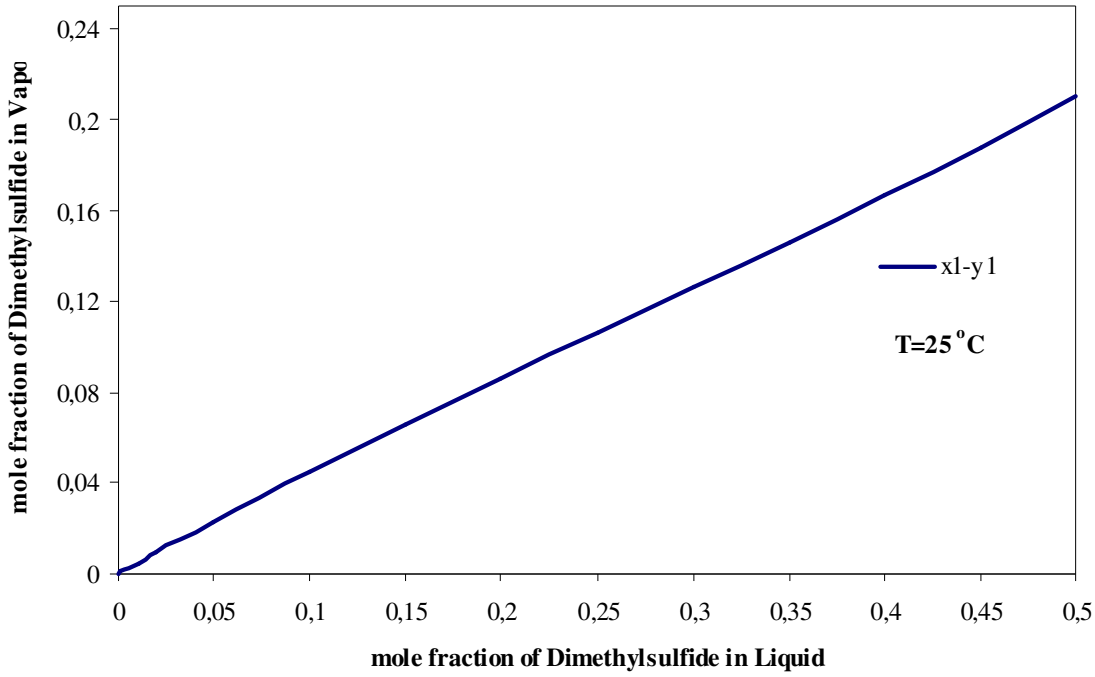

Figure 38: The X-Y diagram for Dimethylsulfide (1) / *n*-Butane (2) at 25 °C. The solid curve shows the COSMOtherm predictions

2.2.4-Trimethyl pentane – n-Butane binary system

The Figure 39 shows the vapor liquid equilibrium data for 2,2,4-triethylpentane (1) / *n*-butane (2) at fixed temperature 25 °C. The Figure shows the amount of 2,2,4 trimethyl pentane in vapor phase equilibrium with amount of 2,2,4 trimethyl pentane liquid phase. Here any point on this curve shows the variations of dimethylsulfide in liquid that is in equilibrium with dimethylsulfide in vapor at different pressures. The remaining mole percentage in both cases is *n*-Butane.

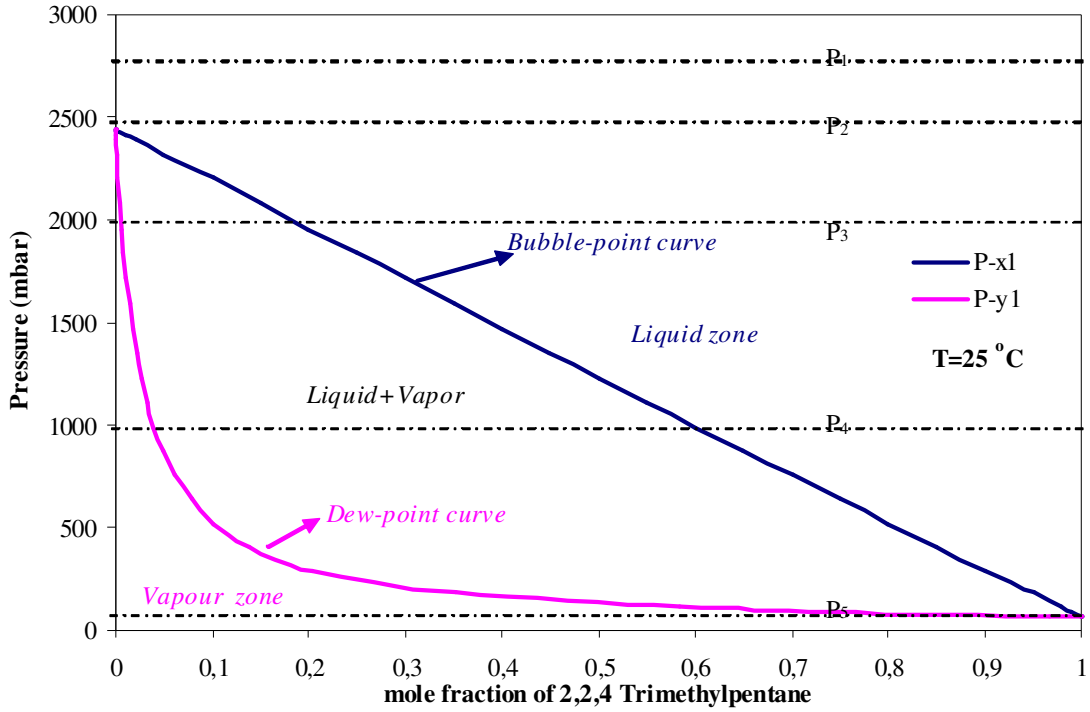

Figure 39: Vapor-Liquid equilibrium for 2, 2, 4Trimethyl-2-pentane (1) / *n*-Butane (2) at 25 °C. The solid curve shows the COSMOtherm predictions

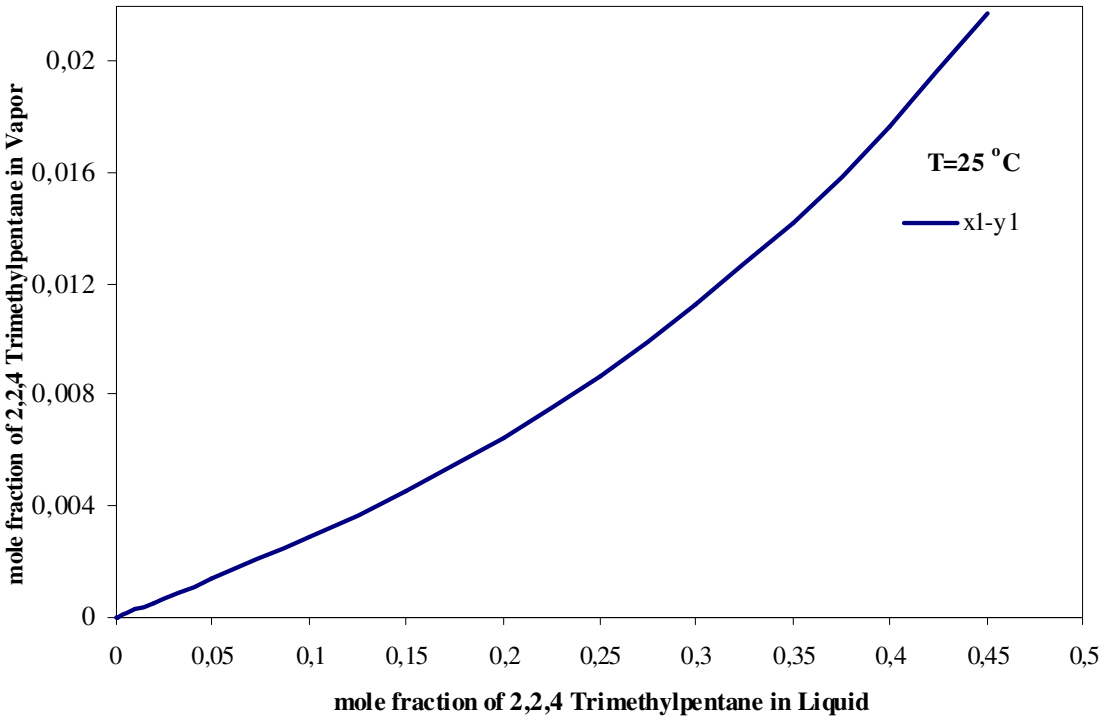

Figure 40: The X-Y diagram for 2, 2, 4 Trimethyl-2-pentane (1) / *n*-Butane (2) at 25 °C. The solid curve shows the COSMOtherm predictions

Picoline – n-Butane binary system

The Figure shows the vapor liquid equilibrium data for 2-methyl pyridine (1)/*n*-butane (2) at fixed temperature 25 °C and the vapor-liquid phase diagram is calculated by using COSMOtherm. The Figure shows the amount of 2-methyl pyridine in vapor and liquid phases. A point on this curve shows the variations of 2-methyl pyridine in liquid that is in equilibrium with 2-methyl pyridine in vapor at different pressures. The remaining mole percentage in both cases is *n*-Butane. In Figure , most of the 2-methyl pyridine is in liquid at room temperature because the boiling point of this compound is very high.

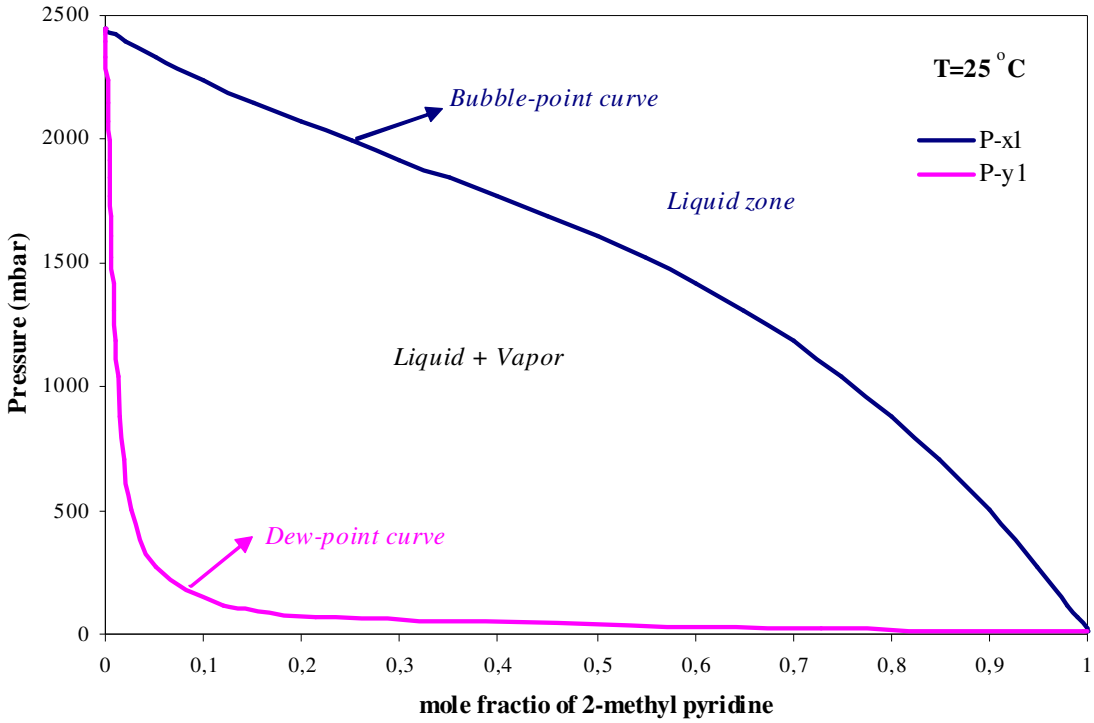

Figure 41: Vapor-Liquid equilibrium for 2-methylpyridine (1) / *n*-Butane (2) at 25 °C. The solid curve shows the COSMOtherm predictions

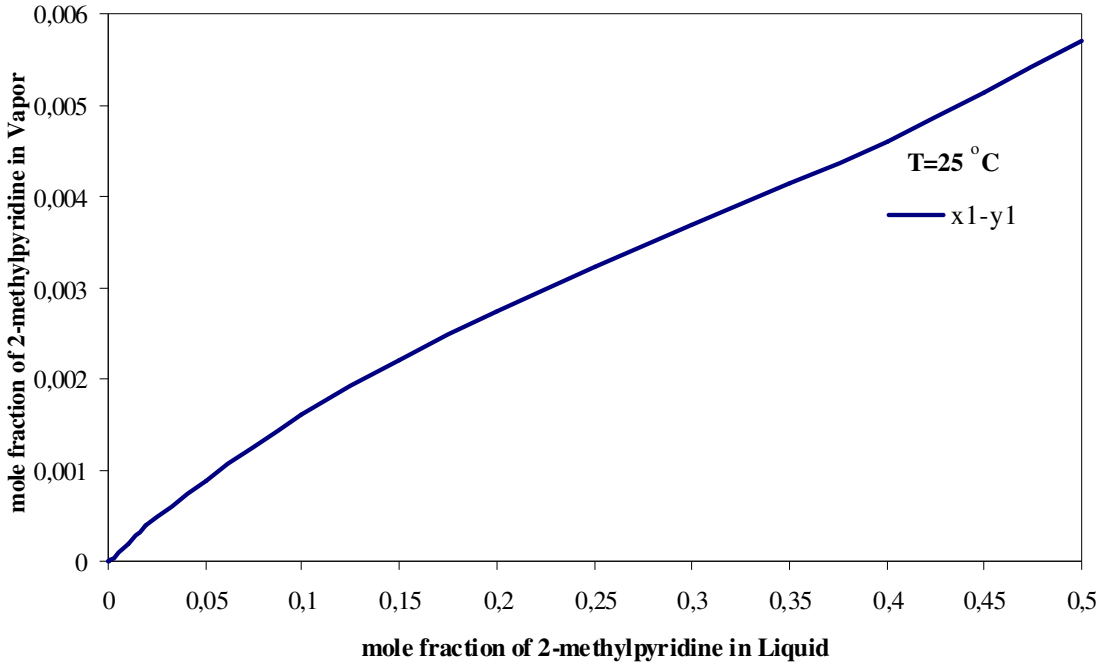

Figure 42: The X-Y diagram for 2-methylpyridine (1) / *n*-Butane (2) at 25 °C. The solid curve shows the COSMOtherm predictions

1.8- Cineole – n-Butane binary system

Figure shows the vapor liquid equilibrium data for 1,8- Cineole (1)/ *n*-butane (2) at fixed temperature 25 °C. The mole fraction of 1,8 cineole in vapor and liquid phases are shown in Figure , In this binary system, a point on the equilibrium curve separated into the mole percentage of the vapor that is substance 1,8- Cineole on the y-axis and the mole percentage of liquid that is 1,8- Cineole on the x-axis. The remaining mole percentage in both cases is *n*-Butane.

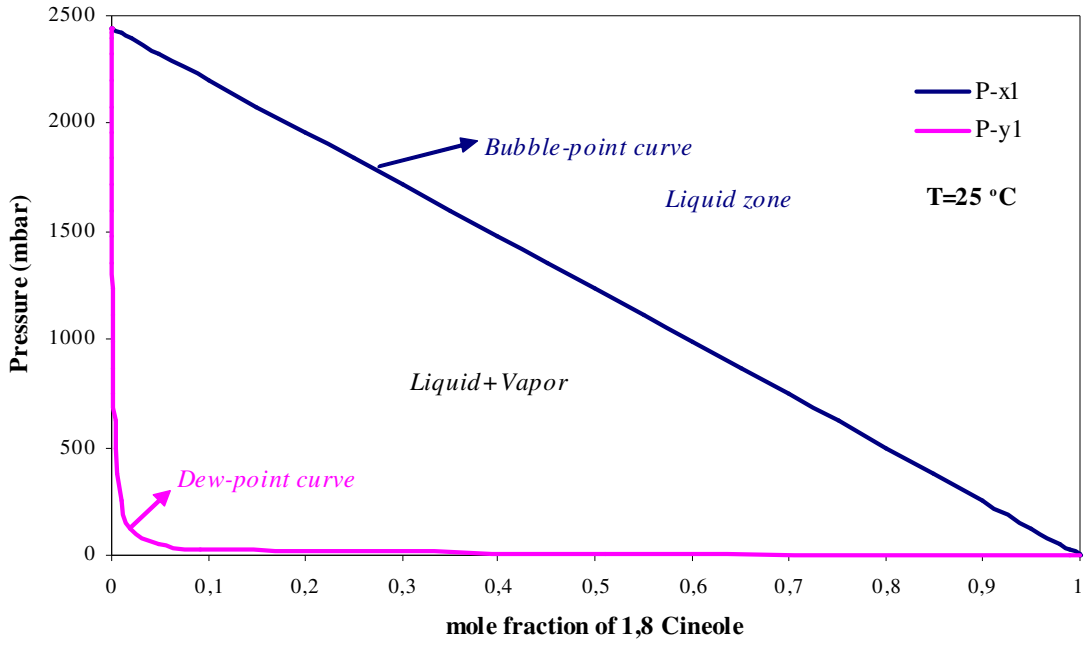

Figure 43: Vapor-Liquid equilibrium for 1, 8 Cineole (1) / *n*-Butane (2) at 25 °C. The solid curve shows the COSMOtherm predictions

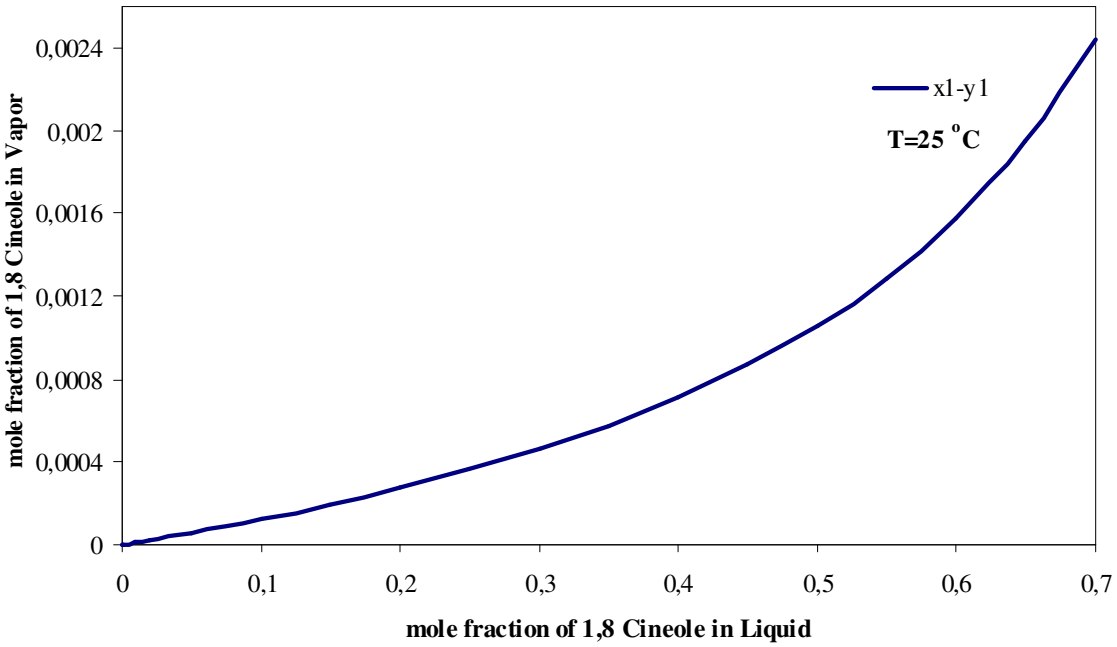

Figure 44: The X-Y diagram for 1, 8 Cineole (1) / *n*-Butane (2) at 25 °C. The solid curve shows the COSMOtherm predictions

Nitrobenzene– n-Butane binary system

Figure shows the vapor liquid equilibrium data for nitrobenzene (1) / *n*-butane (2) at fixed temperature 25 °C. In this diagram, the large amount of nitrobenzene is appearing in mixture zone and liquid zone. The boiling point of nitrobenzene is very high, so small amount of nitrobenzene occur in vapor phase. Figure shows the amount of nitrobenzene in vapor and liquid phases at different pressures.

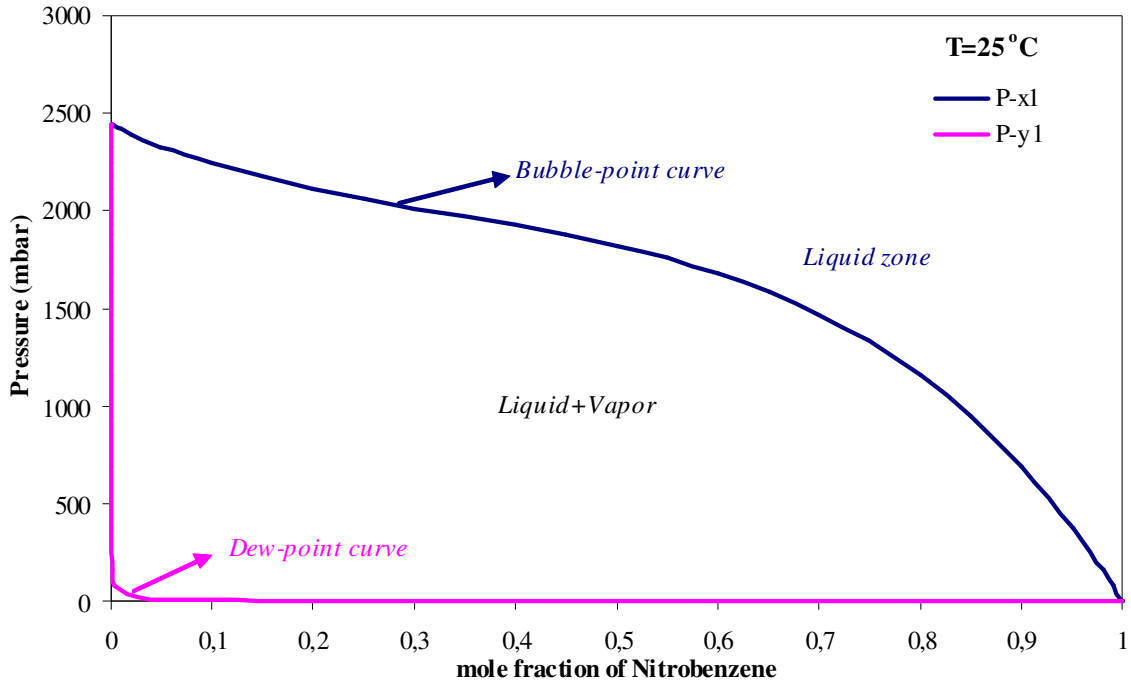

Figure 45: Vapor-Liquid equilibrium for Nitrobenzene (1) / *n*-Butane (2) at 25 °C. The solid curve shows the COSMOtherm predictions

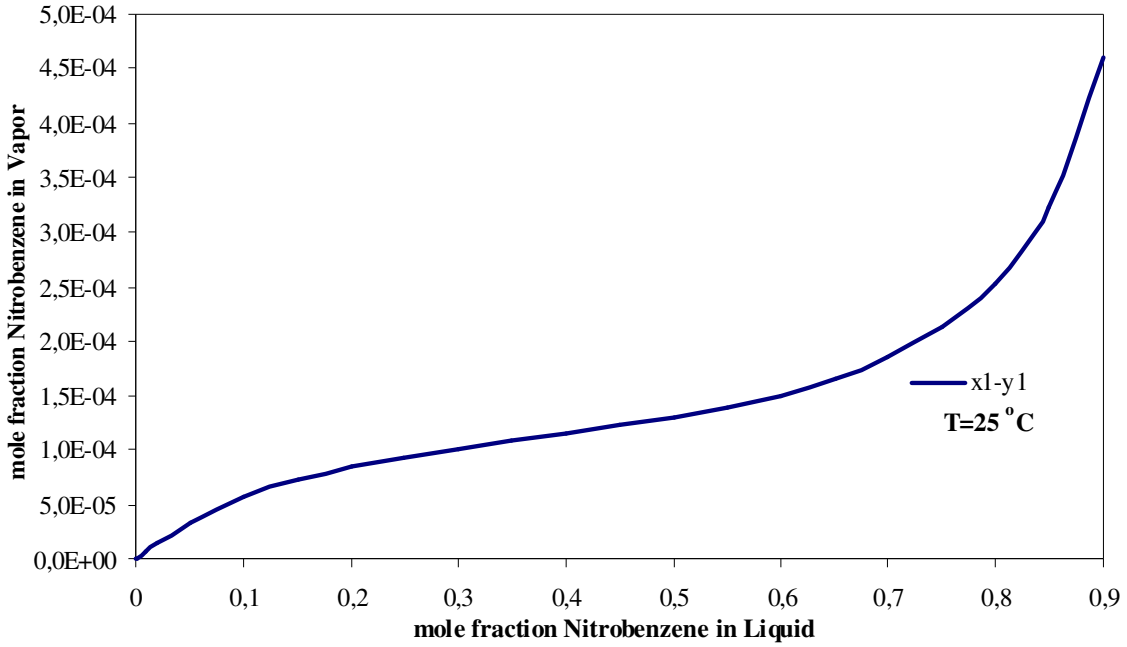

Figure 46: The X-Y diagram for Nitrobenzene (1) / *n*-Butane (2) at 25 °C. The solid curve shows the COSMOtherm predictions

1-Pentanol – n-Butane binary system

Figure shows the vapor liquid equilibrium data for 1-pentanol (1) / *n*-butane (2) at 25 °C. Figure shows the variation of amount of 1-pentanol in vapor phase and the amount of 1-pentanol in liquid phase at different pressures. The remaining mole fraction in both cases is *n*-butane.

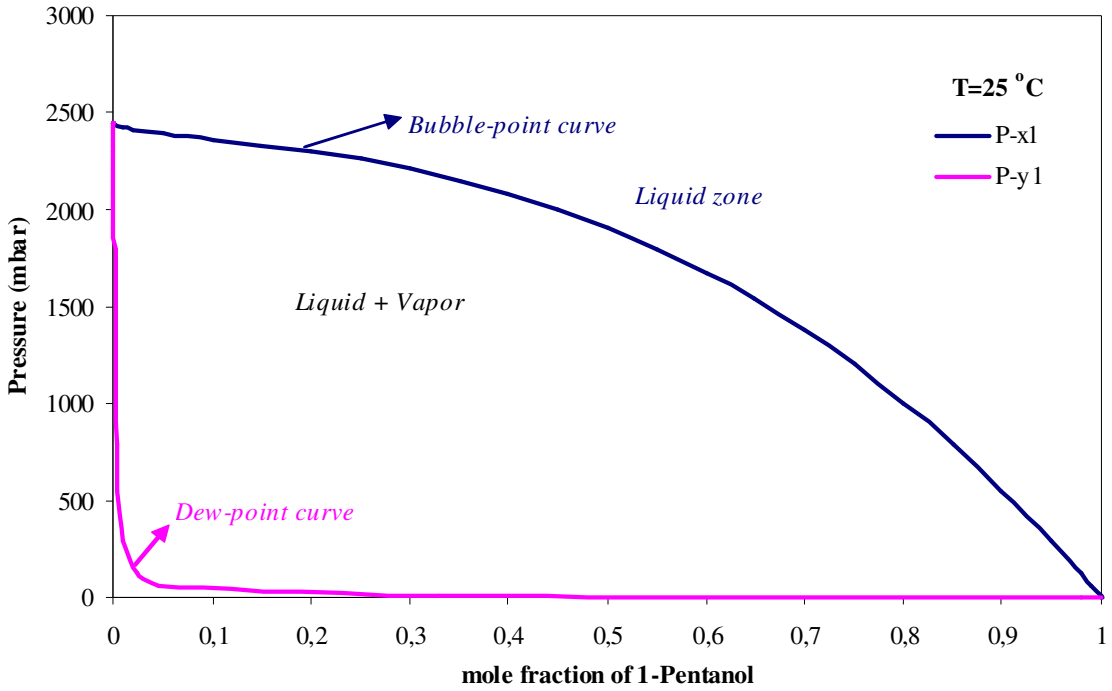

Figure 47: Vapor-Liquid equilibrium for 1-Pentanol (1) / *n*-Butane (2) at 25 °C. The solid curve shows the COSMOtherm predictions

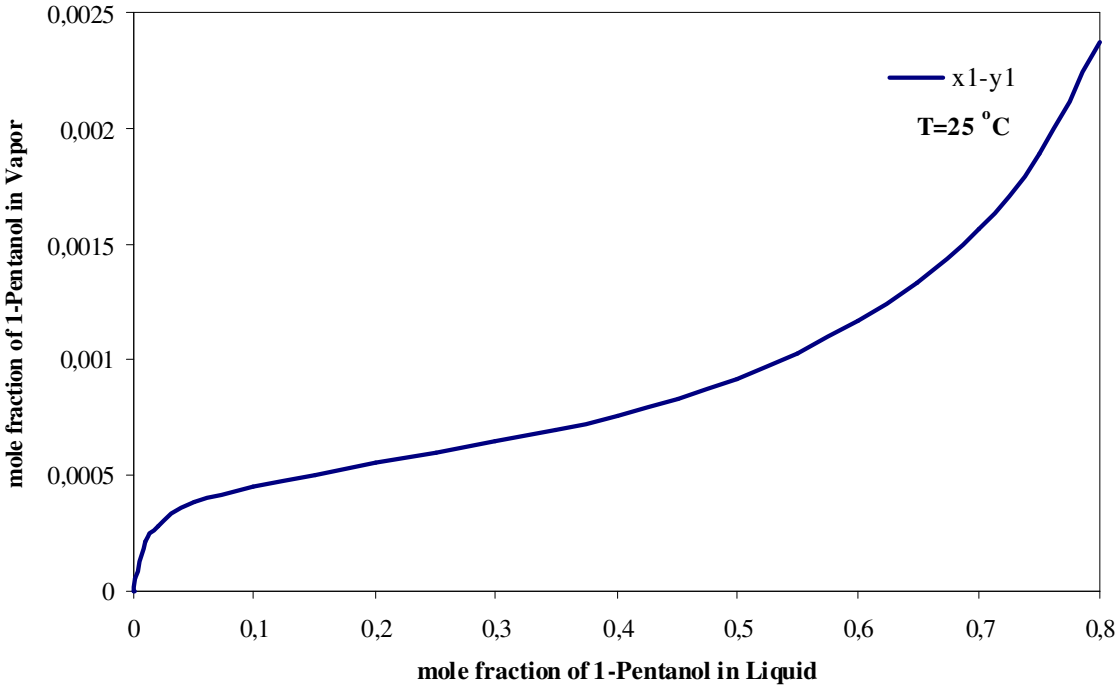

Figure 48: The X-Y diagram for 1-Pentanol (1) / *n*-Butane (2) at 25 °C. The solid curve shows the COSMOtherm predictions

Sulfurylchloride – n-Butane binary system

Figure shows the vapor liquid equilibrium data for sulfurylchloride (1)/*n*-butane (2) at 25 °C and the vapor-liquid phase diagram is calculated by setting isothermal option at a fixed temperature (25 °C) in COSMOtherm. The x-y diagram (Figure) shows the vapor-liquid equilibrium data of this binary system, a point on the equilibrium curve separated into the mole percentage of the vapor that is sulfurylchloride on the y-axis and the mole percentage of liquid that is sulfurylchloride on the x-axis. The remaining mole percentage in both cases is *n*-Butane.

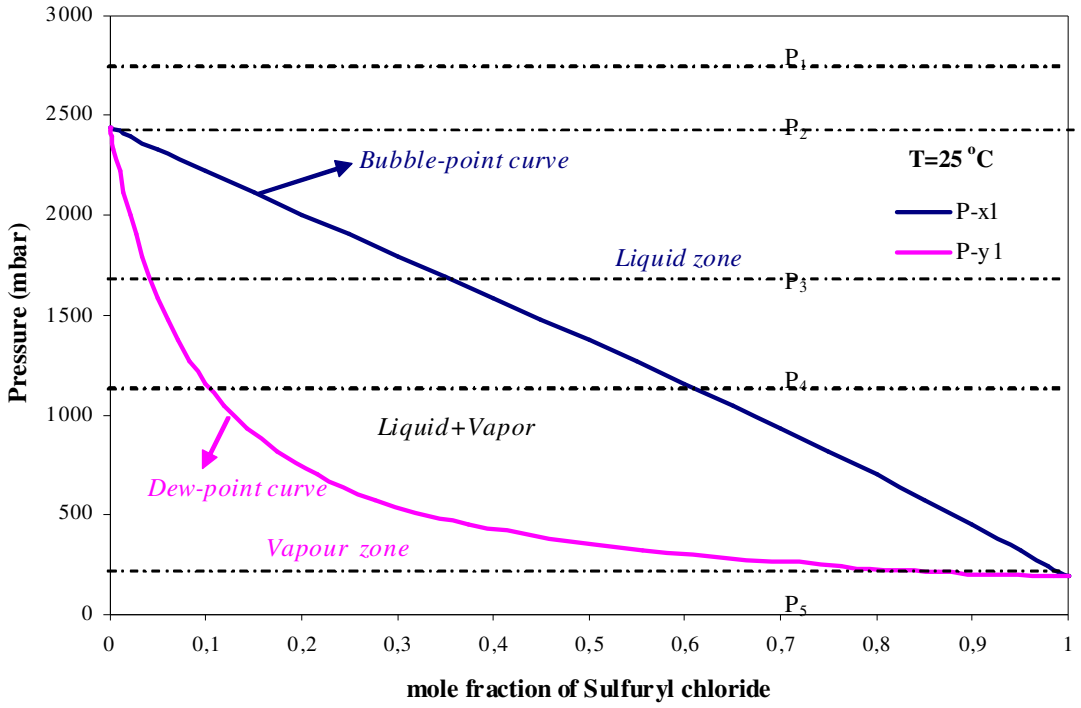

Figure 49: Vapor-Liquid equilibrium for Sulfuryl chloride (1) / *n*-Butane (2) at 25 °C. The solid curve shows the COSMOtherm predictions

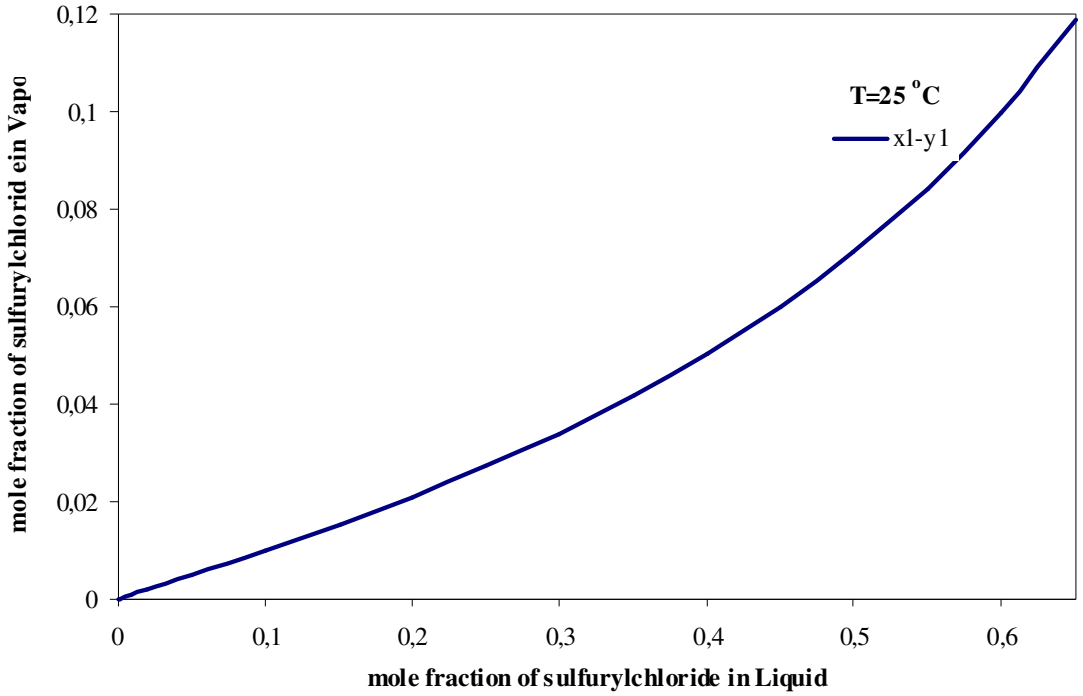

Figure 50: The X-Y diagram for Sulfuryl chloride (1) / *n*-Butane (2) at 25 °C. The solid curve shows the COSMOtherm predictions

Cyanogenchloride – n-Butane binary system

Figure 51 shows the vapor liquid equilibrium data for cyanogenchloride (1)/*n*-butane (2) at 25 °C. The vapor-liquid phase diagram is calculated by using COSMOtherm at fixed temperature 25 °C. In Figure 52, the point A is called an azeotropic point. At this point, the mixture behaves as a pure substance and these azeotropic mixtures cannot separated by ordinary distillation.

Since we are concerned with very low concentrations, this unusual behavior is not relevant here. Figure shows the vapor-liquid equilibrium data, in this binary system, a point on the equilibrium curve separated into the mole percentage of the vapor that is cyanogen chloride on the y-axis and the mole percentage of liquid that is cyanogen chloride on the x-axis. The remaining mole percentage in both cases is *n*-Butane.

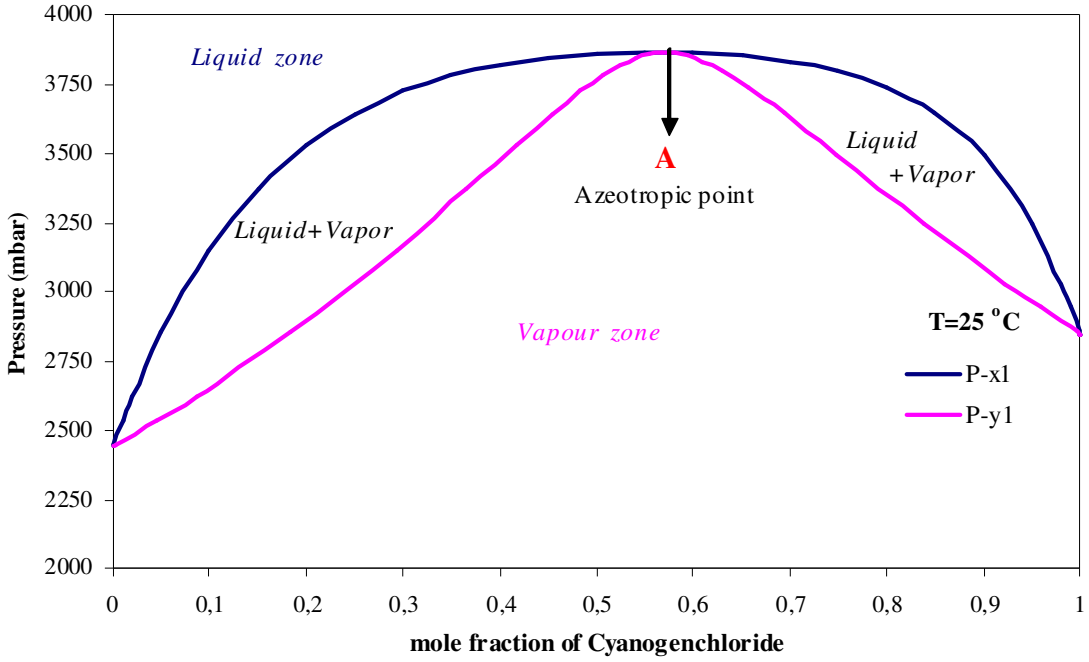

Figure 51: Vapor-Liquid equilibrium for Cyanogen chloride (1) / *n*-Butane (2) at 25 °C. The solid curve shows the COSMOtherm predictions

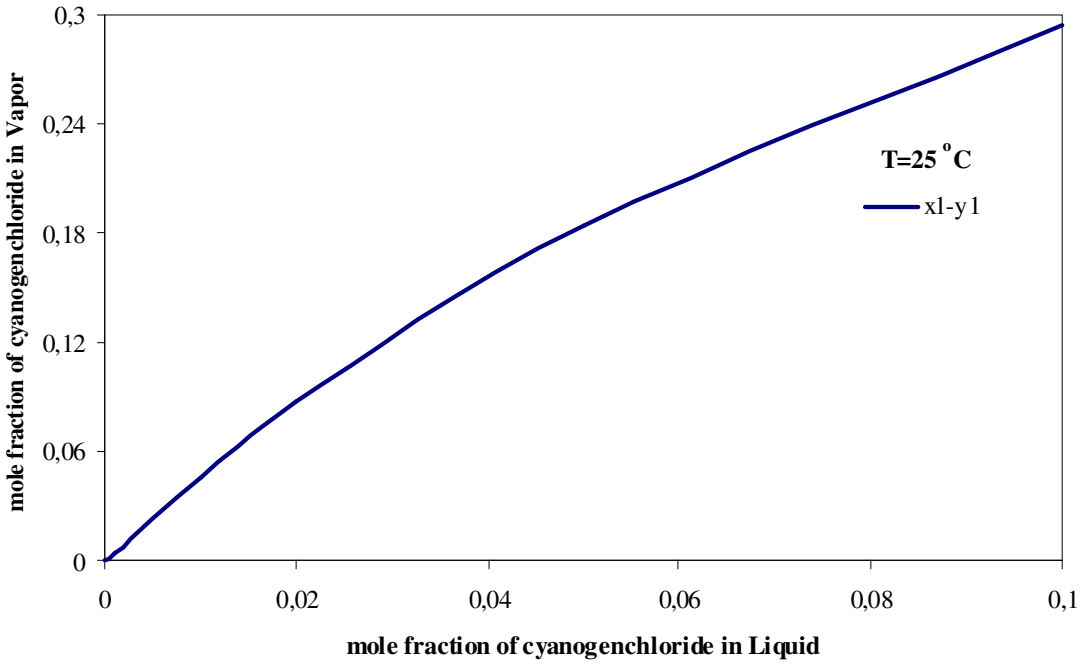

Figure 52: The X-Y diagram for Cyanogen chloride (1) / *n*-Butane (2) at 25 °C. The solid curve shows the COSMOtherm predictions

Based on its phase behaviour properties with *n*-butane, cyanogen chloride is considered a candidate additive, for example the concentrations in each phase are similar (e.g. at a mol fraction of 0.02 in the liquid, the vapor phase concentration is 0.09).

Bis-(2-chloroethyl) sulfide – n-Butane binary system

The phase behavior of this system is shown in figures 53 and 54. It is not considered a good candidate.

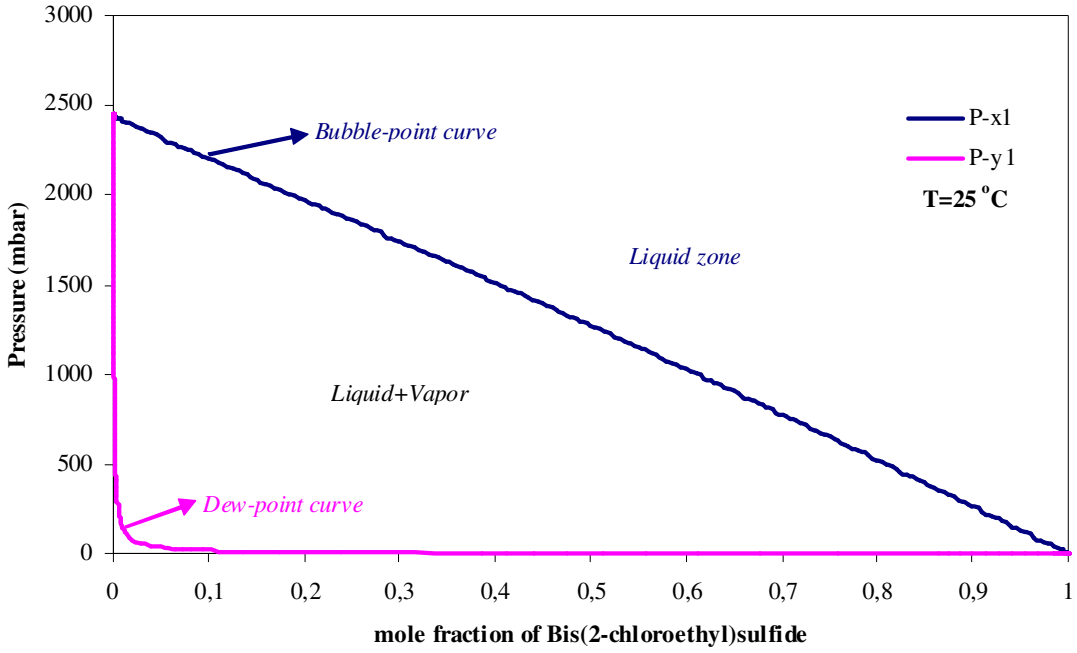

Figure 31: Vapor-Liquid equilibrium for Bis(2-chloroethyl)sulfide (1) / *n*-Butane (2) at 25 °C. The solid curve shows the COSMOtherm predictions

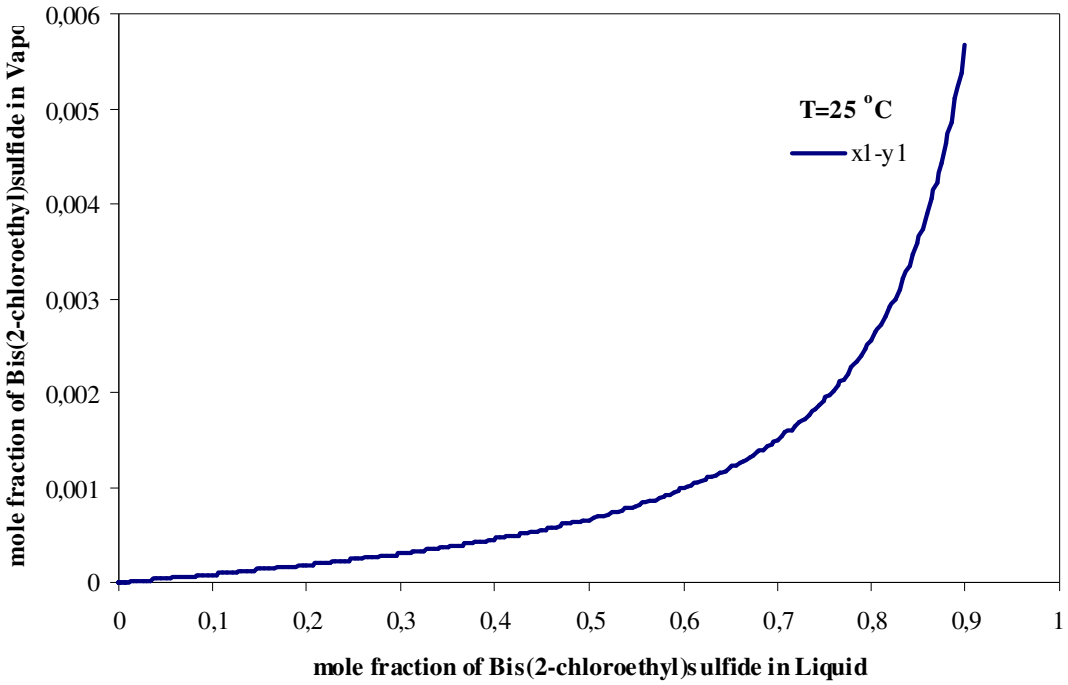

Figure 54: The X-Y diagram for Bis(2-chloroethyl)sulfide (1) / *n*-Butane (2) at 25 °C. The solid curve shows the COSMOtherm predictions

Bis-(2-chloroethyl) ethylamine– n-Butane binary system

The phase behavior of this system is shown in figures 55 and 56. It is not considered a good candidate.

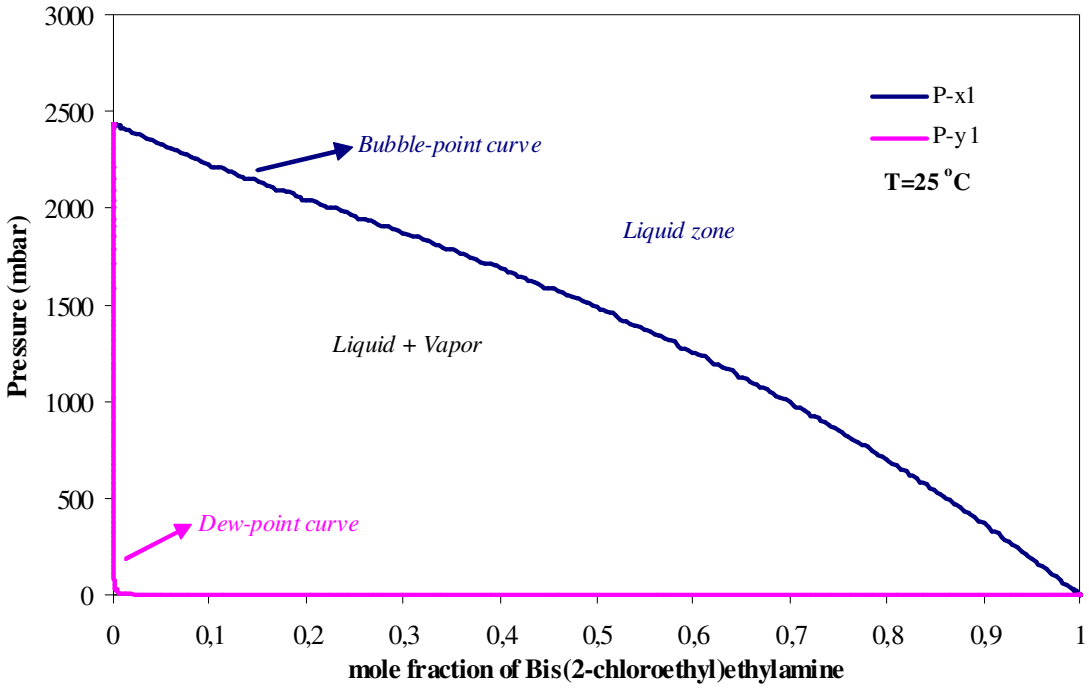

Figure 55: Vapor-Liquid equilibrium for Bis(2-chloroethyl)ethylamine (1) / *n*-Butane (2) at 25 °C. The solid curve shows the COSMOtherm predictions

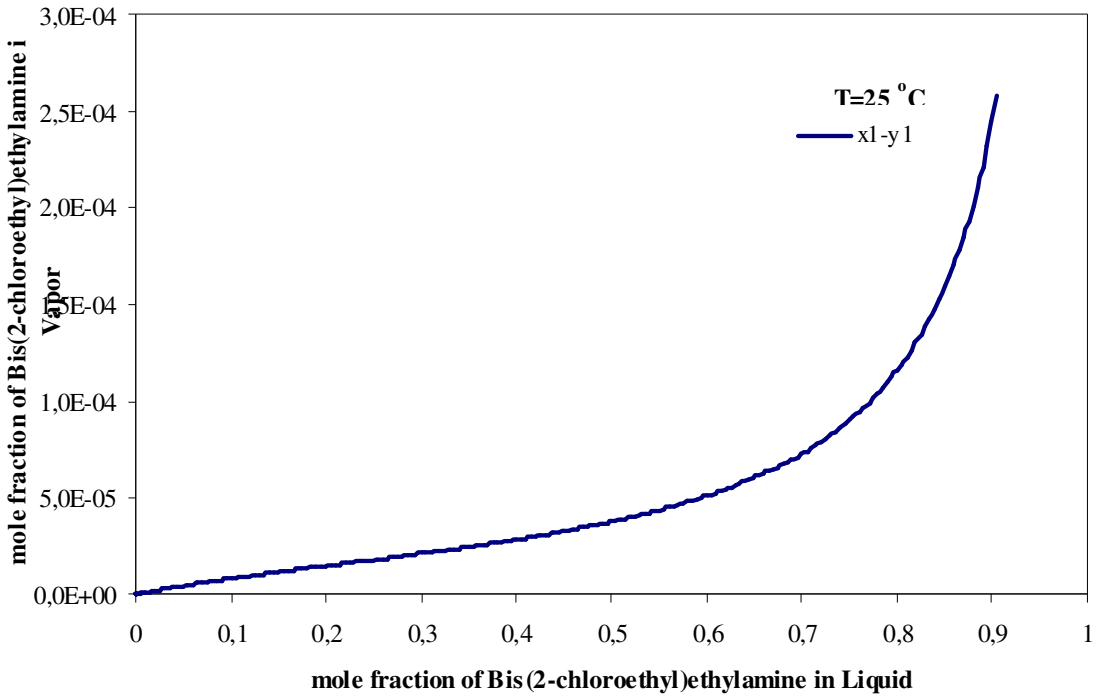

Figure 56: Vapor-Liquid equilibrium for Bis(2-chloroethyl)ethylamine (1) / *n*-Butane (2) at 25 °C. The solid curve shows the COSMOtherm predictions

Dichloroethylarsine – n-Butane binary system

Figure shows the vapor liquid equilibrium data for dichloroethylarsine (1)/*n*-butane (2) at 25°C. Figure shows the variation of mole fraction of dichloroethylarsine in vapor and liquid phases at different pressure. In this binary system, a point on the equilibrium curve represents the mole fraction of the vapor that is dichloroethylarsine on the y-axis and the mole fraction of liquid that is dichloroethylarsine on the x-axis.

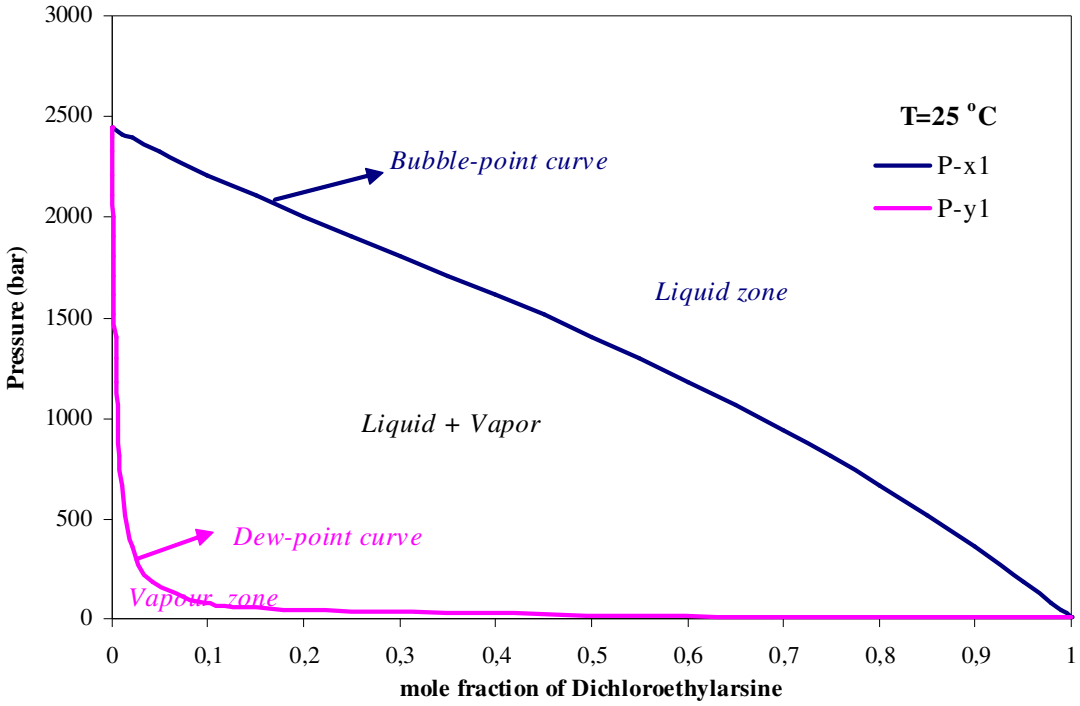

Figure 57: Vapor-Liquid equilibrium for Dichloroethylarsine (1) / *n*-Butane (2) at 25 °C. The solid curve shows the COSMOtherm predictions

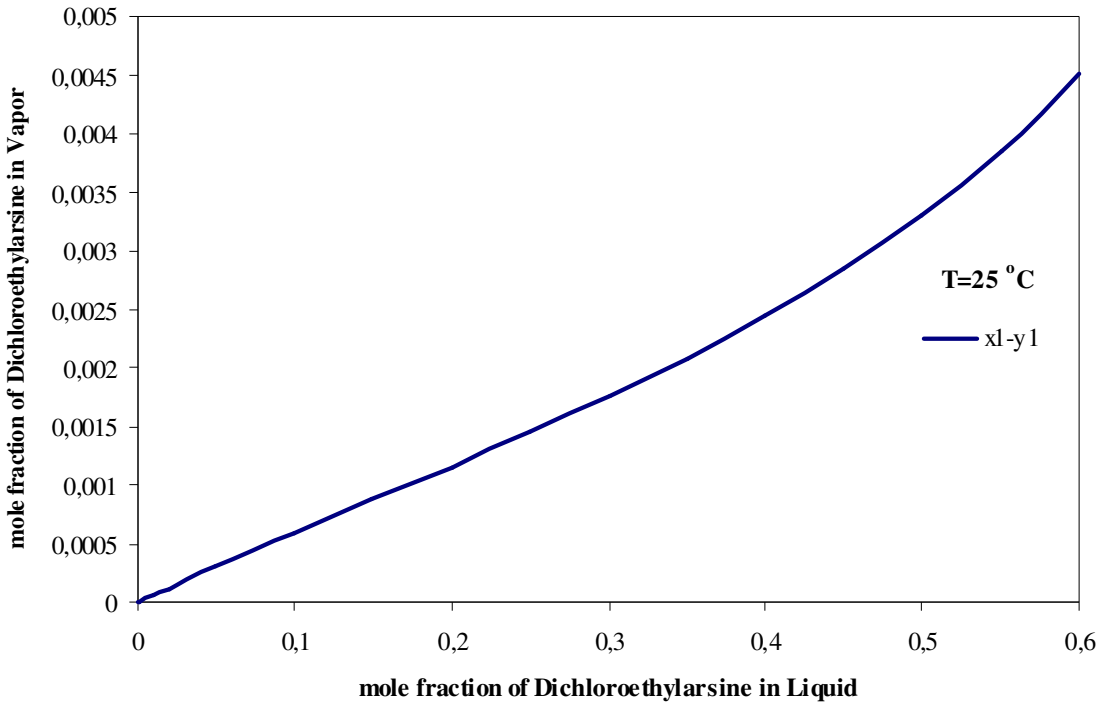

Figure 58: The X-Y diagram for Dichloroethylarsine (1) / *n*-Butane (2) at 25 °C. The solid curve shows the COSMOtherm predictions

Bromobenzylcyanide – n-Butane binary system

Figure shows the vapor liquid equilibrium data for bromobenzylcyanide (1)/*n*-butane (2) at 25°C. Figure shows the variation of mole fraction of bromobenzylcyanide in vapor and liquid phases at different pressure. In this binary system, a point on the equilibrium curve represents the mole fraction of the vapor that is bromobenzylcyanide on the y-axis and the mole fraction of liquid that is bromobenzylcyanide on the x-axis. However it is considered that this very large molecule with a high boiling point would not be a suitable deterrent additive to butane.

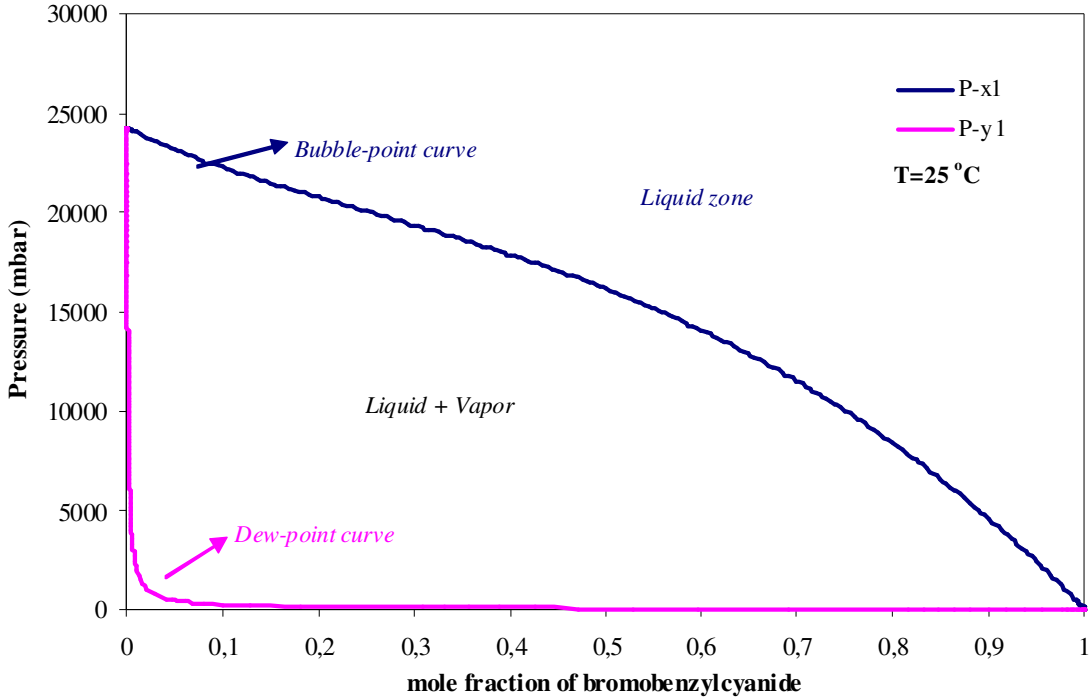

Figure 59: Vapor-Liquid equilibrium for Bromobenzylcyanide (1) / *n*-Butane (2) at 25 °C. The solid curve shows the COSMOtherm predictions

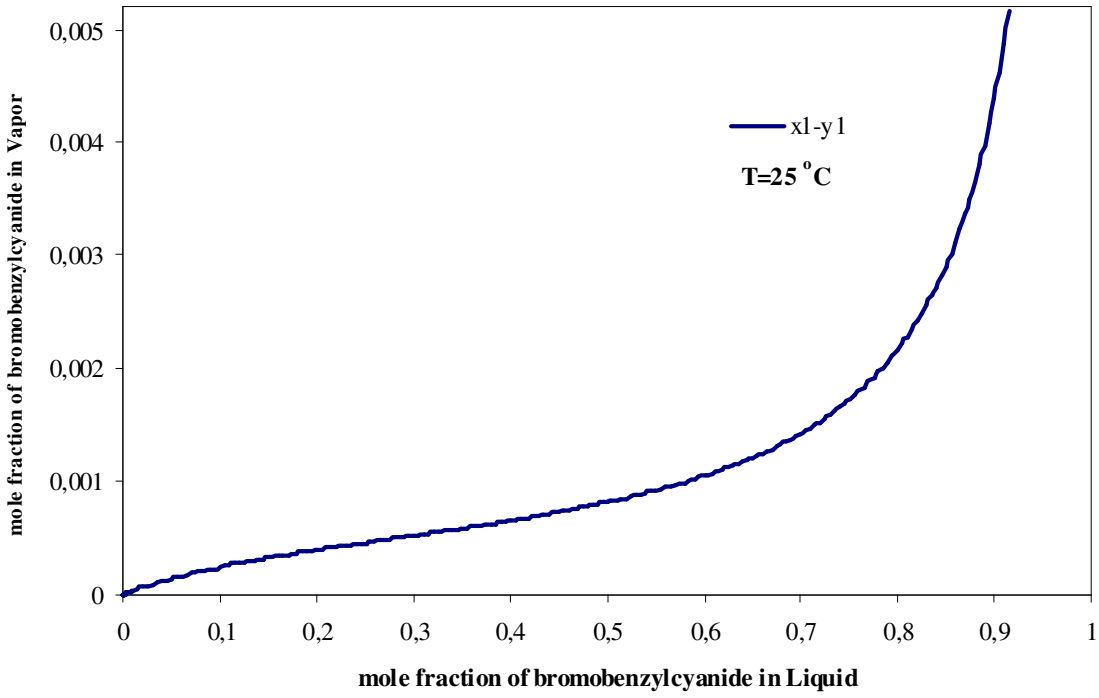

Figure 60: The X-Y diagram for Bromobenzylcyanide (1) / *n*-Butane (2) at 25 °C. The solid curve shows the COSMOtherm predictions

Chloropicrin– n-Butane binary system

Figure shows the vapor liquid equilibrium data for chloropicrin (1)/*n*-butane (2) at 25°C. Figure shows the variation of mole fraction of chloropicrin in vapor and liquid phases at different pressure. In this binary system, a point on the equilibrium curve represents the mole fraction of the vapor that is chloropicrin on the y-axis and the mole fraction of liquid that is chloropicrin on the x-axis. However it is considered that this very large molecule with a high boiling point would not be a suitable deterrent additive to butane.

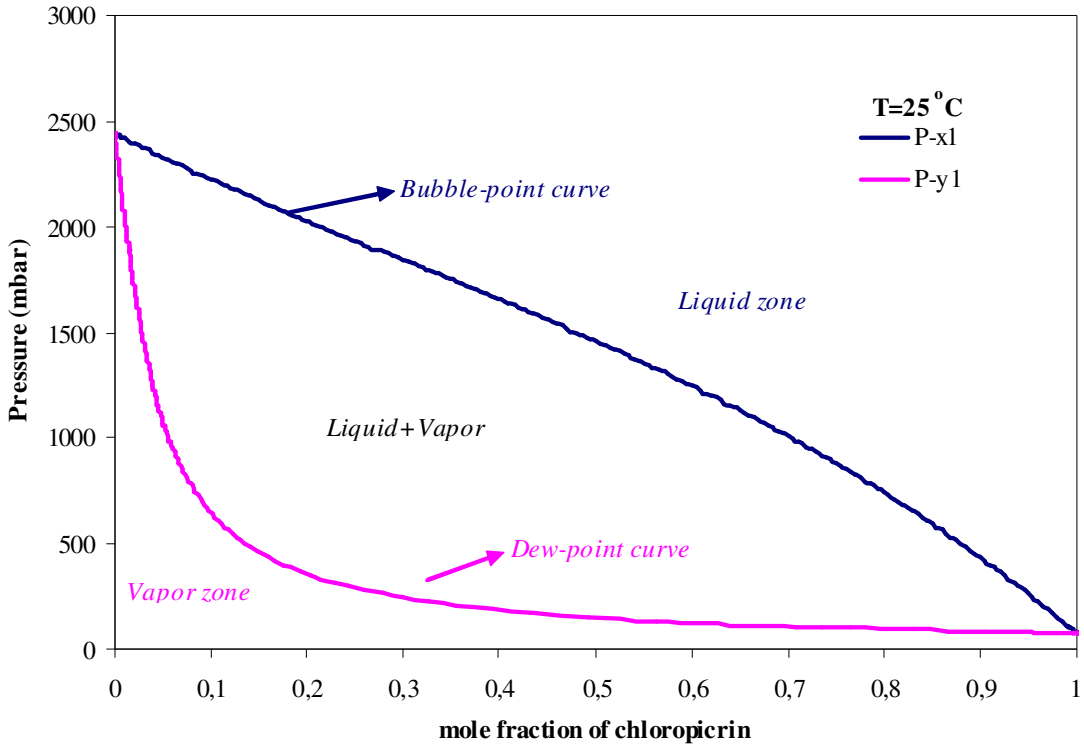

Figure 61: Vapor-Liquid equilibrium for Chloropicrin (1) / *n*-Butane (2) at 25 °C. The solid curve shows the COSMOtherm predictions

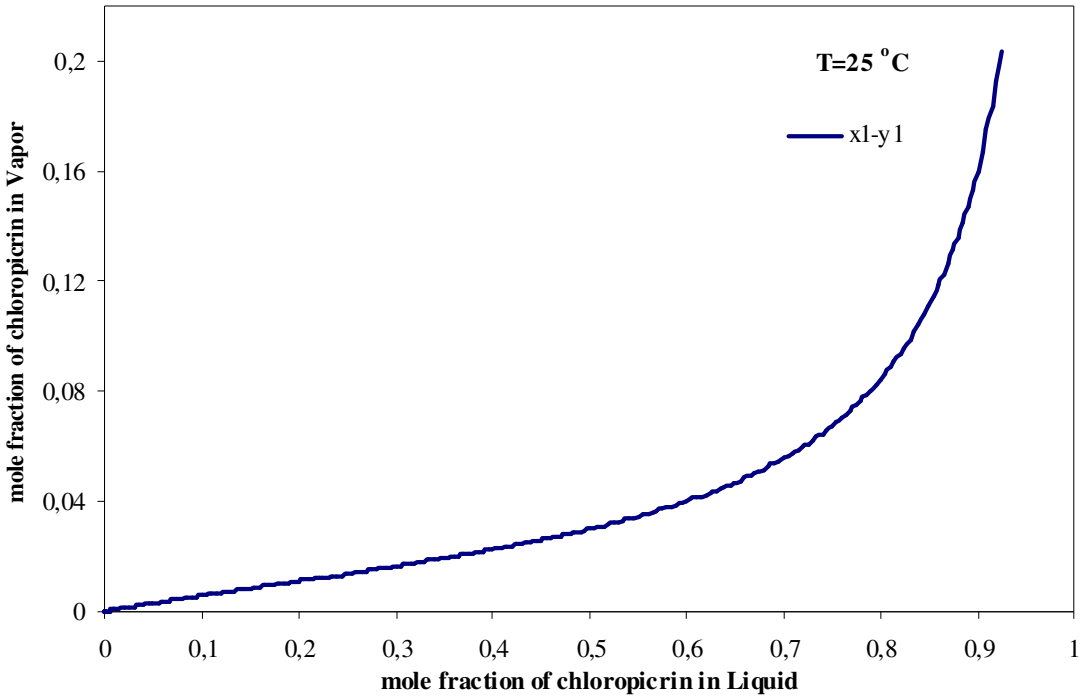

Figure 62: The X-Y diagram for Chloropicrin (1) / *n*-Butane (2) at 25 °C. The solid curve shows the COSMOtherm predictions

Diphenylcyanoarsine– n-Butane binary system

Figure shows the vapor liquid equilibrium data for Diphenylcyanoarsine (1)/*n*-butane (2) at 25 °C. It is considered that this very large molecule with a high boiling point would not be a suitable deterrent additive to butane.

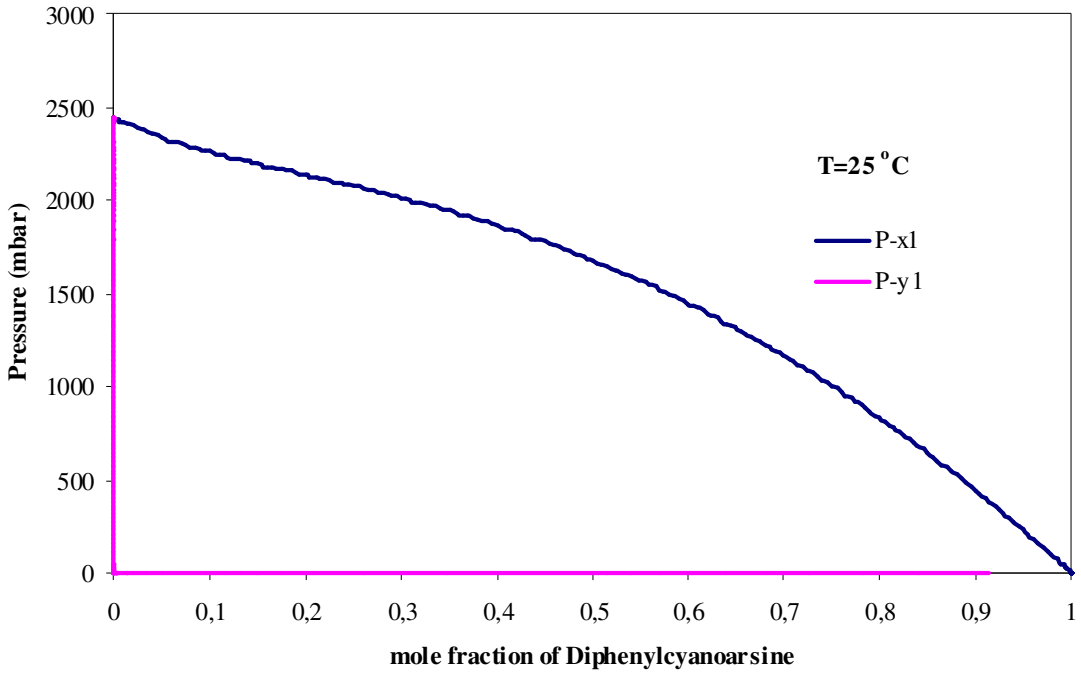

Figure 63: Vapor-Liquid equilibrium for Chloropicrin (1) / *n*-Butane (2) at 25 °C. The solid curve shows the COSMOtherm predictions

Ethylmercaptan – n-Butane binary system

The Figure shows the phase behavior of ethylmercaptan (1)/*n*-butane (2) binary system at 25 °C. The Figure shows the mole fraction of ethylmercaptan in vapor phase and liquid phases at different pressure.

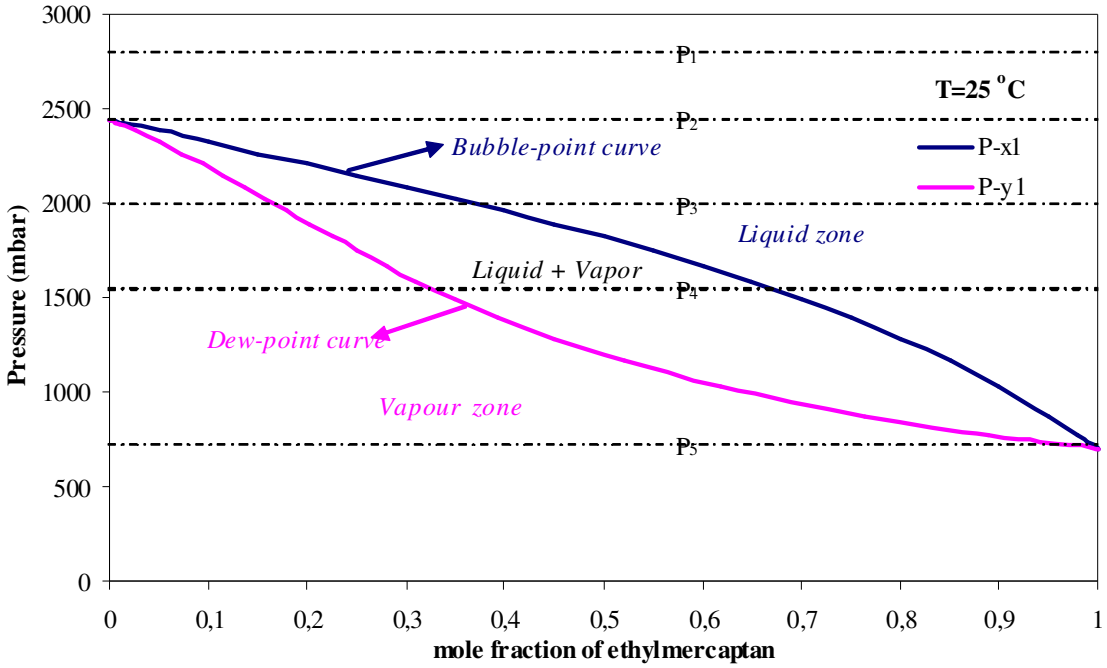

Figure 64: Vapor-Liquid equilibrium for Ethylmercaptan (1) / *n*-Butane (2) at 25 °C. The solid curve shows the COSMOtherm predictions

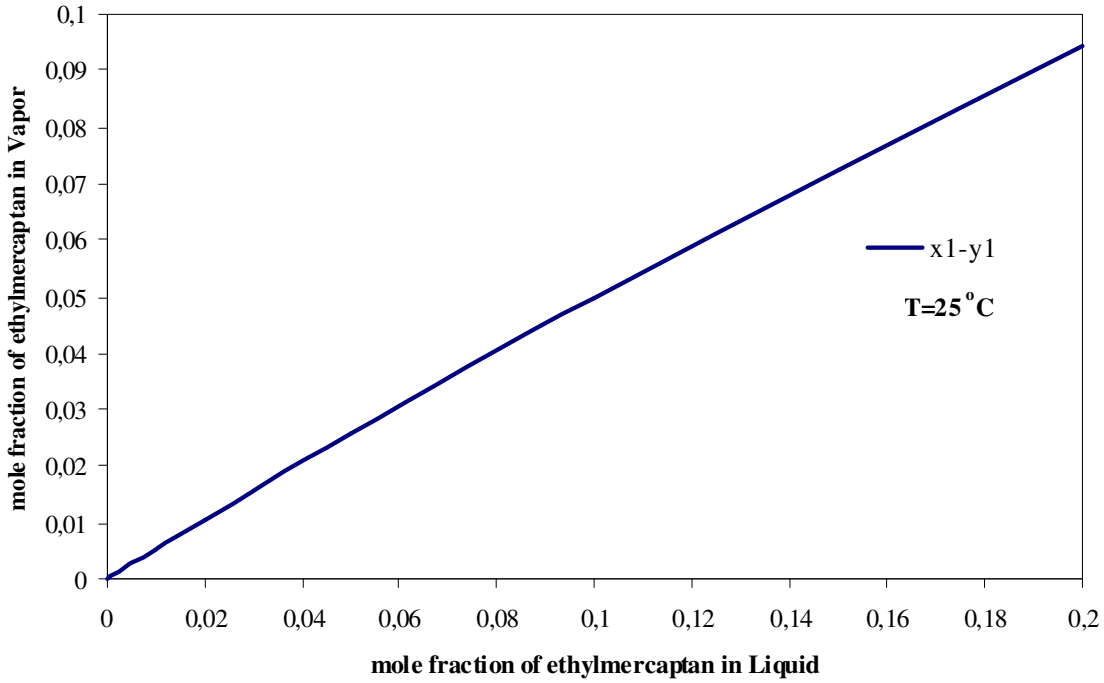

Figure 65: The X-Y diagram for Ethylmercaptan (1) / *n*-Butane (2) at 25 °C. The solid curve shows the COSMOtherm predictions

This compound may be a good candidate, but will not be considered further, as the focus of this work is substances other than mercaptans.

Bis(chloromethyl)ether – n-Butane binary system

The Figure shows the vapor liquid equilibrium data for bis(chloromethyl)ether (1) / *n*-butane (2) at 25 °C. The LLE point found at pressure of 0.2225mbar and the pressure above this, mixture behaves as liquid. So this compound is not suitable to add to butane.

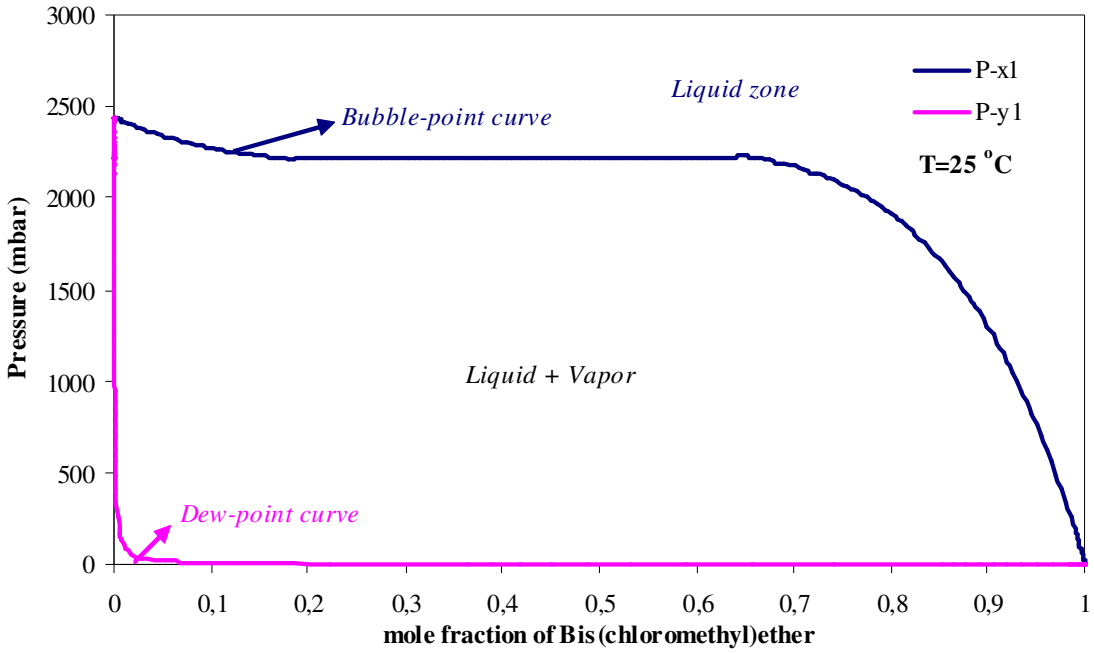

Figure 66: Vapor-Liquid equilibrium for Bis(chloromethyl)ether (1) / *n*-Butane (2) at 25 °C. The solid curve shows the COSMOtherm predictions

2- Aminophenol – n-Butane binary system

The Figure shows the vapor liquid equilibrium data for 2-aminophenol (1) and *n*-butane (2) at 25 °C. The LLE point found at pressure of 0,2423E+04mbar (composition of components (1) and (2) in liquid phase 1 and phase 2 at this pressure x'(1)=0,009119, x'(2)=0,990881, x"(1)=0,85277751, x"(2)=0,14722249) and the pressure above this, mixture behaves as liquid. So this compound is not suitable to add to butane.

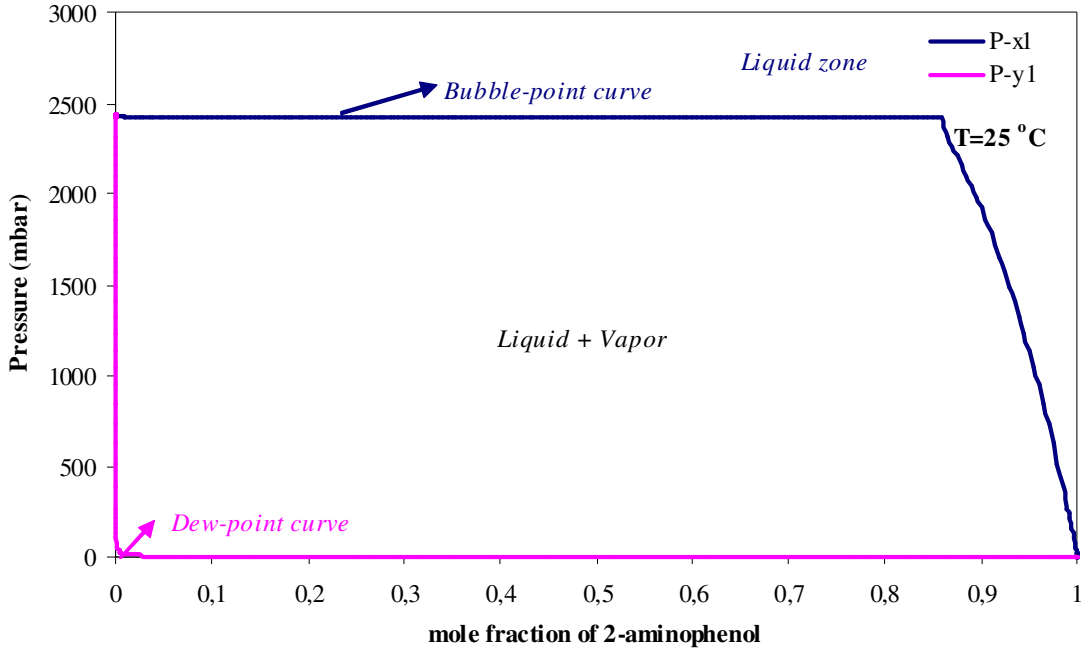

Figure 67: Vapor-Liquid equilibrium for 2-Amino phenol (1) / *n*-Butane (2) at 25 °C. The solid curve shows the COSMOtherm predictions

Propylene glycol – n-Butane binary system

The Figure shows the vapor liquid equilibrium data for propylene glycol (1) and *n*-butane (2) at 25 °C. The LLE point found at pressure of 0,2435E+04mbar (composition of components (1) and (2) in liquid phase 1 and phase 2 at this pressure x'(1)=0,0037, x'(2)=0,9963, x"(1)=0,774, x"(2)=0,226) and the pressure above this, mixture behaves as liquid. So this compound is not suitable to add to butane

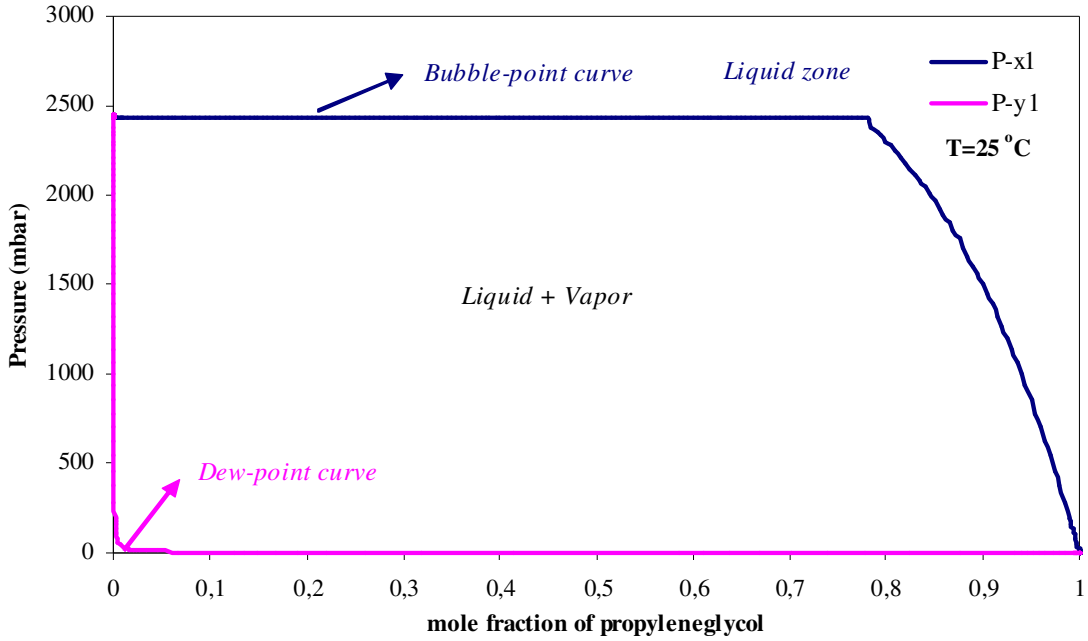

Figure 68: Vapor-Liquid equilibrium for Propylene glycol (1)/ *n*-Butane (2) at 25 °C. The solid curve shows the COSMOtherm predictions

s-Trioxane – n-Butane binary system

The Figure shows the vapor liquid equilibrium data for s-trioxane (1) and *n*-butane (2) at 25 °C. The LLE point found at pressure of 0,2304E+04mbar (composition of components (1) and (2) in liquid phase 1 and phase 2 at this pressure x'(1)=0,0785, x'(2)=0,9215, x"(1)=0,8327, x"(2)=0,1673) and the pressure above this, mixture behaves as liquid.

Chloroacetophenone– n-Butane binary system

The Figure shows the vapor liquid equilibrium data for chloroacetophenone (1) and *n*-butane (2) at 25 °C. The LLE point found at pressure of 0.2267E+04mbar (composition of components (1) and (2) in liquid phase 1 and phase 2 at this pressure x'(1)=0.0175, x'(2)=0.825, x"(1)=0.38, x"(2)=0.62) and the pressure above this, mixture behaves as liquid.

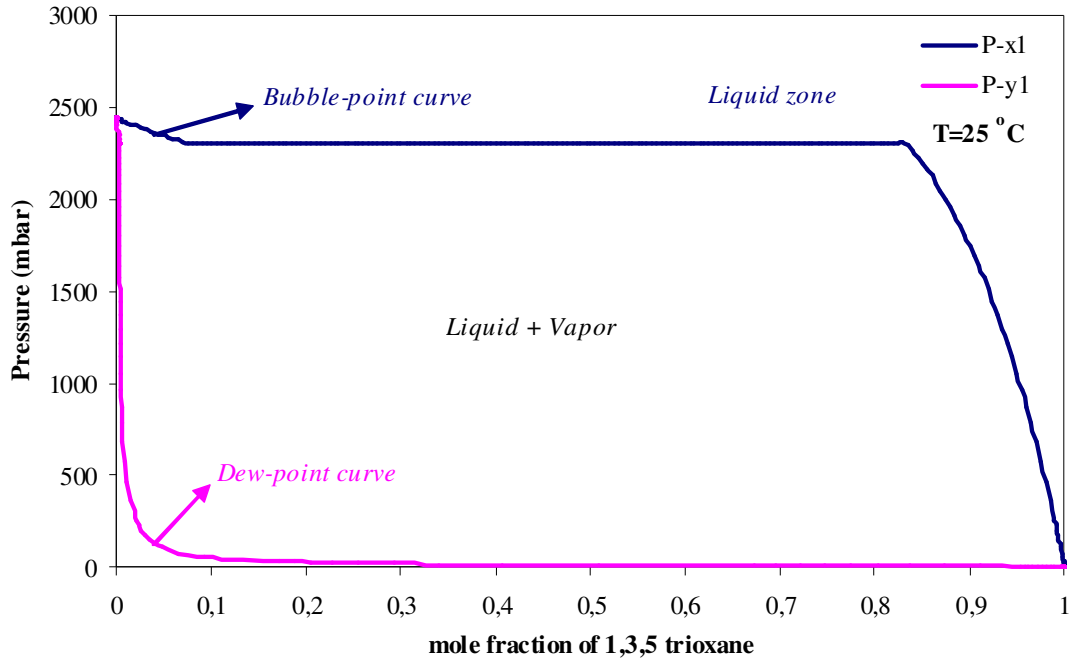

Figure 69: Vapor-Liquid equilibrium for 1, 3, 5 Trioxane (1) / *n*-Butane (2) at 25 °C. The solid curve shows the COSMOtherm predictions

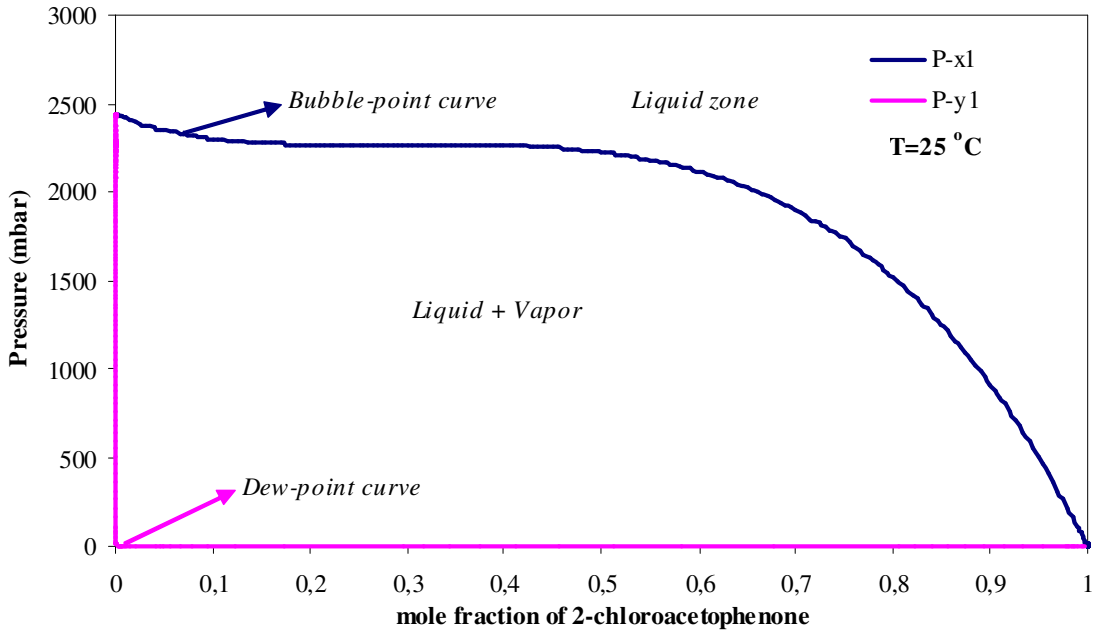

Figure 70: Vapor-Liquid equilibrium for Chloroacetophenone (1) / *n*-Butane (2) at 25 °C. The solid curve shows the COSMOtherm predictions

Indole – n-Butane binary system

The Figure shows the vapor liquid equilibrium data for Indole (1) and *n*-butane (2) at 25 °C. The LLE point found at pressure of 0.2276E+04mbar (composition of components (1) and (2) in liquid phase 1 and phase 2 at this pressure x'(1)=0.155, x'(2)=0.845, x"(1)=0.505, x"(2)=0.495) and the pressure above this, mixture behaves as liquid.

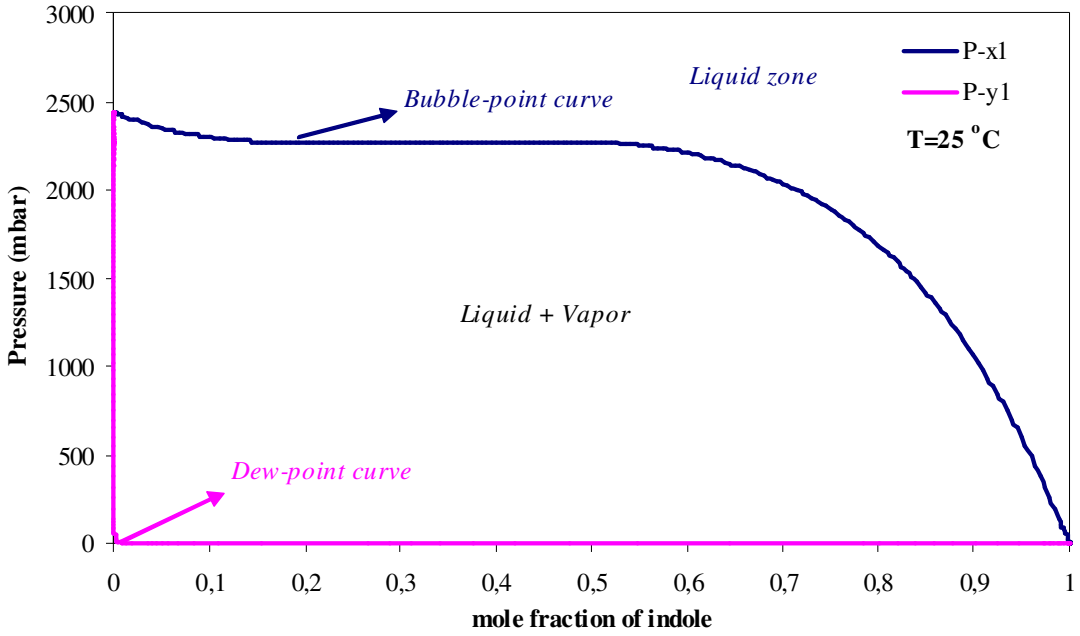

Figure 71: Vapor-Liquid equilibrium for Indole (1) / *n*-Butane (2) at 25 °C. The solid curve shows the COSMOtherm predictions

Pyridine – n-Butane binary system

The Figure shows the vapor liquid equilibrium data for pyridine (1)/*n*-butane (2) at fixed temperature 25 °C and the vapor-liquid phase diagram is calculated by using COSMOtherm. The Figure 32 shows the amount of pyridine in vapor and liquid phases. A point on this curve shows the variations of pyridine in liquid that is in equilibrium with pyridine in vapor at different pressures. The remaining mole percentage in both cases is n-butane.

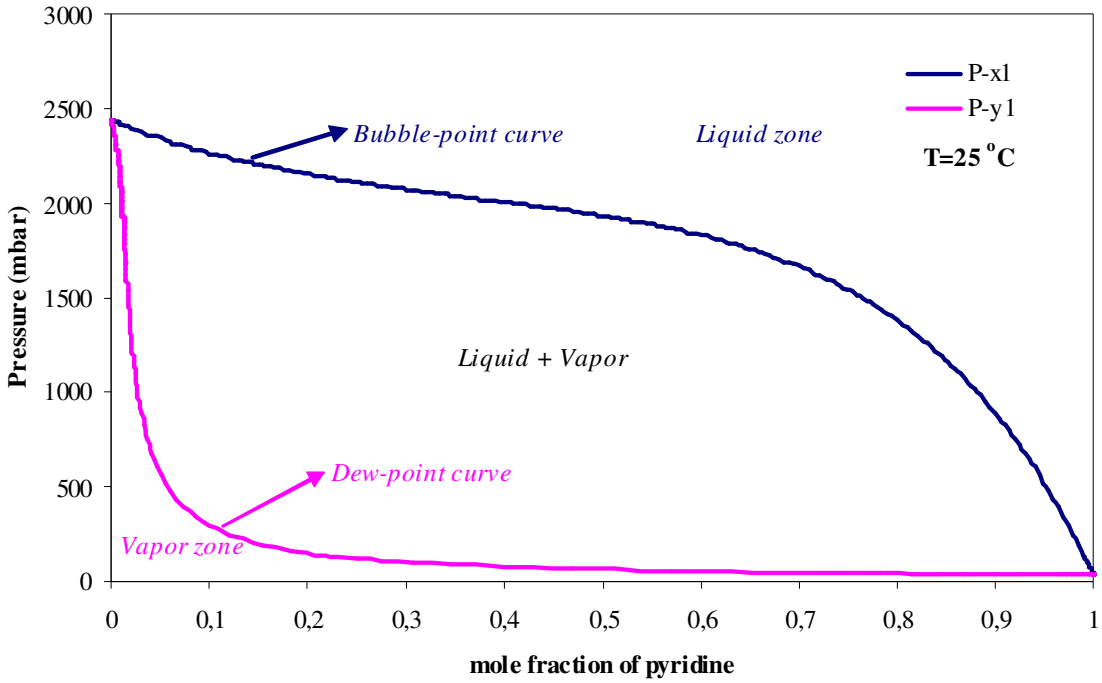

Figure 72: Vapor-Liquid equilibrium for Pyridine (1) / *n*-Butane (2) at 25 °C. The solid curve shows the COSMOtherm predictions

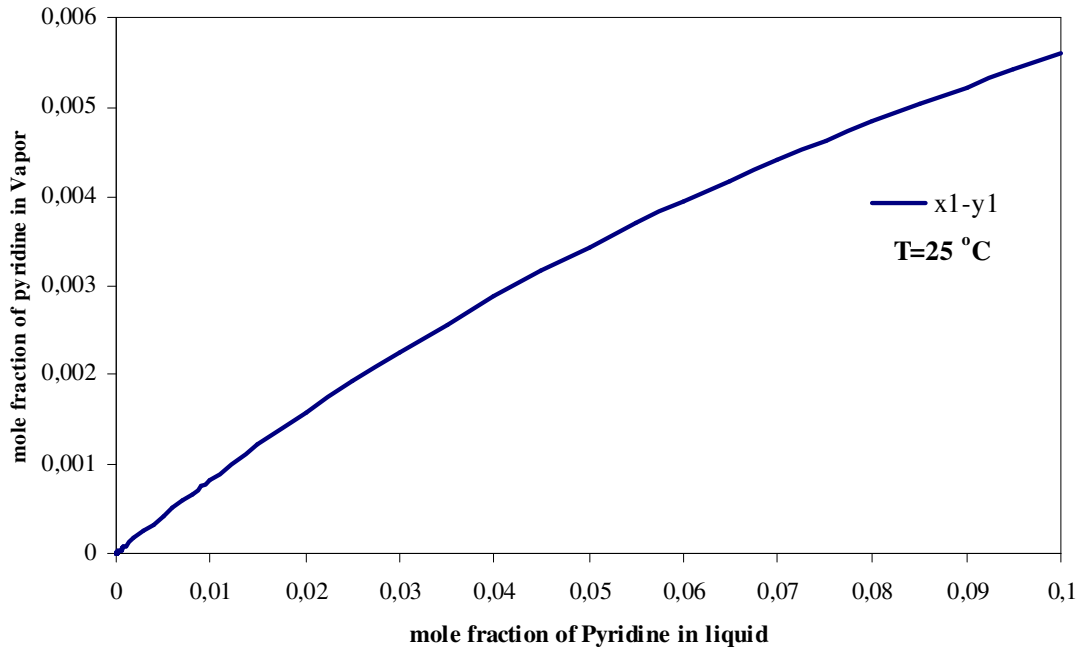

Figure 32: The X-Y diagram for Pyridine (1) / *n*-Butane (2) at 25 °C. The solid curve shows the COSMOtherm predictions

Butyl amine – n-Butane binary system

The Figure shows the vapor liquid equilibrium data for butylamine (1)/*n*-butane (2) at fixed temperature 25 ^{o}C and the vapor-liquid phase diagram is calculated by using COSMOtherm. The Figure shows the amount of butylamine in vapor and liquid phases. A point on this curve shows the variations of butylamine in liquid that is in equilibrium with butylamine in vapor at different pressures. The remaining mole percentage in both cases is *n*-butane.

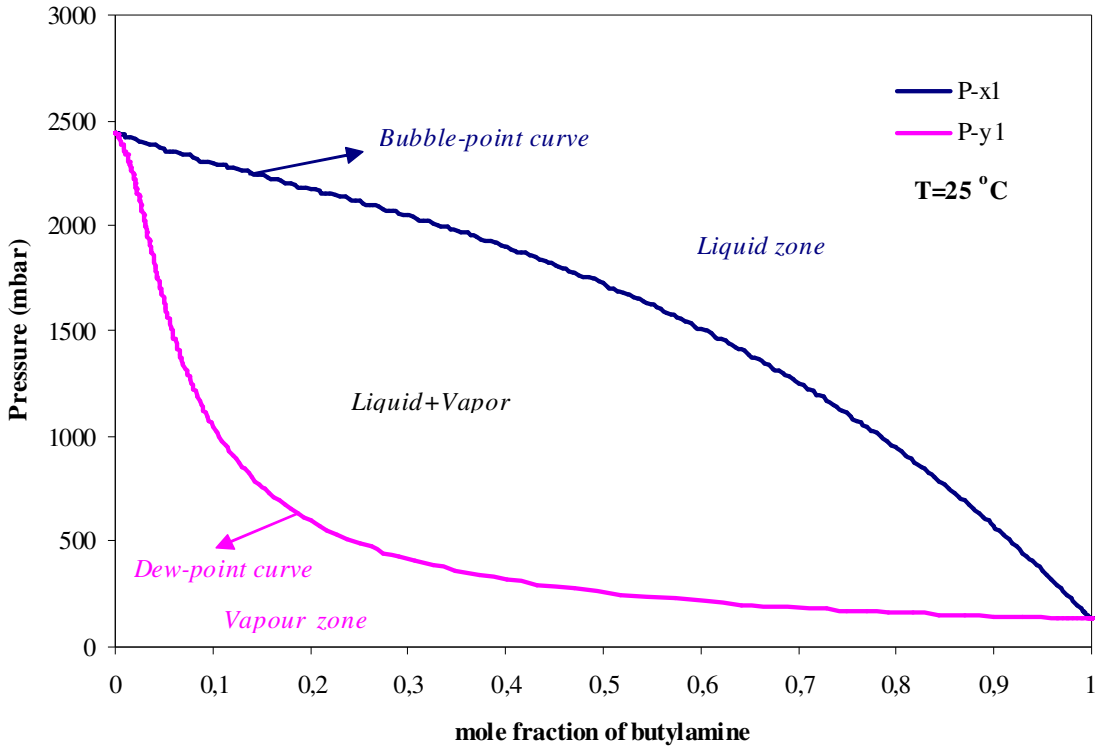

Figure 74: Vapor-Liquid equilibrium for Butylamine (1) / *n*-Butane (2) at 25 ^{o}C. The solid curve shows the COSMOtherm predictions

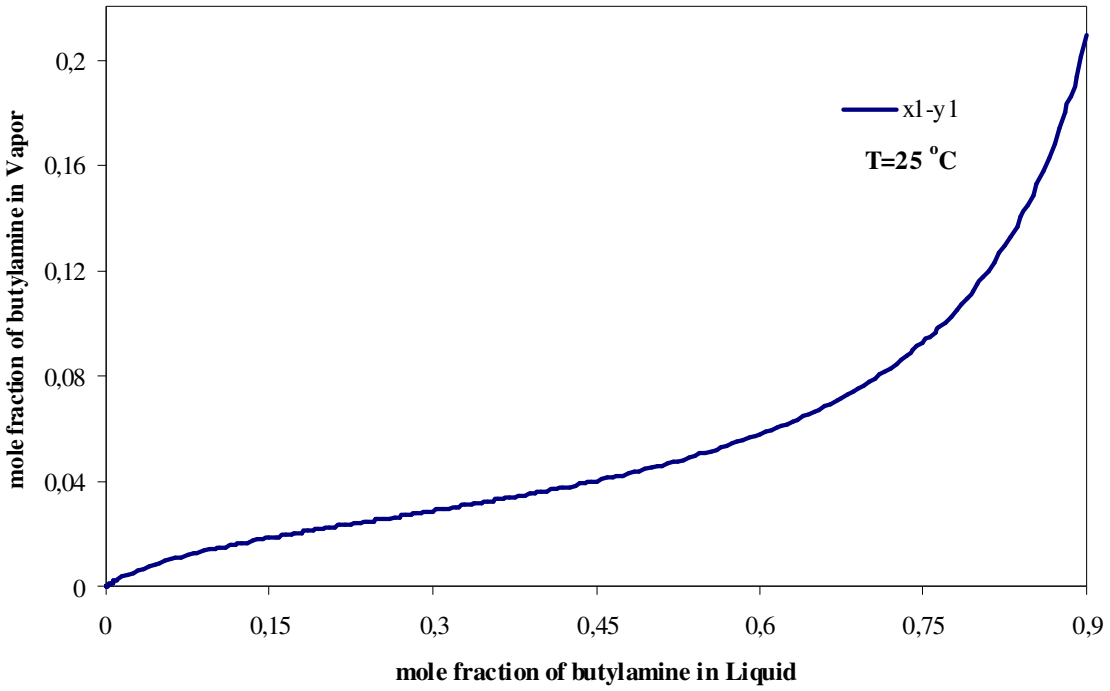

Figure 75: The X-Y diagram for Butylamine (1) / *n*-Butane (2) at 25 °C. The solid curve shows the COSMOtherm predictions

Figure 33 shows the mole fraction of nine compounds which could be possible additives in the vapor phase as a function of its concentration in the liquid phase. This diagram is created from the phase equilibrium calculations of possible candidates made in the preceding section. A point on the equilibrium curve is the mole percentage of additive in the vapor as a function of the mole percentage additive in the liquid, in binary mixtures of the additive and butane.

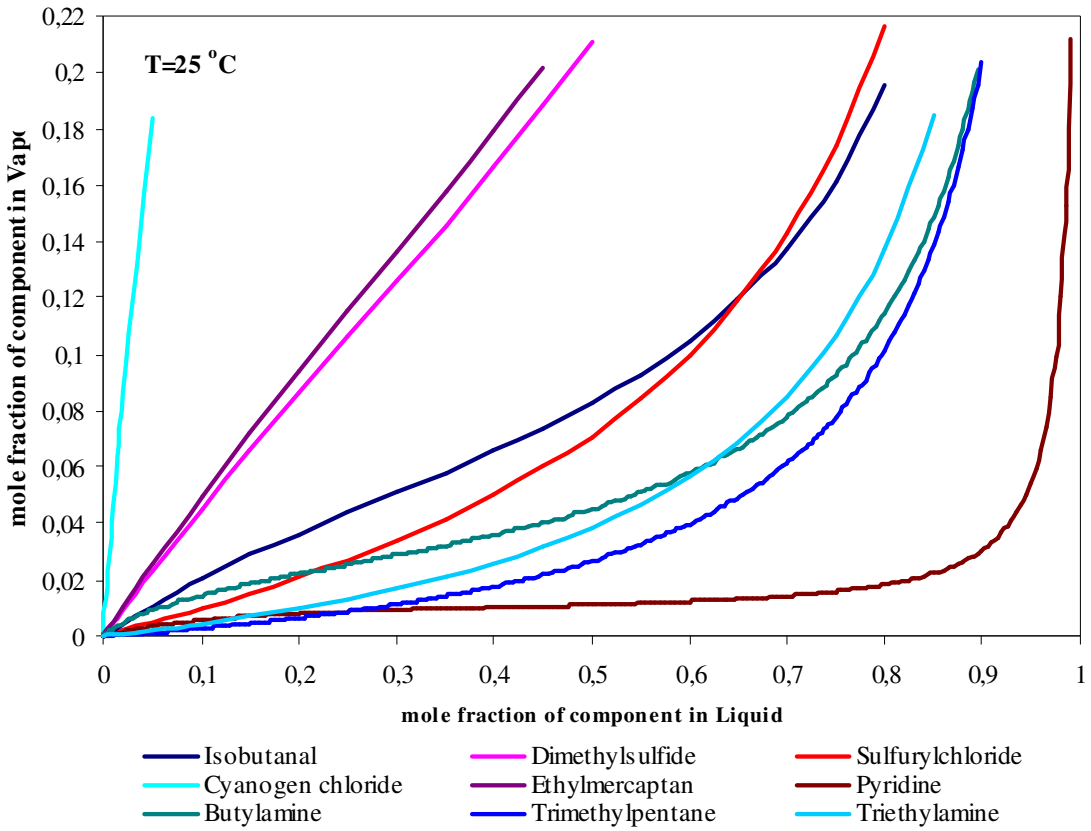

Figure 33: The X-Y diagram for 9 possible additives (1) / *n*-Butane (2) at 25 °C. The solid curve shows the COSMOtherm predictions

8 Conclusion

A list of 27 possible compounds was compiled, selected preliminarily on the basis of deterrent effect and solubility in organic solvents. Phase equilibrium calculations were performed using COSMOtherm, after this software tool had been validated against the available experimental data. From these calculations 9 compounds (triethylamine, isobutyraldehyde, pyridine, dimethylsulfide, sulfurylchloride, cyanogenchloride, 2,2,4 trimethylpentane, ethyl mercaptan and butylamine) were considered as possible additives to prevent inhalation. Some of the remaining compounds: bis(chloromethyl)ether, 2-aminophenol, propyleneglycol, s-trioxane, 2-chloro acetophenone and indole exhibit liquid-liquid equilibrium with butane, others have a vapor pressure which is probably too low to be of interest. These compounds are not considered suitable to add to butane at room temperature.

We conclude that compounds with a similar volatility to butane will be best, since they will not concentrate in the liquid over time (for heavier components), nor will they be largely removed in a short time (for much more volatile components). The amines, cyanogen chloride, and sulfuryl chloride are considered to be the most promising compounds to add to butane. For these substances much more work needs to be done to establish that the effect is sufficient, that the additive is non-toxic in the amount added, that the lighter gas can still be used in a normal way. Again, it must be emphasized that this report represents a technical chemical study as part of a larger study that must consider other aspects – the most important being the health aspects of the proposed additives.

9 References

[1] The final report of the national inhalant abuse task force. *National directions on inhalant abuse*. was endorsed by the ministerial council strategy on 15 May 2006

[2] Hideaki Sugie. Chizuko Sasaki. Chikako Hashimoto. Hiroshi Takeshita. Tomonori Nagai. Shigeki Nakamura. Masataka Furukawa. Tomonori Nagai. Takashi Nishikawa. Katsuyoshi Kurihara *"Three cases of sudden death due to butane or propane gas inhalation: analysis of tissue for gas components"* Forensic Science International 143 (2004) 211-214.

[3] Chiaki Fuke. Tetsuji Miyazaki. Tomonori Arao. Yasumasa Morinaga. Hajime Takaesu. Taichi Takeda. Teruo Iwamasa *"A fatal case considered to be due to cardiac arrhythmia associated with butane inhalation"* Legal Medicine 4 (2002) 134-138.

[4] H.Pfeiffer. M.Al Khaddam. B. Brinkmann. H.Kohler and J. Beike *"Sudden death after isobutane sniffing: a report of two forensic cases"* Int J Legal Med (2006) 120: 168-173.

[5] Suk-Joon Oh. Sang-Eun Lee. Ji*n*-Sik Burm. Chul-Hoon Chung. Jong-Wook Lee. Young-Chul Chang. Dong-Chul Kim *"Explosive burns during abusive inhalation of butane gas"* Burns 25 (1999) 341-344.

[6] A Esmail. L Meyer. A Pottier. S Wright *"Deaths from volatile substance abuse in those under 18 years: results from a national epidemiological study"* Archives of disease in childhood (1993) 69: 356-360.

[7] Tracey L. Kurtzman. B.A.. Kimberly N. Otsuka. M.D.. and Richard A. Wahl. M.D. *"Inhalant abuse by adolescents"* Journal of adolescent health (2001). 28: 170-180.

[8] Raquel A. Crider. Beatrice A. Rouse *"Epidemiology of inhalant abuse: An update"* Division of Epidemiology and statistical analysis. National Institute on Drug Abuse Research Monograph 85. 1988.

[9] A report and recommendations on *"Western Australian Task force on Butane Misuse" October 2006.*

[10] Peter d'Abbs and Sarah McLean *"Volatile Substance misuse: A Review of interventions"* Department of Health and Ageing. 2008

[11] Roger Nicholas *"The policing implications of volatile substance misuse"* Australian Center for Policing Research. December 2004

[12] Mihoko Ago. Kazutoshi Ago and Mamoru Ogata *"A fatal case of n-butane poisoning after inhaling anti-perspiration aerosol deodorant"* Legal Medicine 4 (2002) 113-118.

[13] Isabel Burk *"Inhalant Prevention Resource Guide"* Verginia Department of Education. Division of Instructional Support Services. January 2001.

[14] Andreas Klamt and Frank Eckert *"COSMO-RS: a novel and efficient method for the priori prediction of thermophysical data of liquids"* Fluid Phase Equilibria 172 (2000). 43-72.

[15] Chieh-Ming Hsieh and Shiang-Tai Lin *"Determination of cubic equation of state parameters for pure fluids from first principle solvation calculations"* AICHE J. 54 (August 2008.) 2174-2181.

[16] Tiancheng Mu. Jurgen Rarey. and Jurgen Gmehling *"Performance of COSMO-RS with sigma profiles from different model chemistries"* Ind. Eng. Chem. Res. (2007). 46. 6612-6629.

[17] Shiang-Tai Lin and Stanley I. Sandler *"A prori phase equilibrium prediction from a segment contribution solvation model"* Ind. Eng. Chem. Res. (2002). 41. 899-913.

[18] Eric Mullins. Richard Oldland. Y.A.Liu. Shu Wang. Stanley I. Sandler. Chau-Chyun Chen. Michael Zwolak. and Kevin C. Seavey *"Sigma-profile database for using COSMO-based thermodynamic methods"* Ind. Eng. Chem. Res. (2006). 45. 4389-4415.

[19] Eric Mullins. Y.A.Liu. Adel Ghaderi. and Stephen D. Fast *"Sigma-profile database for predicting solid solubility in pure and mixed solvent mixtures for organic pharmacological compounds with COSMO-based thermodynamic methods"* Ind. Eng. Chem. Res. (2008). 47. 1707-1725.

[20] Kontogeorgis, G. M.; Voutsas, E. C.; Yakoumis, I. V.; Tassios, D. P. Ind. Eng.Chem. Res.1996, 35, 4310-4318.

[21] L. Ruffine, P. Mougin, and A. Barreau *"How to represent Hydrogen sulfide within the CPA Equation of state"* Ind. Eng.Chem. Res.2006, 45, 7688-7699.

[22] Neil F Giles, and Grant M. Wilson "Phase Equilibria on seven Binary Mixtures" J. Chem. Eng. Data, 2000, 45 (2), 146-153.